



HAL
open science

Recovery technologies for indium, gallium, and germanium from end-of-life products (electronic waste) – A review

Kun Zheng, Marc Benedetti, Eric van Hullebusch

► To cite this version:

Kun Zheng, Marc Benedetti, Eric van Hullebusch. Recovery technologies for indium, gallium, and germanium from end-of-life products (electronic waste) – A review. *Journal of Environmental Management*, 2023, 347, pp.119043. 10.1016/j.jenvman.2023.119043 . hal-04221646

HAL Id: hal-04221646

<https://cnrs.hal.science/hal-04221646v1>

Submitted on 28 Sep 2023

HAL is a multi-disciplinary open access archive for the deposit and dissemination of scientific research documents, whether they are published or not. The documents may come from teaching and research institutions in France or abroad, or from public or private research centers.

L'archive ouverte pluridisciplinaire **HAL**, est destinée au dépôt et à la diffusion de documents scientifiques de niveau recherche, publiés ou non, émanant des établissements d'enseignement et de recherche français ou étrangers, des laboratoires publics ou privés.

Recovery technologies for indium, gallium, and germanium from end-of-life products (electronic waste) – A review

Kun Zheng¹, Marc F. Benedetti¹, Eric D. van Hullebusch^{1*}

¹ Université Paris Cité, Institut de Physique du Globe de Paris, CNRS, F-75005 Paris, France

* Corresponding author: vanhullebusch@ipgp.fr (Eric D. van Hullebusch)

Abstract

Advanced high-tech applications for communication, renewable energy, and display, heavily rely on technology critical elements (TCEs) such as indium, gallium, and germanium. Ensuring their sustainable supply is a pressing concern due to their high economic value and supply risks in the European Union. Recovering these elements from end-of-life (EoL) products (electronic waste: e-waste) offers a potential solution to address TCEs shortages. The review highlights recent advances in pre-treatment and hydrometallurgical and biohydrometallurgical methods for indium, gallium, and germanium recovery from EoL products, including spent liquid crystal displays (LCDs), light emitting diodes (LEDs), photovoltaics (PVs), and optical fibers (OFs). Leaching methods, including strong mineral and organic acids, and bioleaching, achieve over 95% indium recovery from spent LCDs. Recovery methods emphasize solvent extraction, chemical precipitation, and cementation. However, challenges persist in separating indium from other non-target elements like Al, Fe, Zn, and Sn. Promising purification involves solid-phase extraction, electrochemical separation, and supercritical fluid extraction. Gallium recovery from spent GaN and GaAs LEDs achieves 99% yield via leaching with HCl after annealing and HNO₃, respectively. Sustainable gallium purification techniques include solvent extraction, ionic liquid extraction, and nanofiltration. Indium and gallium recovery from spent CIGS PVs achieves over 90% extraction yields via H₂SO₄ with citric acid-H₂O₂ and alkali. Although bioleaching is slower than chemical leaching (several days versus several hours), indirect bioleaching shows potential, achieving 70% gallium extraction yield. Solvent extraction and electrolysis exhibit promise for pure gallium recovery. HF or alkali roasting leaches germanium with a high yield of 98% from spent OFs. Solvent extraction achieves over 90% germanium recovery with minimal silicon co-extraction. Solid-phase extraction offers selective germanium recovery. Advancements in optimizing and implementing these e-waste recovery protocols will enhance the circularity of these TCEs.

Keywords: Technology critical elements recovery, pre-treatment methods, hydrometallurgy, biohydrometallurgy, e-waste recycling

Table of contents

RECOVERY TECHNOLOGIES FOR INDIUM, GALLIUM, AND GERMANIUM FROM END-OF-LIFE PRODUCTS (ELECTRONIC WASTE) – A REVIEW.....	I
ABSTRACT.....	II
TABLE OF CONTENTS	III
1 INTRODUCTION	1
1.1 INDIUM	2
1.2 GALLIUM	3
1.3 GERMANIUM.....	4
1.4 THE AQUEOUS CHEMISTRY OF INDIUM, GALLIUM, AND GERMANIUM.....	5
2 END-OF-LIFE PRODUCTS AS A SECONDARY SOURCE FOR INDIUM, GALLIUM, AND GERMANIUM.....	9
2.1 END-OF-LIFE PRODUCTS AS A SECONDARY SOURCE OF INDIUM.....	9
2.1.1 <i>LCDs as a secondary source of indium</i>	13
2.2 END-OF-LIFE PRODUCTS AS A SECONDARY SOURCE OF GALLIUM	14
2.2.1 <i>LEDs as a secondary source of gallium</i>	15
2.2.2 <i>PVs as a secondary source of gallium</i>	17
2.3 END-OF-LIFE PRODUCTS AS A SECONDARY SOURCE OF GERMANIUM.....	17
2.3.1 <i>OFs as a secondary source of germanium</i>	19
3 THE RECOVERY OF INDIUM, GALLIUM, AND GERMANIUM FROM END-OF-LIFE PRODUCTS	19
3.1 KINETIC STUDY.....	21
3.1.1 <i>Kinetic studies of the leaching step</i>	21
3.1.2 <i>Kinetic studies of the recovery step</i>	22
3.2 INDIUM RECOVERY FROM EoL LCDs VIA HYDROMETALLURGICAL AND BIOHYDROMETALLURGICAL ROUTES.....	23
3.2.1 <i>Pre-treatment of EoL LCDs</i>	23
3.2.1.1 Manual dismantling of LCDs to access the ITO film.....	23
3.2.1.2 Removing polarizing films and liquid crystals.....	24
3.2.1.3 Comminution of LCD panels to obtain powder samples	26
3.2.1.4 Characterization methods of LCD samples.....	27

3.2.2	<i>Indium leaching from EoL LCDs via hydrometallurgical and biohydrometallurgical routes</i>	29
3.2.2.1	Indium leaching with strong mineral acids	32
3.2.2.2	Indium leaching with organic acids.....	34
3.2.2.3	Indium bioleaching	34
3.2.3	<i>Indium recovery from EoL LCDs by hydrometallurgical and biohydrometallurgical routes</i>	35
3.2.3.1	Solvent extraction and ionic liquids extraction	37
3.2.3.2	Solid-phase extraction	39
3.2.3.3	Precipitation.....	40
3.2.3.4	Cementation.....	40
3.2.3.5	Electrochemical separation/Electrowinning.....	41
3.2.3.6	Supercritical fluid extraction	41
3.2.3.7	Indium biorecovery	42
3.3	GALLIUM RECOVERY FROM EoL LEDs VIA HYDROMETALLURGICAL AND BIOHYDROMETALLURGICAL ROUTES.....	42
3.3.1	<i>Pre-treatment of EoL LEDs</i>	43
3.3.2	<i>Gallium leaching from EoL LEDs via hydrometallurgical and biohydrometallurgical routes</i>	45
3.3.2.1	Gallium leaching with strong mineral acids and alkaline	47
3.3.2.2	Gallium leaching with organic acids	48
3.3.2.3	Gallium bioleaching	49
3.3.3	<i>Gallium recovery from EoL LEDs via hydrometallurgical and biohydrometallurgical routes</i>	50
3.3.3.1	Solvent extraction.....	52
3.3.3.2	Ionic liquids extraction	52
3.3.3.3	Membrane separation	53
3.3.3.4	Precipitation.....	53
3.3.3.5	Supercritical fluid separation.....	54
3.3.3.6	Indirect biorecovery-based approach	54
3.4	INDIUM AND GALLIUM RECOVERY FROM EoL PVs VIA HYDROMETALLURGICAL AND BIOHYDROMETALLURGICAL ROUTES.....	55
3.4.1	<i>Pre-treatment of EoL PVs</i>	55
3.4.2	<i>Indium and gallium leaching from EoL PVs via hydrometallurgical and biohydrometallurgical routes</i>	56
3.4.2.1	Indium and gallium leaching with acids and alkali	57
3.4.2.2	Indium and gallium bioleaching.....	58

3.4.3	<i>Indium and gallium recovery from EoL PVs via hydrometallurgical and biohydrometallurgical routes.....</i>	<i>58</i>
3.5	GERMANIUM RECOVERY FROM EoL OFs VIA HYDROMETALLURGICAL ROUTES	60
3.5.1	<i>Pre-treatment of end-of-life OFs</i>	<i>60</i>
3.5.2	<i>Germanium leaching from OFs via hydrometallurgical routes</i>	<i>60</i>
3.5.2.1	Germanium leaching with mineral acids.....	61
3.5.3	<i>Germanium recovery from OFs via hydrometallurgical routes</i>	<i>62</i>
3.5.3.1	Solvent extraction.....	62
3.5.3.2	Solid-phase extraction	63
4	FURTHER RESEARCH PERSPECTIVES	63
5	CONCLUSIONS	64
6	CREDIT AUTHORSHIP CONTRIBUTION STATEMENT	66
7	DECLARATION OF COMPETING INTEREST.....	66
8	ACKNOWLEDGMENTS	66
9	REFERENCES.....	67

1 Introduction

2 The ongoing development of novel high-tech applications for communications, renewable
3 energy production, and display purposes strongly depends on technology critical elements
4 (TCEs) such as indium, gallium, and germanium. These elements play important roles in the
5 functionality of liquid crystal displays (LCDs), light emitting diodes (LEDs), photovoltaics
6 (PVs), and optical fibers (OFs). However, the sustainable supply of these elements is a major
7 concern, as their supply to the European Union (EU) manufacturing industry is not secured due
8 to increasing demand and export controls from resource-rich countries (Licht et al., 2015).
9 European Commission has classified these TCEs on the main list of critical raw materials
10 (CRMs: total 30 materials) in view of their high importance to the EU economy and because
11 of the high risk associated with their supply from 2011 to the present (European Commission,
12 2020).

13 The EU proposed a circular economy with efficient energy use, low carbon emissions, efficient
14 resource recovery, and a competitive economy in 2011 (European Commission, 2011). The EU
15 Green Deal Communiqué also adopted a proposal in 2019 to achieve carbon neutrality by 2050.
16 As a result, EU members are continuously working to develop sustainable and efficient
17 processes to recover TCEs needed for electronic applications, therefore contributing to the
18 sustainable supply of these elements. According to the International Telecommunication Union
19 News in 2020, approximately 53.6 million metric tonnes (Mt) of global electronic waste (e-
20 waste) (excluding PV panels) were generated in 2019, and this figure is expected to increase
21 to 74 Mt by 2030 (Forti et al., 2050). Moreover, according to the International Renewable
22 Energy Agency (IRENA), End-of-life (EoL) PVs were projected to reach 1.7-8 Mt in 2030 and
23 70 Mt in 2050 (Stephanie et al., 2016). Global e-waste generation is increasing at an alarming
24 rate of almost 2 Mt per year (Forti et al., 2050).

25 Furthermore, according to the Platform for Accelerating the Circular Economy report, if
26 current trends continue, the amount of global e-waste will double to 120 Mt per year by 2050.
27 Also, Elshkaki and Graedel (2013) reported that the demand for indium, gallium, and
28 germanium will increase by 225%, 224%, and 2,130%, respectively, in 2050 compared to 2010.
29 In addition, production losses account for 70% of total losses for indium and more than 95%
30 for gallium and germanium in the global production processes (Charpentier Poncelet et al.,
31 2022). The recovery of these TCEs from EoL products is seen as a sustainable approach to
32 overcome the foreseeable supply shortages of indium, gallium, and germanium.

33 In contrast to existing reviews, which primarily focus on single TCE type and its recovery from
34 primary resources or pyrometallurgical industry waste streams, this review paper provides a
35 comprehensive exploration of contemporary methodologies dedicated to the recovery of
36 indium, gallium, and germanium from EoL products, such as LCDs, LEDs, PVs, and OFs. In
37 addition, the reliance on energy-intensive pyrometallurgical methods such as thermal
38 decomposition for TCEs recovery hindered by environmental and economic concerns has not
39 been reviewed in the present paper but is discussed elsewhere (Akcil et al., 2019; Fontana et
40 al., 2020; Pradhan et al., 2018; Schaeffer et al., 2017; Zhang et al., 2015). Consequently, the
41 present study encompasses an overview of the above-mentioned TCEs content and distribution
42 in EoL products, as well as a detailed discussion of the full electronic waste treatment chain,
43 including the pre-treatment, and both hydrometallurgical and biohydrometallurgical TCE
44 recovery processes. Further details regarding the methodology for literature selection can be
45 found in Supplementary Material Text S1. This paper presents a complete perspective covering
46 diverse TCEs recovery routes from various types of EoL products and emphasizes recent
47 advances in hydrometallurgical and biohydrometallurgical approaches, contributing to a
48 comprehensive understanding of current research and providing valuable insights for future
49 research.

50 **1.1 Indium**

51 Indium is a silvery white metal. The oxidation states of indium are +1 and +3, but the most
52 stable oxidation state is In(III) (Alfantazi and Moskalyk, 2003; Gunn, 2014; Zhang et al., 2017).
53 Its specific properties, including ductility, scalability, electrical conductivity, and optical
54 transparency, make it attractive for high-tech applications (Ciacci et al., 2019). Indium is used
55 in manufacturing industries to produce a variety of applications to improve the quality of
56 human life, such as flat panel displays (FPDs), PVs, LEDs, batteries, and more (Lokanc et al.,
57 2015). Additionally, the considerable economic value and irreplaceable nature of indium
58 solidify its importance within technological domains (Harper et al., 2015).

59 The scarcity of indium in rocks is obvious by its average crustal abundance of 0.072 mg/kg in
60 oceanic crust and 0.05 mg/kg in continental crust (Gunn, 2014). It is most commonly found in
61 higher concentrations in zinc (sphalerite), copper sulphide (chalcopyrite), and tin ores, often as
62 a by-product of the extraction of elements like Zn, Cu, Pb, and Sn (Ciacci et al., 2019; Mejías
63 et al., 2023). Despite this, its concentration in zinc ores usually remains below 20 mg/kg
64 (Takahashi et al., 2009).

65 Given the limited availability and growing demand, the global indium supply faces challenges.
66 The world produced approximately 900 tons of indium, about 7% less than in 2021, possibly

67 due to global COVID-19 pandemic restrictions (USGS, 2022, 2023). The United States, for
68 instance, relied on a 100% net import from countries such as China (31% in 2017-2020) and
69 the Republic of Korea (32% in 2018-2021), leading to fluctuations in supply (USGS, 2022,
70 2023). This increasing demand has contributed to a rise in the price of indium, reaching \$395
71 (99.99% purity) per kilogram by 2020 (Křištofová et al., 2016; Zhang et al., 2017; USGS,
72 2023). Owing to its high economic importance ($EI \geq 2.8$) and supply risk ($SR \geq 1$), indium
73 ($EI: 3.3$ and $SR: 1.8$) has been classified on the CRMs list by the EU commission from 2011
74 to 2020 (European Commission, 2020).

75 To counteract indium supply shortages, recovering indium from EoL products presents a viable
76 solution (Lokanc et al., 2015). While past indium recovery rates were limited ($< 1\%$) due to
77 technological and economic barriers, the production losses of indium were relatively high (70%)
78 in the global production process (Charpentier Poncelet et al., 2022; Ylä-Mella & Pongrácz,
79 2016). However, efficient indium recovery technologies have been explored for waste
80 electrical and electronic equipment (WEEE) containing significant concentrations of TCEs
81 (Danilo Fontana et al., 2015). In this context, hydrometallurgical and biohydrometallurgical
82 methods stand out, offering lower energy consumption, reduced operating costs, and improved
83 environmental friendliness compared to pyrometallurgical routes (Mejías et al., 2023;
84 Sethurajan et al., 2018, 2019).

85 **1.2 Gallium**

86 Gallium is silvery-white in appearance and a relatively soft metal (Gunn, 2014). It has two
87 valence states of +1 and +3, with Ga(III) being the predominant stable state. The benefits of
88 electronic, optoelectronic, and thermal conductivity properties attract the attention of high-tech
89 industries (Gunn, 2014; USGS, 2018). Gallium is used in electronic circuits, semiconductors,
90 laser diodes, transistors, PVs, and LEDs due to its unique physical and chemical properties,
91 compared to conventional semiconductor materials like silicon (Chen et al., 2018a; Licht et al.,
92 2015; Maarefvand et al., 2020). Therefore, gallium is important in high-tech industries.

93 Gallium usually occurs in trace amounts in nature, although it has an average crustal abundance
94 of 19 mg/kg, similar to other well-known metals, such as lead (10 mg/kg) and tin (2 mg/kg).
95 Not occurring naturally as a pure mineral, gallium replaces similar elements in minerals like
96 iron (Gunn, 2014). Extracted primarily as a by-product of aluminum from bauxite, zinc
97 production from sphalerite (ZnS), and coal, gallium is highly dependent on the production of
98 primary commodities (Licht et al., 2015; Lu et al., 2017). While around 90% of primary gallium
99 production is related to aluminum refining, less than 5% (438 tonnes) can be recuperated from

100 Bayer liquor generated in aluminum refining (Licht et al., 2015). Growing technological needs
101 have increased demand, predicted a more than 200% increase by 2050 from 2010 (Elshkaki
102 and Graedel, 2013). However, as of 2022, global gallium production has already reached 550
103 tonnes per year, a 127% increase from 2021 (USGS, 2023). Dependency on 100% net imports
104 (2017 to 2021), particularly from China (53%), along with the price increase of low-purity
105 gallium to \$420 per kg in 202, may be caused by the pandemic restriction, highlights the global
106 competition driven by limited resources and heaving demand (USGS, 2023). The
107 irreplaceability of gallium drives competition in such dynamics (Frenzel et al., 2017). This
108 explains why the European Commission has identified this element as critical (EI: 3.5 and SR:
109 3.9) (European Commission, 2023).

110 In addition, the growing market for wireless communications and mobile technologies is
111 driving the need to develop gallium recovery from related EoL products (Swain et al., 2015a).
112 Despite this, less than 1% of gallium is recycled from EoL products, and the production loss
113 exceeds 95% in the global production process (Charpentier Poncelet et al., 2022; Chen et al.,
114 2018a). EoL products, such as LEDs and PVs, contain significant amounts of gallium, which
115 is predicted to see over a 12-fold demand increase by 2050 (Ueberschaar et al., 2017).
116 Therefore, hydrometallurgical and biohydrometallurgical approaches are developing as
117 promising routes to recover gallium from EoL products (Chen et al., 2018a; Maarefvand et al.,
118 2020; Nagy et al., 2017; Swain et al., 2015a).

119 **1.3 Germanium**

120 Germanium is greyish-white and brittle semi-metal (Gunn, 2014; Rosenberg, 2009). It has two
121 main valence states, +2 and +4, with Ge(IV) as the stable redox state. It appears as compounds
122 like GeO₂ and GeS₂, and substitutes silicon in silicate minerals due to similar ionic radii (Ge⁴⁺
123 0.53 Å versus Si⁴⁺ 0.40 Å) and similar covalent radii (Ge⁴⁺ 1.22 Å versus Si⁴⁺ 1.17 Å) (Höll et
124 al., 2007). The unique electrical properties of germanium, its high refractive index in
125 transmission, and its low dispersion to avoid chromatic aberrations, make it essential in various
126 applications, such as optical fibers, infrared optics, electronics, and PVs. (Bumba et al., 2018;
127 Licht et al., 2015; Rosenberg, 2009). With escalating semiconductor and optical industry
128 demands, germanium use is projected to increase by 2,130% in 2050 compared to 2010
129 (Elshkaki and Graedel, 2013).

130 Germanium is a rare element in rocks, with an average abundance of 13.8 mg/kg on the earth
131 (1.5 mg/kg for the oceanic crust and 1.6 mg/kg for the continental crust). It does not occur as a
132 free metal in nature, and is found in trace amounts within various rocks, including oxidic and
133 sulfide metalliferous deposits (zinc-copper-lead-gold-silver ores), and non-ferrous metal

134 deposits, such as coal combustion by-products (coal fly ash and flue dust) (Gunn, 2014; Höll
135 et al., 2007; Rosenberg, 2009; USGS, 2022). Global refinery production increased by 113% to
136 140 tonnes in 2021 compared to 2018 (USGS, 2018, 2022). However, net imports, mainly from
137 China (53%) and Russia (9%), are vulnerable to geopolitical factors (i.e. the conflict in Ukraine)
138 (Kot-Niewiadomska et al., 2022). The price of germanium metal was high (\$1,315 per kg of
139 99.999% purity) in 2021 (USGS, 2022). Despite these, germanium supply is scarce and is
140 unable to meet the rising manufacturing demand (Chen et al., 2018b). Consequently, the EU
141 Commission listed germanium as a CRM with an EI value of 3.5 and an SR value of 1.8,
142 emphasizing the urgency for alternative supply solutions (European Commission, 2023).

143 In recent years, around 30% of germanium recovery comes from recycled materials
144 (Charpentier Poncelet et al., 2022), with global production losses exceeding 95% (Chen et al.,
145 2018b; USGS, 2022) (Charpentier Poncelet et al., 2022; Chen et al., 2018b; USGS, 2022). The
146 growing popularity of optics with the development of 5G networks presents an opportunity to
147 recycle EoL fiber optics (Chen et al., 2020). Fiber optics account for 40% of total germanium
148 usage and can assistance in germanium recycling (Chen et al., 2017; Chen et al., 2018b). This
149 emphasizes the importance of EoL products recovery to mitigate germanium supply pressure.

150 **1.4 The aqueous chemistry of indium, gallium, and germanium**

151 The ionic radii of In(III), Ga(III), and Ge(IV) play a role in their behavior (

152 Table 1), together with those of Fe(III), Al(III), and Si(IV). These metals often replace elements
153 with similar ionic radii and charges in various ores, and emerge as by-products, including
154 sphalerite, bauxite, and chalcopyrite (Gunn, 2014). In addition, higher oxidation states and
155 ionic radii lead to the formation of stable complexes with oxygen-bound organic ligands
156 (Hofmann et al., 2020; Höll et al., 2007; Wood & Samson, 2006). Thus, the stability of these
157 metals with organic ligand complexes follows the following order: $\text{In(III)} < \text{Fe(III)} \approx \text{Ga(III)}$
158 $\approx \text{Al(III)}$ and $\text{Ge(IV)} < \text{Si(IV)}$. The above information contributes to utilizing insights from
159 the recovery methods of Fe, Al, and Si and applying them to the recovery of In, Ga, and Ge
160 from EoL products.

161 In aqueous solutions, In(III) and Ga(III) are mainly present in their hydrated forms with
162 octahedral coordination formed by six bonds, while Ge(IV) has tetrahedral coordination
163 formed by four bonds (Lu et al., 2017; Nguyen & Lee, 2019; Höll et al., 2007; Wood & Samson,
164 2006) (

165 Table 1). These metals have a full set of 10 d-orbitals in their electronic configuration, enabling
166 stronger covalent bonding with ligands and forming stable complexes.

167

168 Table 1 Ionic radii of metal ions

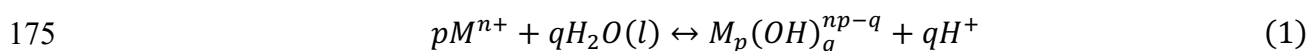
Metal ion	Al ³⁺	Ga ³⁺	Fe ³⁺	In ³⁺	Si ⁴⁺	Ge ⁴⁺
Radius (Å)	0.54	0.62	0.65	0.80	0.26	0.39
Coordination site	Octahedral	Octahedral	Octahedral	Octahedral	Tetrahedral	Tetrahedral

169 Notes: GaCl₄⁻ and InCl₄⁻ belong to the tetrahedral coordination site. Modified from Amthauer et al.
 170 (1982) and Wood & Samson (2006).

171

172 For a better understanding of the metal reaction in aqueous solution, the reaction for hydrolysis
 173 and complexation with ligands is shown below:

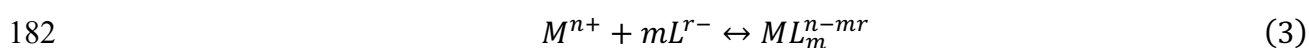
174 1) The hydrolysis reaction of these elements in aqueous medium is defined as:



176 And the equilibrium constant (K_a) is expressed as:

$$177 \quad K_a = \frac{[M_p(OH)_q^{np-q}][H^+]^q}{[M^{n+}]^p[H_2O]^q} \quad (2)$$

178 2) Except for hydroxide complexes, these elements also have different stabilities in
 179 combination with other inorganic ligands, such as fluoride, sulphate and phosphate,
 180 chloride, and bisulphide (Lu et al., 2017; Wood & Samson, 2006). The complex
 181 reaction of these elements with ligands could be written as:



183 And the equilibrium constant (K_b) is expressed as:

$$184 \quad K_b = \frac{[ML_m^{n-mr}]}{[M^{n+}][L^{r-}]^m} \quad (4)$$

185 Where M is metal, n is the relative metal ion charge ($n = 3$ for indium and gallium, $n = 4$ for
 186 germanium), and any ligand of L with ion charge of r .

187 Ionic charges and radii play an important role in metal-ligand complexation (Hofmann et al.,
 188 2020; Höll et al., 2007; Wood & Samson, 2006). Ga(III) ions form stable complexes with hard
 189 ligands such as hydroxide, fluoride, sulphate and phosphate, whereas they form weak
 190 complexes with soft ligands such as chloride and bisulphide (Supplementary Material Table
 191 S1). However, In(III) ion shows an affinity for both hard and soft ligands (hydroxide, fluoride,
 192 sulphate and phosphate, nitrate, chloride and bisulphide). Ge(IV) ion form stable complexes
 193 with hydroxide and fluoride, but limited experimental data for interactions with other ligands

194 due to limiting thermodynamic information and redox chemistry (Filella & May, 2023; Wood
195 & Samson, 2006). However, the well-characterized Ge(IV) acid-base chemistry and the
196 solubility of GeO₂ polymorphs provide insights into its reactivity, interactions, and potential
197 applications (Filella & May, 2023).

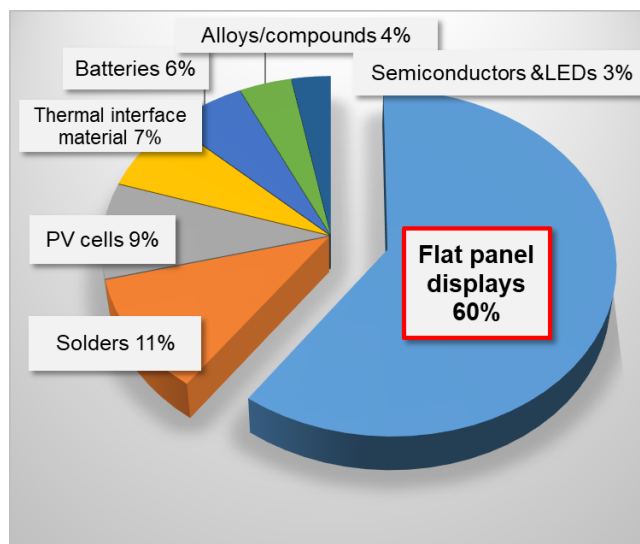
198 In aquatic systems, indium, gallium, and germanium are present at exceedingly low
199 concentrations (0.1 to 72 µg/L for gallium and 0.5 to 130 µg/L for germanium in continental
200 and oceanic geothermal systems) (Wood & Samson, 2006). Their low solubility and difficulty
201 in dissolving pose challenges for recovery methods. The hydrometallurgical and
202 biohydrometallurgical routes for their recovery from WEEE face significant challenges due to
203 their low solubility and the complex environment of non-target metals with high concentrations,
204 such as aluminum, iron, and calcium.

205 **2 End-of-life products as a secondary source for indium, gallium, and** 206 **germanium**

207 **2.1 End-of-life products as a secondary source of indium**

208 EoL products are considered to be a promising secondary source of indium (Lokanc et al.,
209 2015). In the EU, total indium consumption is estimated at 64 tonnes per year from 2012 to
210 2016, with 60% of the total indium used in FPDs, mainly in the form of indium tin oxide (ITO).
211 In addition, 11% and 9% of the consumption is used in solders and PVs, respectively, while
212 the remaining 20% is used in thermal interface materials, batteries, alloys/compounds, and
213 semiconductors & LEDs (Figure 1) (European Commission, 2020). This highlights the
214 importance of considering EoL electronic products as a viable source of indium, particularly
215 for FPDs.

216



217

218 Figure 1 Main uses of indium in the EU. Modified from Critical Raw Materials Factsheets
 219 (European Commission, 2020).

220

221 Table 2 describes the various EoL products that could be used as secondary sources of indium.
 222 As mentioned above, indium is mainly used in FPDs containing ITO thin films. The ITO film
 223 consists of 80-90% indium oxide (In_2O_3) and 10-20% tin oxide (SnO_2) by weight (Fontana et
 224 al., 2015; Silveira et al., 2015). Ylä-Mella and Pongrácz (2016) reported that up to 80% of total
 225 global indium consumption is accounted for by ITO products, which are used in electronic
 226 devices such as smartphones, tablets, and televisions (Assefi et al., 2018). LCDs have the
 227 highest market share among FPDs and are gradually replacing the old cathode ray tube (CRT)
 228 devices because they are lighter and thinner than CRT devices (Zhang et al., 2017). The
 229 increasing use of LCDs and the frequent replacement of devices due to their relatively short
 230 lifespan (less than 10 years) has resulted in the generation of a significant amount of e-waste,
 231 which is typically disposed of in landfills (Lokanc et al., 2015). This is an issue of concern as
 232 spent LCDs contain a significant amount of indium, which is a valuable resource. Savvilotidou
 233 et al. (2015) reported that the concentration of indium in spent LCDs can reach up to 530 mg/kg.
 234 Therefore, collection and recycling of spent LCDs is essential for the recovery of indium. This
 235 approach could significantly reduce the reliance on primary sources of indium and help to
 236 mitigate the environmental impact of electronic waste.

237 Indium and gallium are key semiconductors required in the manufacture of photovoltaic
 238 systems used to generate electricity. Second-generation PV copper indium gallium selenide
 239 (CIGS) is a thin-film solar cell based on the copper indium selenide (CIS) family of
 240 chalcopyrite semiconductors. This technology is gaining popularity and replacing conventional

241 crystalline silicon modules due to their lower costs of materials, lower energy consumption,
242 and thinner and higher stability (Licht et al., 2015).

243 Although the contribution of PV systems to the global indium demand is less than 2%, the
244 output of the global production capacity of CIGS thin-film solar cell systems is expected to
245 cover almost 30% of the total electricity demand (Bleiwas, 2010; Lv et al., 2019). Indium
246 accumulation will start in 2035 and grow, reaching 1,500 tonnes in 2050 in the case of 60 TW
247 scenarios, which is the maximum evaluated by the system for cumulative PV capacity (Gómez
248 et al., 2023). Given this growing demand for indium, the recycling of indium from CIGS thin-
249 film solar cells is expected to be crucial in the future.

250 The versatile use of indium in various electronic devices demonstrates its importance as a
251 critical element for the electronics industry. Indium can also be found in LEDs in the form of
252 indium gallium nitride (InGaN), indium arsenide (InAs), or indium gallium arsenide (InGaAs)
253 (Ciacci et al., 2019; Zhan et al., 2020). LEDs typically exist as LED semiconductor chips and
254 coloured LED lights (Ciacci et al., 2019). To improve the definition and brightness of LCDs,
255 LED semiconductor chips are also used in the LCDs as screen backlighting, which requires an
256 LED-backlit LCD. Currently, colored LED lights are used as lighting devices in homes, cars,
257 instruments, and street-lighting due to their longer life and lower energy consumption than
258 incandescent lamps (Nagy et al., 2017). Other electronic devices, such as DVDs, laser diodes,
259 and printed circuit boards, also contain indium (Licht et al., 2015; Ylä-Mella and Pongrácz,
260 2016). With the increasing demand for electronics, the consumption of indium is expected to
261 continue to grow.

262 In addition to LEDs and LCDs, indium is also found in batteries that contain indium
263 incorporated in indium oxide and have better cyclability and longer cycle life than normal
264 batteries (Nagao et al., 2012; Zhao et al., 2013). It has been reported that the cycle life of
265 batteries with 0.02% In₂O₃ added to the negative active materials is more than four times that
266 of batteries without In₂O₃ (Zhao et al., 2013). The consumption of batteries in the electronics
267 industry is rapidly increasing due to the development of electronic products, such as mobile
268 phones, laptops, recorders, and cameras (Sethurajan et al., 2019). However, the potential for
269 indium recovery from spent batteries has not been fully explored compared to the recovery of
270 other metals (i.e. cobalt and lithium) (Sethurajan et al., 2019; Wang et al., 2016). The recovery
271 of indium could provide additional benefits to the battery recycling industry.

272

273 Table 2 EoL products as a potential secondary source of indium, gallium, and germanium

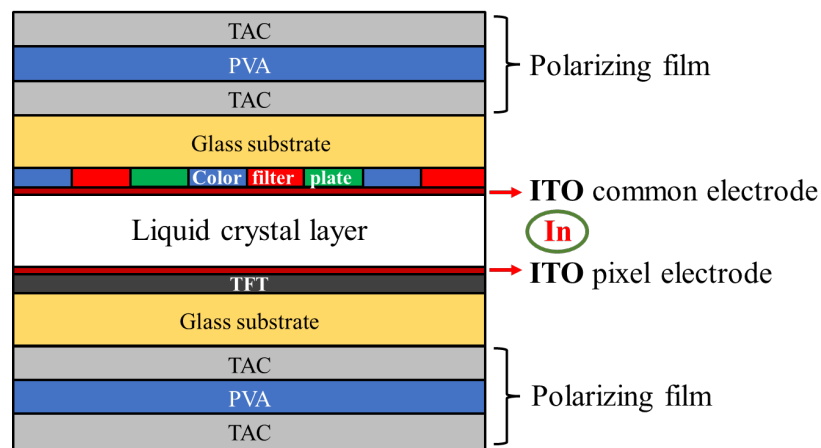
Products	Target metals	EoL products	Advantages
FPDs -LCDs	Indium tin oxide (ITO)	E-books, smartphones, tablets, TVs	Low power consumption, thinness, and light weightness
PV -thin film solar cell	CuInGaSe (CIGS)/ CuInSe (CIS)	Rooftop and building integrated systems, concentrator photovoltaics, and photodetectors	Thinner, less costly, and highly stable
Semiconductors -LEDs	InGaN, InGaAs, InAs, GaAs, GaN, GaP	LED semiconductor chips on LCDs, LED lamps, and monitors	Longer lifespan and lower energy consumption than incandescent lamps
Semiconductors -Others	InP, InN, InGaN, In ₂ Se	DVDs, laser diodes, printed circuit boards	Higher electron velocity and diffusivity, lower base resistance
Batteries -Lithium-ion batterie	Indium thin film (In ₂ O ₃), GaAs, GaN, and GaTe	Mobile phones, laptops, recorders, cameras, nuclear and solar batteries	Good cyclability and longer cycle life
Integrated circuits	GaAs, GaN	PCBs of printers, mobile phones, and computers	Smaller, faster, and less expensive
Laser diodes	GaAs, GaN	DVD, CD, and Blu-ray players	Lasers produced range from infra-red to the UV spectrum
Optical fibers (OFs)	GeO ₂	Communication networks, sensors, and power transmission	Immune to electromagnetic interference compared with metal wires, lower optical losses with germanium than silicon
Infrared (IR) optics	Ge	Night vision systems, camera lenses, IR spectroscopy, military, active car safety systems, satellite systems, and fire alarms	Higher refractive index, transparency and optical uniformity, and low dispersion
Catalyst	GeO ₂	PET and synthetic textile fibers	Colorless by germanium compared with other catalysts, like titanium and antimony

Semiconductor in electronics and solar applications	Ge	Wireless devices, optical communication systems, hard disk drives, GPS, transistors, rectifiers, lasers, and photovoltaic solar cells	Higher speed and lower energy consumption compared with silicon
Catalysts and others	Ge	Catalysts in fluorescent lamps, diodes, transistors, and crystals of X-ray detectors	Germanium detectors are thicker than silicon detectors

274

275 **2.1.1 LCDs as a secondary source of indium**

276 In an LCD module, electrically conductive electrodes are located between two glass panels.
 277 These electrodes are mainly made of ITO. More specifically, the LCD unit is made up of 86.52
 278 wt% glass, 12.81 wt% organic materials and approximately 0.02 wt% indium. Indium is located
 279 in the ITO layer, which is sandwiched between the two glass substrates (Ma and Xu, 2013).
 280 According to Savvilotidou et al. (2015), the thickness of the ITO layer is consistent and stable
 281 at approximately 150 nm, and the indium content is estimated to be more than 100 mg/kg. The
 282 lamination structure of the ITO layer of the LCD panel is shown in Figure 2.



283

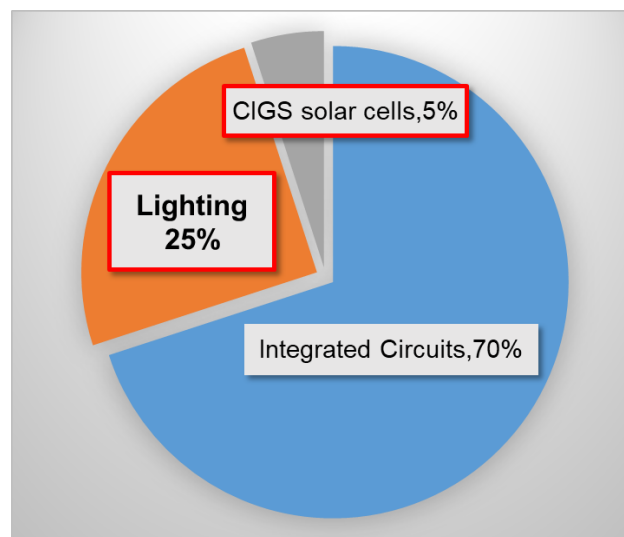
284 Figure 2 Lamination structure of the ITO layer from LCD panel. TAC: cellulose triacetate;
 285 PVA: polyvinyl alcohol; TFT: thin-film transistor; ITO: indium tin oxide. Modified from
 286 Dodson et al. (2012) and Křištofová et al. (2016).

287

288 2.2 End-of-life products as a secondary source of gallium

289 Although gallium is reported to be used in GaAs, InGaN, GaP, GaN, and GaSb semiconductors,
290 the major consumption of gallium is reported for GaAs and GaN. GaAs has higher signal
291 transmittance speed and semiconducting property. It also has higher saturation electron
292 velocity and better radiation hardness than silicon due to its energy band structure in the
293 electronics industry (Chen et al., 2011, 2012; Lee and Nam, 1998). The majority of gallium
294 (almost 99%) is consumed in the form of GaAs and GaN, with 92% of gallium used for GaAs
295 and 8% used for GaN in various EoL products such as integrated circuits, LEDs, laser diodes,
296 PVs, and solar cells. In the EU, integrated circuits account for 70% of total gallium
297 consumption, while lighting accounts for 25%, and CIGS solar cells account for almost 5%
298 (Figure 3) (Chancerel et al., 2013; European Commission, 2020; Licht et al., 2015; Ueberschaar
299 et al., 2017).

300



301

302 Figure 3 Main gallium used in the EU. Modified from Critical Raw Materials Factsheets
303 (European Commission, 2020).

304

305 Table 2 provides information on potential sources of gallium from EoL products. This shows
306 that integrated circuits are a significant source of gallium, as the metal is used in GaAs
307 components, which offer superior performance compared to discrete circuits. Gallium is also
308 present in the printed circuit boards (PCBs) of various electronic devices, including printers,
309 mobile phones, computers, and other applications (Licht et al., 2015). Chancerel et al. (2013)
310 indicate that gallium concentrations in PCBs can range from 2 mg/kg to 140 mg/kg. However,

311 the recovery of gallium from EoL products is limited due to the complexity of integrated circuit
312 chips (Ueberschaar et al., 2017).

313 LEDs have become a popular choice in various applications, including lighting products and
314 backlighting systems for televisions, monitors, and other devices, mainly due to their long
315 lifespan and low energy consumption (Tan et al., 2009). The concentration of gallium in LEDs
316 ranges from 248 to 690 mg/kg and is typically assembled as GaAs, GaN, InGaN, or GaP,
317 depending on the type of LED (Chancerel et al., 2013; Nagy et al., 2017). Gallium is also used
318 in the manufacture of laser diodes, with GaN and GaAs being the most commonly used
319 materials. Laser diodes have a wide range of applications, such as in DVD, CD, and Blu-ray
320 players (Chancerel et al., 2013). Gallium is also found in the production of indium photovoltaic
321 systems, as described in Section 2.1, which are used in solar parks and buildings and supplied
322 to consumers with related products (Schmidt et al., 2019).

323 Gallium compounds (GaTe_x , AsN, GaAs) are used in various batteries, such as secondary
324 lithium batteries, nuclear batteries, and solar batteries (Hoang Huy et al., 2022). For example,
325 gallium can improve the specific capacity, efficiency, cycling, and overcharge resistance of
326 lithium batteries (Nishida et al., 1997; Patil et al., 2015). However, there is a lack of research
327 into the recovery of gallium from lithium batteries.

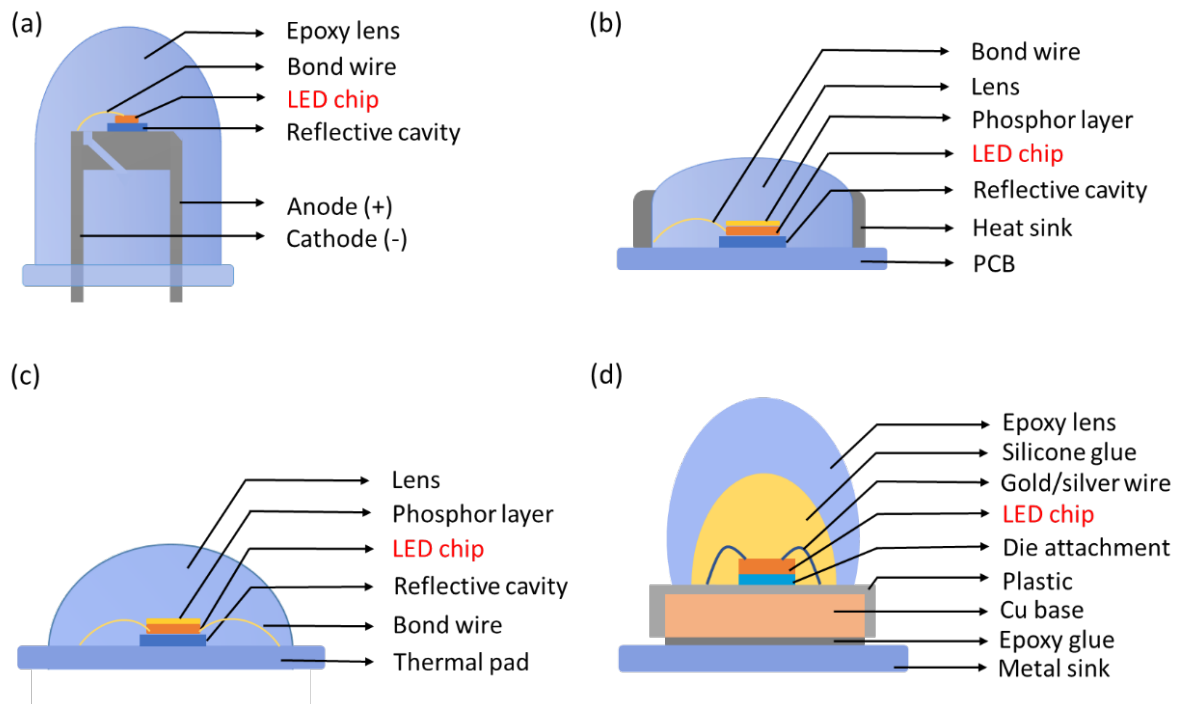
328 **2.2.1 LEDs as a secondary source of gallium**

329 The LED industry produces various types of LED chips, such as GaN, GaAs, InGaN, and GaP.
330 Waste from these materials contains indium and gallium, which can be recycled as a secondary
331 source for the manufacture of related electrical and electronic equipment. However, LEDs also
332 contain major and hazardous materials, including Fe, Cu, Al, Cr, Ni, Zn, Sn, Pb, Ba, and As
333 (Nagy et al., 2017; Pourhossein & Mousavi, 2018; Swain et al., 2015a and 2015b). Therefore,
334 the recycling process needs to carefully consider these factors.

335 Four common types of LEDs have been discussed, which offer essential data support that will
336 help us better understand how to pre-treat these devices and find effective ways to concentrate
337 the desired elements in future studies (Figure 4). The first type is a traditional dual in-line
338 package (DIP) LED, also known as a "pill" or "bullet" due to its shape, which can be easily
339 welded onto circuit boards. DIP LEDs are commonly used in accent tube lamps. The typical
340 structure of DIP LEDs is shown in Figure 4 (a). The second type is surface mounted device
341 (SMD) LEDs, which come in various shapes and sizes, such as SMD 3528 (size: 2.8×3.5 mm)
342 and SMD 5050 (size: 5.0×5.0 mm), and are commonly used in strip lights for decoration,
343 advertising, and backlighting. The basic structure of SMD LEDs is shown in Figure 4 (b). The

344 third type is chip-on-board (COB) LEDs, which consist of multiple diodes in a few individual
 345 modules. These LEDs are more advanced than DIP and SMD types and are used in street
 346 lighting and mobile phone cameras, as shown in Figure 4 (c). The final type is high-power (HP)
 347 LEDs, which can have an operating power of tens of watts (J/s). HP LEDs are designed for
 348 specific high lumen applications such as industrial facilities, mines, sports venues, and urban
 349 landscapes, as shown in Figure 4 (d).

350



351

352 Figure 4 Schematic of four different types of LEDs: (a) DIP LEDs, (b) SMD LEDs, (c) COB
 353 LEDs, and (d) HP LEDs. Modified from Hamidnia et al. (2018), Pourhossein & Mousavi,
 354 (2018), and Tan et al. (2009).

355

356 The critical component of an LED is the LED chip, which is responsible for converting
 357 electricity into light with different colors and brightness levels according to the user's needs.
 358 The LED chip is made up of three different layers that are connected to two electrodes (anode
 359 and cathode) and grown on a substrate, such as sapphire (Al_2O_3), as shown in Supplementary
 360 Material Figure S1. The LED chip utilizes materials such as GaN, GaAs, AlGaInP, or InGaN
 361 in its layers. These materials facilitate the generation of light emission when combined with
 362 electrons and holes (Hamidnia et al., 2018; Pimputkar et al., 2009; Tan et al., 2009; Yam &
 363 Hassan, 2005; Zhan et al., 2015).

364

365 2.2.2 PVs as a secondary source of gallium

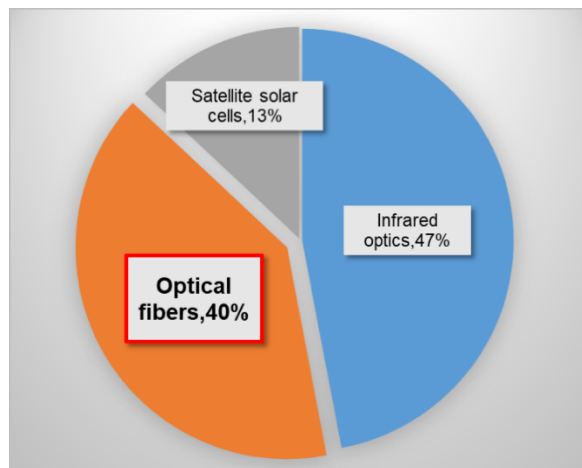
366 Photovoltaics (PVs), or solar cells, have become increasingly popular due to their low-emission
367 properties in response to the global warming problem (Amato and Beolchini, 2019). Second-
368 generation thin-film photovoltaics, including CIGS ($\text{CuIn}_x\text{Ga}_{(1-x)}\text{Se}_2$) PVs and GaAs PVs, have
369 replaced first-generation Si-based technology due to their superior performance and high
370 efficiency. While second-generation PVs currently account for only 10% of total PV electricity
371 production and 2% of CIGS PVs in 2017, they are expected to grow in popularity (Ma et al.,
372 2020; Schmidt et al., 2019). For example, gallium and indium are predicted to increase to 15-
373 20% and 15%, respectively, in CIGS PVs in the near future, and it has been reported that
374 gallium and indium may contain high concentrations in spent CIGS PVs, 530 mg/kg and 2,900
375 mg/kg, respectively (Gu et al., 2018). Therefore, from a long-term perspective, it is important
376 to recover these valuable elements from spent PVs, even if the retirement period of PVs has
377 not yet been reached (which is expected to be about 25 years) (Lv et al., 2019; Ma et al., 2020;
378 Savvilotidou and Gidarakos, 2020).

379 Supplementary Material Figure S2 presents the schematic structure of CIGS PV and GaAs PV.
380 The layers include the back contact layer (often molybdenum), an absorber layer
381 $\text{CuIn}_x\text{Ga}_{(1-x)}\text{Se}_2$ or CuInSe (CIS), a buffer layer (like CdS or emerging materials), and a
382 window layer (primarily ZnO with a multilayer antireflective coating) (Polman et al., 2016;
383 Schmidt et al., 2019; Tang, 2017). GaAs PVs share a similar structure, with n-type GaAs and
384 p-type $\text{Al}_{0.3}\text{Ga}_{0.7}\text{As}$ layers surrounded by AlInP windows for protection (Kim et al., 2022;
385 Polman et al., 2016). This information provides essential insights for dismantling devices and
386 concentrating desired elements in future studies.

387 2.3 End-of-life products as a secondary source of germanium

388 EoL products can be a secondary source of germanium, as shown by studies on the global
389 distribution of EoL products in Figure 5. From 2012 to 2016, a total of 122.6 tonnes of
390 germanium was supplied for manufacturing. The EU accounted for 32% of total germanium
391 consumption, with 38.7 tonnes used for three main manufacturing applications: 47% for
392 infrared optics, 40% for optical fibers, and 13% for satellite solar cells (European Commission,
393 2020). Furthermore, in the United States, optical fibers accounted for 40% of germanium use,
394 followed by 30% in infrared optics, 20% in electronics and solar applications, and 10% in other
395 uses, where germanium is not used in polymerization catalysts (Chen et al., 2018b; Rosenberg,
396 2009).

397



398

399 Figure 5 Main uses of germanium in the EU. Modified from Critical Raw Materials Factsheets
 400 (European Commission, 2020).

401

402 Table 2 shows that the EoL products could be used as a secondary source of germanium. OFs
 403 contain various types of flexible and transparent fibers, which typically contain a core
 404 surrounded by transparent cladding to transmit the information as light pulses (Rosenberg,
 405 2009). OFs are an important source of germanium because they contain germanium oxide
 406 (GeO_2) as a dopant to prevent electromagnetic interference, light absorption, and optical losses.
 407 Germanium is used because it has similar atomic and ionic radii compared to SiO_2 , which helps
 408 to modify the refractive index and achieve lower optical losses (Licht et al., 2015; Rosenberg,
 409 2009). OFs are used as a medium for communication, sensing, and power transmission (Gunn,
 410 2014). The concentration of germanium in spent OFs can be as high as 1,100 mg/kg (Ruiz et
 411 al., 2018).

412 Infrared (IR) optics also contain germanium due to its higher refractive index, transparency and
 413 optical uniformity, and low dispersion (Gunn, 2014; Rosenberg, 2009). GeCl_4 is used in the
 414 fields of night vision systems, optical instruments, IR spectroscopy, IR detectors, active vehicle
 415 safety systems, satellite systems, and fire alarms (Gunn, 2014; Nguyen & Lee, 2021).

416 Germanium is also used as a catalyst in polymerization, mainly in the production of
 417 polyethylene terephthalate (PET) and synthetic textile fibers production. GeO_2 is incorporated
 418 into PET products to produce colourless final product compared to other catalysts, such as
 419 titanium and antimony (Gunn, 2014).

420 In electronics and solar applications, germanium is used as a semiconductor and applied for
 421 germanium-based wafers are used in wireless devices, optical communication systems, hard
 422 disk drives, GPS, transistors, rectifiers, lasers, and space-based PV solar cells (Gunn, 2014;
 423 Licht et al., 2015; Rosenberg, 2009).

424 Germanium semiconductors have higher speed and lower energy consumption than silicon
425 semiconductors, making them an attractive option for optoelectronic and electronic
426 applications. Germanium is also used as a catalyst in fluorescent lamps, diodes, and transistors,
427 and as a crystal in X-ray detectors, which are thicker and more sensitive than silicon detectors
428 (Gunn, 2014; Rosenberg, 2009).

429 In summary, OFs, which account for 40% of total germanium consumption in the EU, contain
430 a higher concentration of germanium and are easier to collect and pre-treat than other
431 germanium-containing EoL products. Therefore, several studies have described the recovery
432 of germanium from OFs.

433 **2.3.1 OFs as a secondary source of germanium**

434 Supplementary Material Figure S3 shows the typical structure of OFs, which are a potential
435 source of germanium as they contain a small amount of germanium in their core. The core of
436 OFs consists of pure silica glass with GeO₂ added as a dopant to improve the optical properties
437 (European Commission, 2020; Nguyen & Lee, 2021). OFs consist of fiber bundle tubes,
438 reinforcements, and plastic sheaths, with the fiber bundle tubes consisting of acrylic resin
439 coating and fiber optic (Zhang et al., 2019). X-ray fluorescence (XRF) analyses have shown
440 that OFs contain 99% silicon and less than 1% germanium (Chen et al., 2020; Zhang et al.,
441 2019). However, the concentration of germanium (> 1000 mg/kg) in OFs can be higher than
442 that in primary sources such as coal and sulfide ores. Therefore, OFs are a potential secondary
443 source of germanium, and several studies have focused on the recovery of germanium from
444 spent OFs (Chen et al., 2017; Ruiz et al., 2018).

445 **3 The recovery of indium, gallium, and germanium from end-of-life** 446 **products**

447 The recovery of indium, gallium, and germanium from EoL products is currently carried out
448 using different technologies such as pyrometallurgy, hydrometallurgy, and biohydrometallurgy.
449 Pyrometallurgy, which operates at high temperatures and generates high energy costs and toxic
450 gas emissions, is not discussed in this review (Savvilotidou et al., 2015). However,
451 hydrometallurgical and biohydrometallurgical technologies, which are considered to have
452 better performance, have been reviewed in detail.

453 The hydrometallurgical approach is probably one of the most advanced ways to recover indium,
454 gallium, and germanium from EoL products because this process has the advantages of being
455 versatile, flexible, and highly efficient (Akcil et al., 2019; Sethurajan et al., 2019). In this

456 process, the target products are leached after e-waste pre-treatment with mineral and organic
457 acids, followed by selective recovery of dissolved TCEs from generated leachates by solvent
458 extraction, solid phase extraction, precipitation, cementation, electrochemical
459 separation/electrowinning, or supercritical fluid extraction. However, due to the stringent
460 conditions generated during leaching, highly complex leaching solutions in terms of elemental
461 composition require multiple purification steps to remove unwanted elements, such as iron,
462 among others prior to any selective recovery of the target elements (Erüst et al., 2013;
463 Nancharaiah et al., 2016; Sethurajan et al., 2018; Yu et al., 2020).

464 The influencing parameters for indium, gallium, and germanium recovery are discussed in the
465 present paper. In the leaching process, the most important influencing parameters are pH, the
466 selection and concentration of leaching agent(s), the ratio of solid e-waste samples to liquid in
467 the leaching system, the particle size fraction of samples, reaction time, temperature, and
468 agitation rate (Akcil et al., 2019; Chen et al., 2017; de Oliveira et al., 2021; Fontana et al., 2020;
469 Mir et al., 2022; Tao et al., 2021). Thoughtful optimization of these parameters can exert a
470 profound influence on the dissolution and leaching yields of indium, gallium, and germanium.
471 For instance, a more acidic leaching system has been found to achieve higher indium leaching
472 yields. Similarly, smaller particle sizes, higher leachant concentrations, longer reaction times,
473 and elevated temperatures have shown favourable effects. However, it is essential to conduct
474 preliminary tests with complex pre-treated e-waste samples as different parameters may
475 interact differently. The establishment of optimal conditions often requires a combination of
476 various favourable parameters. In contrast, in the recovery process, factors influencing
477 extraction efficiency include the choice of extracting agents, metal ion concentration in the
478 leaching solution, extraction temperature and duration, and the distribution ratio between
479 phases (Akcil et al., 2019; Chen et al., 2017; de Oliveira et al., 2021; Fontana et al., 2020; Mir
480 et al., 2022; Tao et al., 2021). Proper optimization of these factors is also crucial for effectively
481 recovering indium, gallium, and germanium from the leaching solution. The determination of
482 optimal conditions may vary depending on the specific e-waste leachate composition,
483 necessitating also to perform preliminary tests with different parameter combinations.

484 The biohydrometallurgical approach uses microorganisms to convert insoluble TCEs into their
485 dissolved forms and then selectively recover soluble metal ions from leachates (Nancharaiah
486 et al., 2016). The bioleaching process can take place via the acidolysis, complexolysis, or
487 redoxolysis processes. The biorecovery process, such as bioprecipitation, biosorption,
488 bioreduction, or bioaccumulation, have been widely used to recover target metals from dilute
489 solutions (Nancharaiah et al., 2016; Sethurajan et al., 2018). The key influential parameters
490 include microbial activity and adaptation, environmental conditions (i.e. pH and temperature),

491 and substrate concentration (i.e. minerals and nutrients). These kinetic factors determine the
492 recovery rates of target metals. In recent years, biohydrometallurgy has been considered as a
493 promising and green technique to recover and recycle TCEs from e-waste due to its superior
494 value of selectivity, friendly environment, cost-effectiveness, and non-toxic reagents (Dodson
495 et al., 2012; Işıldar et al., 2019; Sethurajan et al., 2018). However, the development of
496 biohydrometallurgy protocols to recycle TCEs from EoL products such as LCDs, LEDs, PVs,
497 and OFs is still in its infancy and requires in-depth attention before full-scale implementation.

498 **3.1 Kinetic study**

499 In the process of recovering indium, gallium, and germanium from EoL products, various
500 hydrometallurgical recovery approaches are utilized. These methods include complex chemical
501 reactions and mass transfer processes. This part aims to provide illustrations of leaching and
502 recovery methods to explore their principles and emphasize the significance of kinetic studies.
503 The biohydrometallurgical routes are not addressed here, as specific explanations will be
504 provided in the sections “Indium/Gallium bioleaching” and “Indium/Gallium biorecovery”.

505 **3.1.1 Kinetic studies of the leaching step**

506 Strong acids such as hydrochloric acid, sulfuric acid, and mixed strong acids are commonly
507 utilized for the purpose of dissolving indium, gallium, and germanium from EoL products into
508 solution via an acidolysis process (Chen et al., 2018b; Gabriel et al., 2020; Hu et al., 2014;
509 Maarefvand et al., 2020). Furthermore, the addition of catalysts such as oxidants like MnO₂
510 and H₂O₂ has been shown to accelerate reactions and enhance dissolution efficiency via a
511 redoxolysis process (Swain et al., 2016a; Zeng et al., 2015; Zhang et al., 2021). The mechanism
512 of strong acid leaching involves the dissolution of metal ions within an acidic environment
513 facilitated by H⁺ ions. Additionally, hydrofluoric acid is working for the dissolution of
514 germanium from silicate glass matrices (W. Chen et al., 2017).

515 Organic acids such as oxalic acid are also utilized for the recovery of indium and gallium via a
516 complexolysis process. These organic acids can be involved in chelation reactions with metal
517 ions, forming soluble complexes (Cui et al., 2019). For instance, indium ions (In³⁺) can form
518 complexes with carboxyl groups in oxalic acid, resulting in complexation. The higher solubility
519 of these complexes allows for the transfer of indium ions from e-waste to the solution.

520 In these leaching processes, the significance of kinetic studies lies in the profound
521 comprehension of reaction rates and mechanisms. This understanding helps in optimizing
522 operational conditions, thus enhancing metal recovery rates and purity. By regulating reaction

523 conditions such as acid concentration, reaction temperature, solid-liquid ratio, particle size of
524 samples, reaction and agitation time, and catalysts, more efficient transformations and
525 dissolution of metal ions can be achieved. Moreover, kinetic studies contribute to a deeper
526 understanding of the interaction between strong mineral and organic acids with metal ions,
527 ultimately leading to improved recovery efficiency.

528 **3.1.2 Kinetic studies of the recovery step**

529 In solvent extraction methods, the transfer of substances between organic and aqueous phases
530 relies on chelation reactions between extractants and metal ions. For instance, bis(2-ethylhexyl)
531 phosphoric acid as an organic phase extractant can engage in chelation reactions with indium
532 ions, forming complexes (Gupta et al., 2007; Virolainen et al., 2011; J. Yang et al., 2013).
533 Kinetic studies examine the coordination of the extractant with metal ions and the rates of
534 chelation reactions. Subsequently, stripping involving the use of strong acids such as HCl can
535 redissolve metal ions previously complexed in the organic phase, facilitating the purification
536 and refinement of indium.

537 Ionic liquid extraction methods employ ionic liquids as the organic phase to form chelation
538 complexes with metal ions, achieving separation and extraction. For instance, phosphonium
539 ionic liquid (i.e. Cyphos IL 104) can form complexes with indium ions (Dhiman & Gupta,
540 2020). Kinetic studies focus on the structure of ionic liquids and the rates of chelation reactions
541 with metal ions. The stripping process similarly employs strong acids (i.e. HCl) to dissolve
542 metal ions from previously formed complexes in the organic phase, enabling further
543 purification.

544 Solid-phase extraction (ion exchange) employs ion exchange resins with specific functional
545 groups to adsorb and separate metal ions. For instance, Amberlite™ resin can adsorb indium
546 ions, and kinetic studies centred around adsorption rates and resin performance (Ferella et al.,
547 2016). The stripping process similarly employs strong acids (i.e. H₂SO₄) to dissociate indium
548 ions from the resin, laying the foundation for subsequent purification steps.

549 Precipitation methods rely on chemical reactions to generate hydroxide precipitates for metal
550 ion recovery. Adjusting pH using NH₄OH and precipitate Na₂S, for instance, can lead to indium
551 precipitation (Fang et al., 2019; Hu et al., 2014; Silveira et al., 2015). Kinetic studies focus on
552 precipitation rates and the effects of conditions. In this process, metal ions combine with
553 hydroxide ions and sulfide ions to form solid precipitates, which can be obtained through
554 filtration or precipitation separation techniques.

555 Additionally, cementation is a chemical process involving the deposition of one metal onto the
556 surface of another metal to achieve separation and extraction. Through contact with zinc
557 powder, indium ions undergo reduction reactions, successfully recovering indium (Rocchetti
558 et al., 2016). Kinetic studies observe reduction rates and reaction mechanisms. This process
559 involves the reduction and deposition of metal ions on a metal surface, with kinetic studies
560 contributing to the optimization of operational conditions for enhanced recovery efficiency.

561 Electrowinning involves the reduction of metal ions to metal through electrochemical reactions,
562 generating metal precipitates in the electrolyte. Indium ion recovery, for example, can be
563 achieved through low-current electrolysis (D. Choi et al., 2014). Kinetic studies focus on
564 electrolysis rates and electrode reaction mechanisms. During electrolysis, metal ions are
565 reduced to metal on the electrode surface, forming solid deposits and thus enabling successful
566 recovery.

567 Supercritical fluid separation leverages the properties of supercritical fluids to separate and
568 extract target substances from solid samples or liquid mixtures (Argenta et al., 2017; Zhan et
569 al., 2020). The combination of supercritical CO₂ and co-solvents has been demonstrated to
570 enhance the efficiency of recovery reaction kinetics, aiding in the transformation of indium
571 from a solid state to a soluble ionic state (Argenta et al., 2017). Kinetic studies emphasize the
572 solubility of supercritical fluids and the rates of chelation reactions. Under supercritical
573 conditions, fluid density, and solubility change with variations in temperature and pressure,
574 and kinetic studies contribute to a better understanding of these influencing factors.

575 Through these specific recovery method examples, we gain deeper insights into the principles
576 and kinetic characteristics of each technique, thereby providing more precise guidance and
577 understanding for optimizing the recovery process. These kinetic studies not only uncover the
578 behavior of metal ions in different methods but also provide robust scientific foundations for
579 achieving efficient metal recovery. Simultaneously, these studies offer crucial clues for
580 controlling operational conditions, enhancing recovery rates, and ensuring purity.

581 **3.2 Indium recovery from EoL LCDs via hydrometallurgical and biohydrometallurgical** 582 **routes**

583 **3.2.1 Pre-treatment of EoL LCDs**

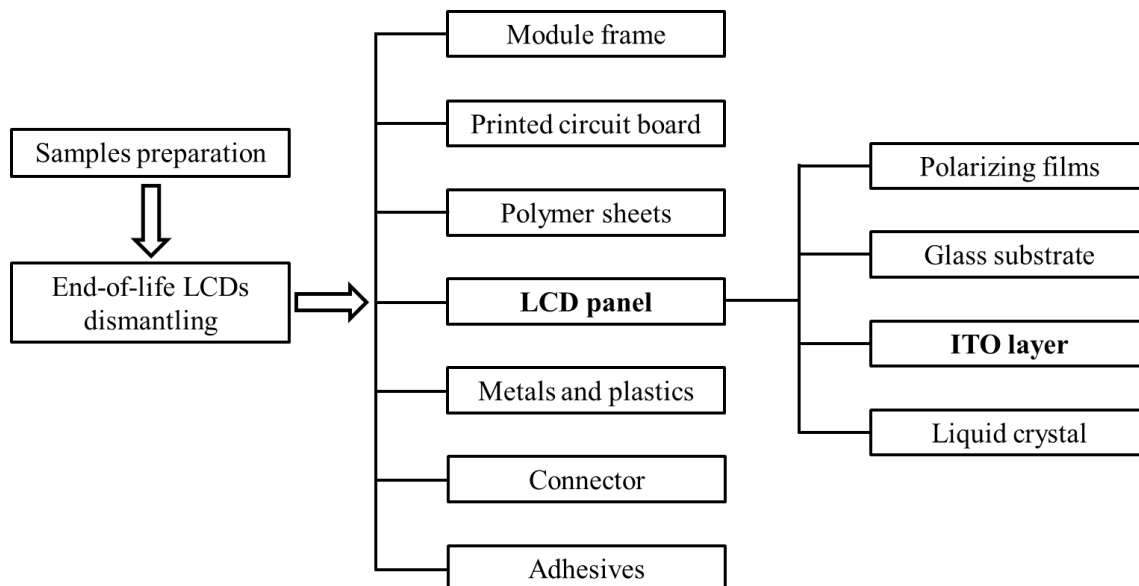
584 **3.2.1.1 Manual dismantling of LCDs to access the ITO film**

585 Pre-treatment of end-of-life LCDs involves dismantling and separating valuable parts, such as
586 the LCD panel, from other parts, such as the module frame, printed circuit board, polymer

587 sheets, metal and plastics, connectors, and adhesives. The first step is to manually disassemble
588 the LCDs to access the ITO film layer (Figure 6).

589

590



591

592 Figure 6 Manual dismantling of spent LCDs

593

594 3.2.1.2 Removing polarizing films and liquid crystals

595 After manual disassembly, polarizing films and liquid crystals should be removed from the
596 LCD panel in the next pre-treatment step (Cui et al., 2020; Danilo Fontana et al., 2015).
597 Polarizing films generally consist of a layer of iodine-doped polyvinyl-alcohol (PVA)
598 sandwiched between two protective layers of cellulose triacetate (TAC) (Dodson et al., 2012).
599 In addition, the removal of organic materials of PVA and TAC from LCD panels is required
600 for more efficient grinding of LCD panels (Silveira et al., 2015). Therefore, thermal and
601 chemical treatments were tested to remove polarizing films from previous studies, as shown in
602 Table 3.

603 The optimal method for removing polarizing films is thermal treatment (Ferella et al., 2016;
604 Fontana et al., 2015; Lee et al., 2013; Li et al., 2009; López-Yáñez et al., 2019; Savvilotidou
605 et al., 2015). As detailed in Ferella's study, thermal treatment with liquid nitrogen does not
606 damage the surface of LCD glass, and liquid crystals are cleaned using ultrasound (Ferella et
607 al., 2016; Fontana et al., 2015). In addition, Li et al. (2009) reported that thermal shock at 230-

608 240 °C could be used to remove up to 90 wt% of the polarizing film. Ultrasonic treatment was
 609 then used to remove liquid crystals (10 min of 40 kHz (P = 40W)).

610 Based on the energy consumption and pollutant emission of thermal treatment, chemical
 611 treatment has also been proposed to remove polarizing films and liquid crystals (Cui et al.,
 612 2020; Fontana et al., 2015; Silveira et al., 2015; Wei et al., 2016). Without heating, a longer
 613 treatment time (i.e. 20 h) is required to remove polarizing films with acetone (Silveira et al.,
 614 2015). Acetone in a hot water bath of 80-100 °C can reduce the reaction time to 35 min (Cui et
 615 al., 2020).

616 Savvilotidou et al. (2015) used a combination of thermal and chemical treatments to remove
 617 the polarizing films by implementing a thermal shock at 200 °C. It was observed that the
 618 polarizing film started to soften and bulge after 7 min, after which the glue and liquid crystals
 619 remaining on the panel were removed by acetone liquid. Since acetone is considered toxic, the
 620 polarizing films can be removed manually, but this task is time-consuming (Li et al., 2020;
 621 Zhang et al., 2017). It may not be necessary to remove the polarizing films prior to
 622 hydrometallurgical leaching (Assefi et al., 2018; Gabriel et al., 2020; Upadhyay et al., 2021).
 623 However, it is better to remove polarizing films and liquid crystals for biohydrometallurgy due
 624 to their physiological toxicity for microorganisms (Cui et al., 2020). Therefore, thermal
 625 treatment combined with ultrasound and acetone should be considered as a pre-treatment to
 626 remove polarizing films and liquid crystals from waste LCDs.

627

628 Table 3 The common methods of removing polarizing films and liquid crystals from spent LCD
 629 panels

Method	For polarizing films	For liquid crystals	Time	Reference
Thermal treatment	Liquid nitrogen	Ultrasonic treatment 35 kHz	10-20 min	(Fontana et al., 2015)
	230-240 °C	Ultrasonic treatment 40 kHz		(Li et al., 2009)
Chemical treatment	Acetone	Acetone	20 h	(Silveira et al., 2015)
	Water bath of 80-100 °C for 5-20 min and then acetone bath for 30 min		Total 35-50 min	(Cui et al., 2020)
Thermal and chemical	Thermal shock 200 °C for 7 min and then soaking in acetone		> 7 min	(Savvilotidou et al., 2015)
Others	Manually peeled	Acetone with 4 h	> 4 h	(Zhang et al., 2017)
	Manually peeled	Without treatment		(Li et al., 2020)

630

631 3.2.1.3 Comminution of LCD panels to obtain powder samples

632 Comminution methods of spent LCD panels reported in the literature over the last decade are
633 described in Table 4. In general, LCD panels are manually crushed to produce small pieces (3-
634 5 cm) that are easily ground into powder by mills (Gabriel et al., 2018, 2020; Jowkar et al.,
635 2018). The traditional method is ball milling, which has been studied by many researchers who
636 have investigated different parameters such as temperature and grinding time (Dhiman &
637 Gupta, 2020; Ferella et al., 2016; Gabriel et al., 2020; Jowkar et al., 2018; Silveira et al., 2015;
638 Yen et al. 2016). Silveira et al. (2015) compared three mills and found that a porcelain ball mill
639 was optimal for obtaining small particle sizes (average 150 μm) in 120 min with minimal
640 material loss (0.18 wt%) compared to knife and hammer mills. Other mills, such as cutting
641 mills, blade mills, planetary ball mills, ring mills, and rod mills can also be used. Ferella et al.
642 (2016) found that the rod mill was a good option to achieve a 52 wt% finest fraction (average
643 212 μm) with the highest indium concentration in 30 min. Yen et al. (2016) found that planetary
644 ball milling for 120 min at 300 rpm was required to achieve a particle size of about 96 μm ,
645 while Assefi et al. (2018) found that the ring mill could grind LCDs to powder with a particle
646 size of 10 μm within 1 min after grinding with a guillotine blade.

647 For a more efficient method, high-energy ball milling in a planetary ball mill with a jar and 5
648 mm balls made of ZrO_2 is performed within a short time of 1 min, obtaining LCD powder with
649 a minimum particle size of 7.5 μm (Lee et al., 2013; Qin et al., 2021; Zeng et al., 2015). The
650 LCD panel can also be crushed by a multi-function disintegrator at 31,000 rpm and achieve a
651 particle size of 250 μm , saving time up to 10 min (Xie et al., 2019). A high-speed crushing
652 shear is used to crush LCD panels for a short time of 5 min and achieve a smaller particle size
653 ($< 75 \mu\text{m}$) (Luo et al., 2019). These grinding methods significantly reduced the working time.
654 After obtaining the finer particle powder, the ground samples were dried in a vacuum oven (the
655 temperature range of 60-110 $^{\circ}\text{C}$) until a constant weight was reached (Ferella et al., 2016; Xie
656 et al., 2019).

657

Method	Operative parameters	Time	Particle size (μm)	References
Ball milling		4 h	< 37	(Jowkar et al., 2018)
Ball milling	Porcelain ball mill with 60 rpm	2 h	150	(Silveira et al., 2015)
Ball milling	Alumina ball with polarizing films	4 h	< 5	(Gabriel et al., 2020)
Ball milling	Rod ball with wet condition (water)	0.5 h	< 212 of 52 wt%	(Ferella et al., 2016)
Ball milling	Planetary ball mill with 300 rpm	2 h	96	(Yen et al., 2016)
Ring mill		1 min	10	(Assefi et al., 2018)
High energy ball milling	Planetary mill with a jar and balls of 5 mm size made of ZrO_2	1 min	7.5	(Lee et al., 2013)
High energy ball milling	Planetary mill with a jar and balls of 5 mm size made of ZrO_2	0.5 h	< 75 of 97.6 wt%	(Qin et al., 2021)
Multi-function disintegrator	31,000 rpm	10 min	250	(Xie et al., 2019)
High-speed crushing shear		5 min	< 75	(Luo et al., 2019)

659

660 3.2.1.4 Characterization methods of LCD samples

661 The collected LCD treated samples can be characterized using various qualitative and
662 quantitative methods (Table 5). X-ray diffraction (XRD) helps to identify the crystalline
663 mineral phases (Li et al., 2020; Luo et al., 2019; Zhang and Xu, 2016). Scanning electron
664 microscope (SEM) analyzes the surface structure and morphology (Cadore et al., 2019; Cui et
665 al., 2019; Li et al., 2020; Luo et al., 2019). Energy dispersive X-ray fluorescence spectrometer
666 (EDX) and energy dispersive spectrometer (EDS) analyze elemental composition (Maarefvand
667 et al., 2020; Yang et al., 2013), as well as X-ray fluorescence (XRF) analyses, provide
668 elemental compositions information (Ferella et al., 2016; Gabriel et al., 2020; Silveira et al.,
669 2015; Zeng et al., 2015). Field emission scanning electron microscopy (FE-SEM) and laser
670 light diffraction analyze the particle size of samples (Dhiman & Gupta, 2020; Gabriel et al.,
671 2020). X-ray photoelectron spectroscopy (XPS) analyzes binding energy and intensity (D. Choi
672 et al., 2014; Cui et al., 2019; Krishna Rama et al., 2015). Laser-induced breakdown

673 spectroscopy (LIBS) spectra and the parallel factor analysis (PARAFAC) model characterize
674 different elements (Castro et al., 2020). Instrumental Neutron Activation Analysis (INAA)
675 detects the concentration of metals in solid samples (Andrade et al., 2019). Brunauer-Emmett-
676 Teller (BET) theory gives the surface area of LCD powder according to gas sorption (Lee et
677 al., 2013).

678 Various methods have been employed to determine the precise concentration of different
679 elements in solid WEEE samples, including the common use of strong acids like aqua regia.
680 However, the analysis of WEEE demands suitable reference materials, which has been
681 addressed by Andrade et al. (2019) for printed circuit boards using dilute aqua regia (50% v/v)
682 with 1/100 of S/L ratio in the microwave system at 240 °C. Nonetheless, the application of this
683 method to LCDs is limited due to their different composition. Consequently, current
684 characterization techniques lack accuracy for the wide range of elements present in LCD waste,
685 necessitating the development of specialized techniques. Overcoming this limitation is crucial
686 for advancing our understanding of elemental composition and enhancing e-waste recycling.
687 In this context, further research and innovation are required to address these challenges.

688 Microwave plasma-atomic emission spectrometer (MP-AES), inductively coupled plasma-
689 optical emission spectrometer (ICP-OES), and inductively coupled plasma mass spectrometry
690 (ICP-MS) are then used to detect the concentration of metals in the leachate (Akcil et al., 2019;
691 Assefi et al., 2018; Cui et al., 2019; Yen et al., 2016; Zeng et al., 2015; Zhang et al., 2015).

692

E-waste	Characterization methods	Major elements	Reference
LCD screens	Alkaline fusion and analyzed by ICP-OES, XRD, and SEM	Sr, Co, Zn, Fe, Cu, and Ni	(Jowkar et al., 2018)
LCD screens	HNO ₃ -HCl-HF-H ₂ O ₂ (3:1:1:1, v/v) mixture digestion and analyzed by ICP-OES		(Xie et al., 2019)
Discarded LCD screens	Aqua regia method digestion and analyzed by MP-AES, FE-SEM, EDX, and XRD	Sn, Zn, Fe, Al, Mn, Ca, and Sr	(Dhiman and Gupta, 2020)
LCDs	Mixed acids (HNO ₃ , HCl) digestion and analyzed by ICP-MS		(Savvilotidou et al., 2015)
LCD screens of discarded cell phones	Aqua regia digestion, XRF, SEM and EDS	Si, Sr, Ca, Al, Ba, Sb, and Sn	(Silveira et al., 2015)
LCD panel glass	Aqua regia digestion and analyzed by ICP-OES, SEM, and EDX	Al, Fe, Zn, Sn, Mg, Ni	(Yang et al., 2013)
LCD monitors	XRF and laser light diffraction	Si, Al, Ca, As, K, Sn	(Gabriel et al., 2020)
LCD glass	XRF, XRD, SEM, EDS, FTIR, and ICP-AES	Si, Al, Ba, Sr, Ca, Fe, Mg	(Zeng et al., 2015)
LCD panels	SEM, XRD, XPS, XRF, and ICP-OES	Si, Al, B, Ca, Sr, Fe, Mg, Ba, Sn, Cr, Na, K and Cu	(Cui et al., 2019)
LCDs	SEM and XRD	Al	(Luo et al., 2019)

694

695 3.2.2 Indium leaching from EoL LCDs via hydrometallurgical and 696 biohydrometallurgical routes

697 Table 6 summarizes the techniques for indium leaching from spent LCDs using
698 hydrometallurgy and biohydrometallurgy as reported in the literature. In general, single strong
699 mineral acids, such as HCl, H₂SO₄, and HNO₃, are commonly used to leach elements from solid
700 samples (Ferella et al., 2016; Fontana et al., 2015; Gabriel et al., 2020; Pereira et al., 2018; Qin
701 et al., 2021; Silveira et al., 2015). The mixture of strong mineral acids has also been tested with
702 different concentration ratios and temperatures (Assefi et al., 2018; Lee et al., 2013; Li et al.,
703 2009; Savvilotidou et al., 2015). Organic acids, produced by microorganisms, including
704 bacteria and fungi from organic waste streams, have been reported as promising for the
705 recovery of indium from spent LCDs compared to conventional inorganic acids (Argenta et al.,
706 2017; Cui et al., 2019; Li et al., 2020; López-Yáñez et al., 2019). Oxidizing and reducing
707 chemical agents (i.e. H₂O₂ and MnO₂ as oxidants, and N₂H₄ as reductant) have been considered

708 in the mineral acid leaching process to increase the leaching reaction rate and improve the
 709 leaching yield of target metals (Dhiman & Gupta, 2020; López-Yáñez et al., 2019; Swain et al.,
 710 2016a; Zeng et al., 2015). Nevertheless, the recovery of target metals from leachates generated
 711 by strong inorganic acids or organic acids is complicated because many major elements have
 712 been dissolved in the low pH leachates. Therefore, selective leaching, such as bioleaching,
 713 produces less complex solutions that facilitate selective recovery steps (purification and
 714 separation) (Jowkar et al., 2018; Xie et al., 2019; Yang et al., 2013)

715

716 Table 6 Methods for indium leaching and bioleaching from spent LCDs

E-waste	Total In content (mg/kg)	Leachant	Optimum conditions (S/L: g/mL)	Leaching yield (%)	Other metals	Reference
Mineral acid leaching process						
LCD monitors	300	6 M HCl 0.5 M H ₂ SO ₄ 4 M HNO ₃	60 °C, 4 h; Room temperature, 2 h; 4 M HNO ₃ , 60 °C, 4 h	99.3% 98.2% 87%	Si, Al, Ca, As, K, and Sn	(Gabriel et al., 2020)
LCD glass	260	6 M HCl	1/3 of S/L, 25 °C, without shredding, 6 h	90%	Sn, Al, and Cr	(Fontana et al., 2015)
LCDs (non- crushing)	120	0.8 M HCl	300 W ultrasonic waves at room temperature, 1 h	96.8%	Al, Fe, In, Ca, Mg, Sr, and Mo	(Zhang et al., 2017)
LCDs	330	3 M HCl	1/2 of S/L, 0.5 h	70%	Al, Ca, Fe, Zn and Cu	(Yen et al., 2016)
LCDs of mobile phone		1 M H ₂ SO ₄	1/20 of S/L, 90 °C, 500 rpm agitation, 1 h	96.7%	Sn	(Pereira et al., 2018)
LCD panels		1 M H ₂ SO ₄	1/10 of S/L, 80 °C, 3 h,	100%	Al, Si, Fe, Sn, Zn, and Cr	(Ferella et al., 2016)
LCD screens of cell phones	0.614% (XRF)	1 M H ₂ SO ₄	1/50 of S/L, 90 °C, 500 rpm agitation, 1 h	96.4%	Si, Sr, Ca, Al, Ba, Sb, and Sn	(Silveira et al., 2015)
LCD panels	100	2 M H ₂ SO ₄	1/5 of S/L, 80 °C, 10 min	50%-90%	Al, Ca, Fe, Mn, Mo, and Sn	(Rocchetti et al., 2015)

LCDs	530	3:2 of HCl: H ₂ O	1/5 of S/L, 80 °C, mild agitation, 1 h	60%	As and Sb	(Savvilitid ou et al., 2015)
LCD panels	261	45:5:50 of 38%HCl:69% HNO ₃ :H ₂ O	1/1 of S/L, 0.5 h	86%	Sn	(Lee et al., 2013)
LCD panels	156	0.4 M H ₂ SO ₄	1/2 of S/L, 70 °C, 0.5 h	99.5%		(Houssaine Moutiy et al., 2020)
LCD panels	30	Aqua regia of 3 M HCl and 0.5 M HNO ₃	1/1 of S/L, 70 °C, ultrasonic wave, 0.5 h	99.5%		(Assefi et al., 2018)
Discarde d LCD screens		3 M HCl with oxidant 30 % H ₂ O ₂	75 °C, 400 rpm agitation, 2 h	98.7%	Sn, Zn, Fe, Al, Mn, Ca, and Sr	(Dhiman and Gupta, 2020)
LCD glass		5 M HCl with oxidant 10 % H ₂ O ₂	1/2 of S/L, 75 °C, 400 rpm agitation, 2 h	44%	Sn	(Swain et al., 2016a)
LCD glass	In ₂ O ₃ 0.057% (XRF)	3 M HNO ₃ with oxidant 1 g MnO ₂	3/1000 of S/L, 50 °C with particle size < 75 µm, 3 h	92.6%	Si, Al, Ba, Ca, Fe, Mg, Cr, As and Ni	(Zeng et al., 2015)
Organic acid leaching process						
LCD panels	576	0.5 M Oxalic acid	1/20 of S/L, 70 °C, 45 min	100%	Si, Al, B, Ca, Sr, Fe, Mg, Ba, Sn, Cr, Na, K and Cu	(Cui et al., 2019)
LCD screens	535	0.2 M Oxalic acid	3/10 of S/L, 90 °C, stirring at 500 rpm, 10 min with particle size <74 µm	100%	Cr, Mg, Fe, Ba, Sr, and Ca	(Li et al., 2020)
LCD screens of cell phones	602	1 M Citric acid with 5% H ₂ O ₂ 1 M Malic acid with 5% H ₂ O ₂	1/20 of S/L, 90 °C, 2 h	74.5% (citric acid); 70.9% (malic acid)		(Argenta et al., 2017)
Waste LCD panels		1 M Citric acid with reductant 0.2 M N ₂ H ₄	1/50 of S/L, pH = 5, 16.6 h	98.9%		(López- Yáñez et al., 2019)

Bioleaching process						
LCD screens	405	Adapted <i>A. thiooxidans</i>	4/25 of S/L, pH 2.6, initial 8.6 g/l of sulfur, within 15 days	100%	Sr, Co, Zn, Fe, Cu, and Ni	(Jowkar et al., 2018)
LCD screens	300	<i>A. thiooxidans</i>	3/200 of S/L, pH 2, 10 g/L sulfur and a 10% bacterial suspension	100%	B, Al, Mg, Fe, Ba, Sn, Cr, As	(Xie et al., 2019)
Mobile phone touch screen	69	Adapted <i>A. ferrooxidans</i>	1/4 of S/L, pH 2, 2% (v/v) inoculums, 10 days	100%	Al, Sr, Mn	(Rezaei et al., 2018)
LCD panels	0.0906 % (XRF)	mixed culture of <i>A. ferrooxidans</i> and <i>A. thiooxidans</i>	1/100 of S/L, iron, and sulfur medium inoculated with mixed bacteria	94.7 % after 35 days	Sn, Cu, Pb, Al	(Willner et al., 2022)
Indirect bioleaching-based process						
LCD panels	580	<i>Aspergillus niger</i>	Fermentation broth with pH 4, 125 rpm, 50 g/L of sucrose for 15 days, 70 °C with 1.5 h of leaching	100%	Al, Ca, Sr, Fe, Mg, Ba, Sn, Cr	(Cui et al., 2021)

717

718 3.2.2.1 Indium leaching with strong mineral acids

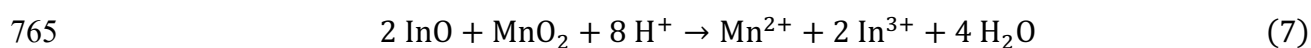
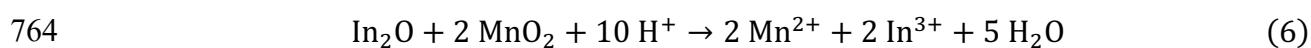
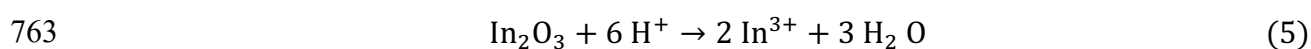
719 Strong mineral acids have been tested for the leaching of indium from waste LCDs using HCl,
720 HNO₃, and H₂SO₄. According to Gabriel et al. (2020), HCl and H₂SO₄ were found to be more
721 effective than HNO₃, with the best indium leaching yield obtained using 6 M HCl at 60 °C
722 within 4 h, resulting in a 99.3% indium leaching yield. At the same time, the 0.5 M H₂SO₄
723 leaching process can also leach 98.2% of the total indium at room temperature in 2 h. However,
724 the leaching efficiency of indium with HNO₃ was found to be lower, dissolving less than 50%
725 of the indium in the leachate. Similar results have been reported by other researchers comparing
726 the leaching of indium with strong mineral acids (HCl, HNO₃, and H₂SO₄) (Fontana et al., 2015;
727 Yang et al., 2013). The reaction of indium oxide with HCl is the fastest, and the reaction with
728 HNO₃ is the slowest (Gabriel et al., 2020; Yang et al., 2013). The amount of indium dissolved
729 in 6 M HCl takes 2 h to reach an equilibrium value, while the reactions with HNO₃ and H₂SO₄
730 take twice as long to reach the same situation (Yang et al., 2013). HCl as a reagent for indium
731 leaching from EoL products helps to limit the dissolution of non-target metals (i.e. Mo), thus
732 contributing to the reduction of metal impurities in the leaching solution (Zhang et al., 2017).

733 On the other hand, leaching with H₂SO₄ shows the best potential for indium leaching from EoL
734 products in terms of economic aspects, energy consumption, and corrosiveness (Ferella et al.,
735 2016; Gabriel et al., 2020; Pereira et al., 2018; Silveira et al., 2015). Ruan et al. (2012) also
736 reported that the use of H₂SO₄ to leach indium from LCDs could reduce the dissolution of toxic
737 arsenic, which is also present in LCDs.

738 Indium leaching from EoL products has also been investigated using different acid mixtures,
739 such as HCl mixed with HNO₃ and HCl mixed with H₂SO₄ (Lee et al., 2013; Savvilotidou et
740 al., 2015). It was reported that HCl mixed with HNO₃ was an effective method at high
741 temperatures, while HCl mixed with H₂SO₄ had lower indium leaching capacity due to the
742 lower activity of H₂SO₄ (Assefi et al., 2018; Lee et al., 2013; Li et al., 2009; Savvilotidou et
743 al., 2015). In addition, Li et al. (2009) reported that a strong oxidative acid, such as HNO₃,
744 mixed with another strong acid, such as HCl, can accelerate the dissolution of indium. However,
745 a mixture of strong oxidative acids and strong acids could contribute to the formation of Sn
746 black precipitate (SnO), which was found to affect the extraction of indium.

747 Increasing the reaction temperature by reacting with ultrasonic waves was found to improve
748 the leaching efficiency of indium (Ferella et al., 2016; Silveira et al., 2015; Zhang et al., 2017).
749 It was reported that single and mixed acid leaching combined with ultrasonic waves improved
750 the indium leaching yield (more than 95%) due to the combination of energy input and
751 percussion. In addition, the ultrasonic waves allow the solution to undergo convective motions
752 that bring fresh H⁺ to the surface of the solid and remove metal ions. Another advantage of this
753 approach is that non-target metals from spent LCDs were rarely affected by ultrasonic agitation
754 (except for In and Al).

755 Oxidants, such as H₂O₂ and MnO₂, were also tested with the aim of increasing the indium
756 leaching efficiency (Dhiman and Gupta, 2020; Swain et al., 2016a; Zeng et al., 2015). When
757 the leaching process was tested using 3 M HCl and 1 M 30% H₂O₂ as oxidant, under magnetic
758 stirring at 400 rpm for 2 h, 98.7% of the total indium was leached (Dhiman and Gupta, 2020).
759 To improve the indium leaching efficiency and avoid undesirable side-stream reactions such
760 as the formation of toxic Cl₂, the addition of MnO₂ as an oxidant to the leaching solution limits
761 the galvanic interaction of indium oxides (In₂O and InO) (Zeng et al., 2015). The related
762 reactions of In₂O₃, In₂O and InO are as follows:



766 Considering the low concentration of indium in the leachate with a single leaching step, the
767 concentrated technique of the multistep leaching approach (the same leachate for leaching fresh
768 waste samples in the multi-steps) was used in LCDs to achieve quantitative leaching. Rocchetti
769 et al. (2015) tested six steps of the above approach to leach indium from spent LCDs. In the
770 fifth step, the concentration of indium in the leachate reached almost 3 times (117 mg/L) that
771 of the first step using 2 M sulfuric acid at 80 °C for 10 min (each step). Although this method
772 can concentrate indium in the leachates to save reagents and reduce CO₂ emission, it does not
773 achieve a good leaching yield, which reaches about 50% after the sixth step. Therefore, other
774 techniques were tested for indium leaching with a low concentration, such as the use of organic
775 acids.

776 3.2.2.2 Indium leaching with organic acids

777 Organic acids have been used for indium leaching from EoL products because they are milder,
778 more selective, less toxic, more biodegradable under aerobic and anaerobic conditions, and
779 easier to control during metal extraction than mineral (Argenta et al., 2017; Cui et al., 2019;
780 Fontana et al., 2020; Li et al., 2020). Oxalic acid has shown good leaching efficiency and has
781 been used for indium leaching from LCDs because this organic acid can maintain the proton
782 concentration level to ensure efficient indium dissolution while limiting the dissolution of other
783 non-target metals (Cui et al., 2019). Cui et al. (2019) reported that indium leaching yield could
784 reach 100% with 0.5 M oxalic acid at an S/L ratio of 1/20 g/mL at 70 °C in 45 min. Li et al.
785 (2020) proposed a method using a temperature-controlled acidic stirred reactor with oxalic acid,
786 which could improve the leaching efficiency and reduce the consumption of oxalic acid
787 compared to the study by Cui et al. (2019). Citric and malic acids were also used to leach
788 indium from discarded LCD screens, and nearly 76.5% of indium was extracted after 3 h with
789 a S/L ratio of 1/20 g/mL at 70 °C (Argenta et al., 2017). In addition, the addition of the oxidant
790 H₂O₂ and reductant N₂H₄ to the media can further improve the leaching yield, as shown in
791 previous research on strong mineral acids (Argenta et al., 2017; López-Yáñez et al., 2019).

792 3.2.2.3 Indium bioleaching

793 Bioleaching is considered a promising approach for leaching indium from WEEE due to the
794 abundance and versatility of microorganisms. This technique has the advantage of being low-
795 cost and environmentally friendly (Jowkar et al., 2017; Ogi et al., 2012; Pennesi et al., 2019;
796 Xie et al., 2019). However, few biological studies are related to indium leaching from e-waste.
797 Microorganisms such as *Acidithiobacillus ferrooxidans* (*A. ferrooxidans*), *Acidithiobacillus*
798 *thiooxidans* (*A. thiooxidans*), and *Aspergillus niger* fermentation broth have been reported to

799 reach 100% indium leaching yield. Jowkar et al. (2018), who published the first report on
800 indium bioleaching using the acidolysis mechanism, involved adapted *A. thiooxidans* from
801 LCDs, resulting in a 100% indium leaching yield. The main reaction involves the acidolysis by
802 the biogenic sulfuric acid produced by bioleaching bacteria (Sethurajan et al., 2018). In addition,
803 Xie et al. (2019) also reported that the use of *A. thiooxidans* could accelerate the leaching rate
804 of indium with a S/L ratio of 3/200 g/mL at pH 2 in the presence of 10 g/L sulfur and a 10%
805 bacterial suspension. In the work of Rezaei et al. (2018), indium could also be leached from
806 the touch screen of the mobile phone using adapted *A. ferrooxidans* with a 100% leaching yield
807 within 10 days. The involved bioleaching mechanism can be classified as redoxolysis, wherein
808 *A. ferrooxidans* catalyzes the oxidation of ferrous (Fe^{2+}) to ferric ions (Fe^{3+}). Subsequently, the
809 ferric ions further oxidize target insoluble metals, converting them into soluble metals
810 (Sethurajan et al., 2018). Furthermore, Willner et al. (2022) demonstrated that mixed bacteria
811 of *A. ferrooxidans* and *A. thiooxidans* inoculated with iron and sulfur medium could achieve a
812 high leaching yield of both indium (94.7%) and tin (98.2%). *Aspergillus niger* fermentation
813 broth has also been explored for indium recovery from waste LCDs through an indirect
814 bioleaching-based process, and indium bioleaching exhibited a significant achievement with a
815 100% yield of indium attained within a short time (1.5 h at 70 °C) (Cui et al., 2021). The
816 primary reaction mechanism involves the production of organic acids using bacteria
817 *Aspergillus niger*, which subsequently release H^+ from acidic functional groups of organic
818 acids and proteins of fermentation broth, facilitating bioleaching of indium. While there are
819 relatively few studies related to bioleaching and indirect bioleaching-based approaches for
820 indium from e-waste, the potential for exploring new bacteria and improving the efficiency of
821 these processes makes them an area of ongoing interest for researchers in the field.

822 **3.2.3 Indium recovery from EoL LCDs by hydrometallurgical and** 823 **biohydrometallurgical routes**

824 Table 7 summarizes the major techniques tested for indium recovery from spent LCD leachates
825 generated by hydrometallurgical and biohydrometallurgical approaches. These techniques,
826 including solvent extraction, ionic liquid extraction, solid-phase or ion-exchange extraction,
827 precipitation, cementation, electrowinning, supercritical fluid separation, and biorecovery,
828 have been tested and achieved good recovery yields when implemented under optimal
829 conditions.

830

831

832 Table 7 Methods for indium recovery from spent LCD leachates

E-waste	Method of extractant	Initial In content (mg/L)	Optimum conditions (O/A: organic and aqueous phase ratio; S/L: g/mL)	Recovery yield	Other metals	Reference
Solvent extraction						
LCD panel glass	DEHPA for extraction and HCl for stripping	200 in H ₂ SO ₄ leachate	0.1 M DEHPA diluted in kerosene, 1 M HCl, 1/1 of O/A, 1500 rpm agitation, 10 min	99% (90% of purity)	Al, Fe, Zn, and Sn	(Yang et al., 2013)
LCD screen wastes	DEHPA for extraction and HCl for stripping	740 in H ₂ SO ₄ leachate	1.5 M HCl		Sn	(Virolainen et al., 2011)
TFT-LCD scrap	D ₂ EHPA for extraction and HCl for stripping	30.2 in H ₂ SO ₄ leachate	30% D ₂ EHPA, 1/5 of O/A, 5 min for extraction, 4 M HCl, 5/1 of O/A for stripping for stripping	97%	Al, Sr, Fe, As, Zn, Ti, Cu, Sn, and Cr	(Ruan et al., 2012)
LCDs of mobile phone	D ₂ EHPA for extraction and HCl for stripping	32.6 in H ₂ SO ₄ leachate	30% D ₂ EHPA diluted in kerosene, 1/40 of O/A, pH 0.5, 20 min for extraction, 4 M HCl for stripping, 10/1 of O/A, 10 min for stripping	96.7% extraction and 61.10% stripping	Sn	(Pereira et al., 2018)
LCDs	A hollow fiber-supported liquid membrane with strip dispersion using D ₂ EHPA as an extractant	141 in HCl leachate	0.25 M D ₂ EHPA, pH 2, 20 min for extraction, 2 M HCl for stripping	94% extracted	Al, Ca, Fe, Zn and Cu	(Yen et al., 2016)
LCD glass	polyethylene glycol (PEG) 1,10 phenanthroline as a ligand, ammonium sulphate	85 in HCl leachate	25% w/w of [PEG 3,350] and 12% w/w of [(NH ₄) ₂ SO ₄], 2 h	80-95% in the bottom phase and 5-20% in the top phase	Sn, Al, and Cr	(Fontana et al., 2015)
Ionic liquids extraction						
Discarded LCD screens	Phosphonium ionic liquid (<i>Cyphos IL 104</i>) for extraction, HNO ₃ for stripping	160 in HCl leachate	0.1 M Phosphonium ionic liquid (<i>Cyphos IL 104</i>) diluted in toluene, 2/3 of O/A for extraction, 4 M HNO ₃ , 3/2 of O/A for stripping	98.9% extraction with a purity of 100%	Sn, Zn, Fe, Al, Mn, Ca, and Sr	(Dhiman and Gupta, 2020)
LCDs	Betainium bis (<i>trifluoromethylsulfonyl</i>) imide ([Hbet][Tf2N])	30 in acid	10 mL 50% (v/v) ionic liquid/ascorbic acid, 1/50 of S/L, 90 °C, 24 h	98.63% In was extracted	Al	(Luo et al., 2019)
Solid-phase extraction (ion exchange)						
LCD screens of mobile phone	Nylon 6/DEHPA nanofibers for extraction, HCl for stripping	32.6 in H ₂ SO ₄ leachate	Nylon 6/30% DEHPA nanofibers, pH 0.5, 7.5 min, 1/300 of S/L for extraction, 1.5 M HCl 1/20 of S/L, 5 min for stripping	74% extraction and 92% stripping	Sn	(Cadore et al., 2019)
LCD panels	5% wt/vol Amberlite™ resin, 2 M H ₂ SO ₄	26.8 in H ₂ SO ₄ leachate	5% wt/vol Amberlite™ resin, pH 3, 1/10 of S/L, 24 h for extraction, 2 M H ₂ SO ₄ , 2/5 of S/L, 1 h for stripping	100%	Al, Si, Fe, Sn, Zn, and Cr	(Ferella et al., 2016)

LCD panels	Macroporous resin (Lewatit TP 208) for extraction, HCl for stripping	30 in mineral acids	0.5 g Lewatit TP 208, pH 2, 25 °C, 30 min for extraction, 2M HCl, 500 rpm agitation, 5 min for stripping	99.5%		(Assefi et al., 2018)
Precipitation						
LCD screens of discarded cell phones	NH ₄ OH	0.2992 kg	NH ₄ OH (28.0-30.0 vol % of NH ₃), pH 7.4	99.8 wt% In was extracted	Si, Sr, Ca, Al, Ba, Sb, and Sn	(Silveira et al., 2015)
Cementation						
LCDs	Zn powder		100 g/L of Zn powder, pH 2-3	99.8%	Al, Ca, and Fe	(Rocchetti et al., 2016)
Electrowinning						
TFT-LCD panels	Low current electrolysis with the Potentiostat/Galvanostat		Current density at 0.2 A cm ⁻² in 15 wt% NaNO ₃ electrolytes for 30 min.	75% for ITO	Sn	(D. Choi et al., 2014)
Supercritical fluid separation						
LCD screens of cell phone	scCO ₂ extraction with 1 M citric acid and 5% H ₂ O ₂	602 mg/kg	1/20 of S/L, 15 MPa, 100 °C, 30 min	94.6%	Sn	(Argenta et al., 2017)
Biorecovery						
Aqueous solutions (InCl ₃) metal-system with indium and iron	Gram-negative bacterium <i>Shewanella algae</i>	115	Room temperature, pH 2.4–3.9, 10 min	100% In was extracted		(Ogi et al., 2012)
	Nature and waste biomass of brown alga <i>Ascophyllum nodosum</i>		pH 3	63 mg/g in nature biomass, 48 mg/g in waste biomass	Fe	(Pennesi et al., 2019)
Discard LCD screens	The hyper-accumulator plant <i>Eleocharis acicularis</i>	300 and 600 in HNO ₃ leachate	24 ± 1 °C, pH 5, 15 days	60 mg and 122 mg uptake		(Upadhyay et al., 2021)

833

834 3.2.3.1 Solvent extraction and ionic liquids extraction

835 Solvent extraction, also known as liquid-liquid extraction, is a widely used separation
836 technique for recovering indium from EoL product leachates. It is based on different solubilities
837 in two different immiscible liquids, usually an aqueous solution (polar) and an organic solvent
838 (non-polar) (Fontana et al., 2020). The advantages of this method are that the extraction process
839 is simpler, and the solvents can be reused (Pradhan et al., 2018). Numerous studies have tested

840 a wide variety of extractants to recover indium from LCD leachate. Typically, different
841 organophosphate extractants such as bis(2,4,4-trimethylpentyl) phosphinic acid (Cyanex 272),
842 trialkylphosphine oxide mixture (Cyanex 923), tributyl phosphate (TBP), and bis(2-ethylhexyl)
843 phosphoric acid (DEHPA) also known as di-2-ethylhexyl phosphoric acid (D₂EHPA) are added
844 to the extraction system (Pereira et al., 2018; Ruan et al., 2012; Virolainen et al., 2011; Yang
845 et al., 2013; Yen et al., 2016).

846 DEHPA has so far been confirmed as a widely used and best extractant for the selective
847 separation of indium and tin from LCD leachate due to the advantages of high loading capacity
848 and good selectivity over other metals (i.e. Fe, As, Cu, Cd, and Zn) (Fontana et al., 2020;
849 Virolainen et al., 2011; Yang et al., 2013). In the work of Yang et al. (2013), different organic
850 systems such as Cyanex 272, Cyanex 923, TBP, and DEHPA were reported for indium
851 extraction from acidic leachate generated from discarded LCD panels. The results showed that
852 DEHPA is a good option and more than 99% indium with 90% purity was extracted from low
853 concentration sulfuric acid by 0.1 M DEHPA diluted in kerosene after stripping with 1 M HCl.
854 Virolainen et al. (2011) also studied three types of solvent systems, including TBP, DEHPA,
855 and a mixture of the two, which suggested that DEHPA could extract both indium and tin from
856 H₂SO₄ and separated indium after stripping with 1.5 M HCl, while the stripping efficiency for
857 indium was 94%.

858 In addition, up to 97% of the total indium concentration was recovered from scrap thin-film
859 transistor (TFT) LCDs by H₂SO₄ leaching and solvent extraction with 30% D₂EHPA within 5
860 min after stripping with 4 M HCl (Ruan et al., 2012). Pereira et al. (2018) applied solvent
861 extraction with D₂EHPA to concentrate indium from EoL mobile phone LCDs, and after
862 adjusting the best conditions, the indium concentration was 236 times higher than the initial
863 concentration, reaching 7,712 mg/L of indium after stripping.

864 However, the disadvantages of using D₂EHPA extraction technique make it poor to separate
865 iron from indium, because the concentration of iron in the solution is similar to that of indium
866 and co-extracted with indium to the organic solution (Yang et al., 2013; Yen et al., 2016).
867 Nevertheless, a novel solvent extraction using crown ethers of 12C5 as the extractant has been
868 proposed and has shown good selectivity for In (III) over Sn (II). Therefore, it is expected to
869 demonstrate selective recovery of indium from waste LCD leachate in the future (Xu et al.,
870 2021).

871 Compared with the classical solvent extraction, a supported liquid membrane with strip
872 dispersion (SLM-SD) has been developed for the extraction of indium from spent LCDs due
873 to the advantages of a good mixing system, which avoids emulsification and enables more

874 efficient indium extraction. More than 94% of indium can be extracted with 0.25 M D₂EHPA
875 after stripping with 2 M HCl for 20 min using the SLM-SD technique (Yen et al., 2016). In
876 addition, polyethylene glycol (PEG)-based aqueous biphasic systems are also used to recover
877 indium from e-waste LCDs due to their characteristics of low toxicity, low corrosiveness, and
878 low flammability. In a study by Fontana et al. (2015), using a PEG-(NH₄)₂SO₄-water system
879 with 1,10-phenanthroline as a ligand, they found that indium can enter the lower (salt-rich)
880 phase at 80-95% and the upper (PEG-rich) phase at 5-20%. They also found that indium
881 separation is the independent composition in this system, and the indium concentration
882 increased by nearly 30% when the PEG concentration increased.

883 To overcome the lack of flammability and toxicity of traditional separation organic solvents in
884 the hydrometallurgical methods. Ionic liquids (ILs) are considered green extraction solvents,
885 and they are a promising and developing technique for indium extraction and recovery from
886 EoL products (Alguacil & López, 2020; Dhiman & Gupta, 2020). Recently, [tetradecyl-
887 (trihexyl) phosphonium bis-(2,4,4-trimethylpentyl) phosphinate] (Cyphos IL104), one of the
888 phosphonium ionic liquids, diluted in toluene, was used as an extractant to recover indium from
889 discarded LCD leachate (98.9% recovery yield) (Dhiman and Gupta, 2020). In addition, Luo
890 et al. (2019) reported that the use of ILs can be a more convenient way to recover indium
891 directly from discarded LCDs. They used the functionalized ionic liquid betainium
892 bis(trifluoromethylsulfonyl)imide ([Hbet][Tf₂N]), and achieved 98.6% indium recovery from
893 solid LCD samples after cooling and stratification under the optimal conditions within 24 hours.

894 3.2.3.2 Solid-phase extraction

895 Recently, solid-phase extraction has been recognized as a promising technique for indium
896 recovery from EoL products. It has the potential to replace conventional solvent extraction due
897 to the advantages of low solvent consumption, low cost, shorter time, and easier process
898 operation (Assefi et al., 2018; Cadore et al., 2019; Ferella et al., 2016; Płotka-Wasyłka et al.,
899 2016). However, there are very few reports using solid-phase extraction to recover indium from
900 LCDs.

901 Cadore et al. (2019) reported the use of Nylon 6 polymer nanofibers modified with DEHPA
902 extractant to selectively recover indium from spent LCD mobile phone screens. Cation-
903 exchange resin in solid-phase extraction has also been used to extract indium from LCDs.
904 According to Ferella et al. (2016), Amberlite™ IRC748 resin, a chelating resin with a high
905 affinity for metal cations (i.e. indium), was used in indium recovery. The indium extraction
906 yield was 100% with 5% wt/vol Amberlite™ resin in the optimum condition at pH 3 with a

907 S/L ratio of 1/10 g/mL within 24 h. The use of macroporous resins for the selective recovery
908 of indium from scrap LCD panels was reported because macroporous styrene-divinylbenzene
909 resins show a more practical approach to metal absorption with the advantages of high
910 performance and simple operation. Three macroporous polystyrene-divinylbenzene resins,
911 including Lewatit TP 208, Lewatit TP 260, and Amberlite IRA 743, were successfully used to
912 adsorb indium. The Lewatit TP 208 showed a higher recovery yield of 99.5% for the adsorption
913 of indium from scrap LCD panels due to the most symmetric and lower steric effect in the
914 interaction with indium, compared to other resins of Lewatit TP 260 and Amberlite IRA 743
915 (Assefi et al., 2018).

916 **3.2.3.3 Precipitation**

917 Precipitation is an alternative method for the extraction of indium from EoL products leachates.
918 The use of ammonium hydroxide (NH₄OH) solution to precipitate indium as indium hydroxide
919 from spent LCDs leachate obtained by H₂SO₄, the results of the experiment showed that 99.8
920 wt% of indium present in the solution with the good condition at pH 7.4 and standing for 24 h
921 (Silveira et al., 2015).

922 However, the precipitation method has its limitations. Other elements (i.e. aluminum) that have
923 similar properties to indium, may also precipitate along with the desired indium. As a result,
924 the indium is not selectively leached, resulting in a lower indium purity. Therefore, it is critical
925 to explore alternative methods that can selectively extract indium while avoiding the
926 precipitation of other elements. Further research is needed to optimize the precipitation method
927 and to develop alternative methods to extract indium selectively from e-waste.

928 **3.2.3.4 Cementation**

929 Cementation is a well-established and suitable method for recovering indium from EoL
930 products, especially in the presence of zinc as a cementing agent. Rocchetti et al. (2016)
931 reported the recovery of indium sponge by cementation with zinc powder, since zinc has a
932 lower reduction potential than indium and this process allows the reduction of trivalent indium
933 to metallic indium. It was found that a pH range of 2 to 3 provided the most efficient operating
934 conditions, resulting in the recovery of 99.8% of indium. In addition, the indium cementation
935 process has the added benefit of reducing the need for reagents during the recovery process,
936 although the final indium product may contain impurities such as aluminum, calcium, and iron.

937 However, additional research is needed to achieve a significant level of indium purity when
938 using zinc as a cementing agent for the purpose of extracting indium from LCD leachates.

939 Further studies are needed to optimize process conditions and to explore alternative methods
940 to achieve higher indium purity levels when using zinc as a cementing agent in the recovery of
941 indium from LCD leachates.

942 **3.2.3.5 Electrochemical separation/Electrowinning**

943 The use of electrochemical separation in recovering and recycling indium from EoL products
944 is rarely reported, especially from discarded LCD screens. This is explained by the fact that the
945 indium recovery process is strongly influenced by different factors, such as electrolyte
946 composition as well as the presence of complexing agents in the leachates (J. H. Choi et al.,
947 2014; Grimes et al., 2017). However, D. Choi et al. (2014) reported the recovery of ITO from
948 obsolete TFT LCD panels using an electrochemical technique, which could obtain 75% of ITO
949 (In_2O_3 and SnO_2) from the recovery process. But the recovered indium could not be reused
950 directly due to the unsuitable ratio of indium and tin. According to Grimes et al. (2017), the
951 extraction and the separation of indium from very dilute solutions that contain indium, tin, and
952 lead, which simulated the leaching solution composition of LCDs, was successful by using a
953 novel cylindrical mesh electrode electrolysis system under the optimum conditions. In the
954 three-stage process, indium was recovered 98% of total indium in the presence of the indium
955 hydroxide phase at the anode of the cylindrical mesh electrode cell by using a complexing agent
956 of 0.1 M thiocyanate (SCN^-) within 24 h. Furthermore, the electrolytic refining technique
957 integrated solvent extraction using 2-ethylhexyl phosphonic acid mono-2-ethylhexyl ether
958 (PC88A) as an extractant could be used to purify indium concentration to a maximum of 99.99%
959 from etching e-waste (Kang et al., 2011).

960 **3.2.3.6 Supercritical fluid extraction**

961 Supercritical Fluid Extraction (SFE) is a promising new technique for recovering indium from
962 LCDs, and it is considered to be more attractive than conventional recovery methods. SFE has
963 several advantages, including high diffusivity, low viscosity, high solubility, and no surface
964 tension, which are essential for efficient recovery. In addition, the use of CO_2 as a solvent in
965 SFE is more environmentally friendly due to its non-toxic, non-flammable, economical, and
966 recyclable properties (Argenta et al., 2017; Pradhan et al., 2018).

967 Supercritical CO_2 with co-solvents has been shown to increase the efficiency of the recovery
968 reaction kinetics by facilitating the conversion of indium from a solid form to a soluble ionic
969 form. Argenta et al. (2017) reported a recovery yield of 94.6% of indium from waste LCD
970 mobile phone screens using supercritical CO_2 and co-solvents (1 M citric acid and 5% H_2O_2)

971 within 30 min. This process was found to be six times faster than the conventional method of
972 using citric and malic acids.

973 In addition to its speed and efficiency, the SFE technique was shown to selectively leach indium
974 without leaching tin, demonstrating its ability to extract indium while avoiding the loss of other
975 valuable metals. As a result, SFE shows great potential for recovering high-purity indium from
976 EoL products such as LCDs. However, further research is needed to optimize the SFE process
977 and to determine its feasibility and scalability for industrial applications.

978 **3.2.3.7 Indium biorecovery**

979 Microbial biosorption is a promising technology for metal recovery due to the ability of some
980 microorganisms to selectively bind and concentrate specific metals from dilute solutions.
981 However, few studies have focused on the biosorption of indium from very low concentrations.

982 In the first report by Ogi et al. (2012), a novel recovery system was constructed using the Gram-
983 negative bacterium *Shewanella algae* to recover indium from aqueous InCl_3 solutions. They
984 found that indium can be recovered rapidly, with complete recovery within 10 min, and that
985 indium can be concentrated more than 4,300 times even from very low concentrations (< 1
986 mg/L). Furthermore, Pennesi et al. (2019) found that indium could be adsorbed by natural and
987 waste biomass of the brown alga *Ascophyllum nodosum*, with the maximum sorption capacity
988 estimated at 63 mg/g and 40 mg/g , respectively. However, competition with iron may affect
989 indium adsorption in real waste LCD leachates. Alternatively, phytoextraction with the hyper-
990 accumulator plant *Eleocharis acicularis* was applied for indium extraction from waste LCD
991 leachates (usually acidic and saline) by its biomass based on high acidity and salinity tolerance.
992 The results showed that the biomass accumulation of indium was achieved at 122 mg/g in dry
993 weight, and the final product of indium-exposed plant biomass can be a candidate for graphite
994 biocomposites (Upadhyay et al., 2021).

995 Therefore, microbial biosorption and phytoextraction are potential alternative technologies for
996 the recovery of indium from waste LCD leachates, although further research is needed to
997 optimize the processes and improve their efficiency.

998 **3.3 Gallium recovery from EoL LEDs via hydrometallurgical and biohydrometallurgical** 999 **routes**

1000 Gallium recovery from EoL products is still a challenge, according to the latest European
1001 Commission report (European Commission, 2020). Currently, industrial waste streams such as
1002 Metal-Organic Chemical Vapor Deposition (MOCVD: a system for depositing high-purity

1003 crystalline compound for LEDs) dust and GaN/GaAs waste are commonly used as secondary
1004 sources to supply gallium to industry (Chen et al., 2018a; Hu et al., 2014; Swain et al., 2015a
1005 and 2015b). However, there is limited experimental data on gallium leaching and recovery
1006 from spent LEDs. Therefore, a knowledge gap persists regarding gallium recovery from spent
1007 LEDs. Lu et al. (2017) reported that the structures of LEDs are more complex than other
1008 gallium secondary sources, such as GaAs scrap, because the chips with GaN-combined quartz
1009 substrates are denser and more difficult to separate and recover. Nevertheless, the increasing
1010 amount of EoL LEDs is still a good source of gallium due to its higher concentration compared
1011 to primary ores. Several preliminary research studies have been conducted on gallium recovery
1012 from spent LED chips containing GaN, GaAs, and InGaN (Maarefvand et al., 2020;
1013 Pourhossein & Mousavi, 2019; Van den Bossche et al., 2019; Zhan et al., 2020; Zhang et al.,
1014 2021; Zhou et al., 2019). Various pre-treatment methods and hydrometallurgical and
1015 biohydrometallurgical technologies have been tested at a laboratory scale for gallium recovery
1016 from spent LEDs.

1017 The pre-treatment of spent LEDs plays a critical role in the dissociation of their complex
1018 structures. Therefore, this review focused on different approaches dedicated to the pre-
1019 treatment of different types of spent LEDs. Although some studies have focused on
1020 pyrometallurgy, more environmentally friendly routes such as hydrometallurgy and
1021 biohydrometallurgy are discussed.

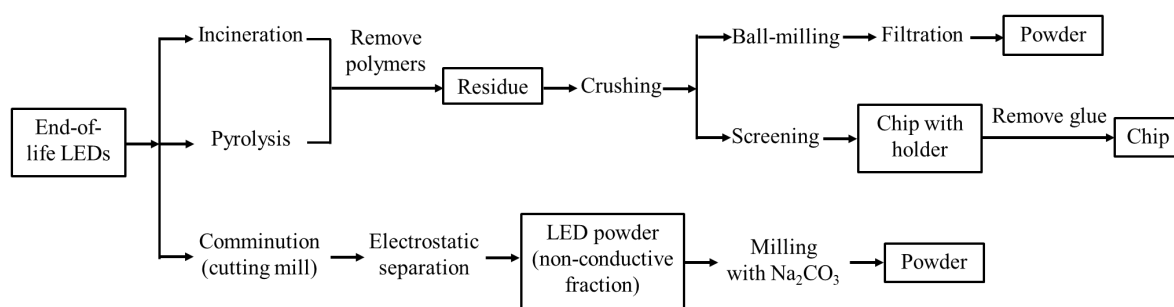
1022 **3.3.1 Pre-treatment of EoL LEDs**

1023 Pre-treatment of EoL LEDs is an important step in the recovery of valuable materials and
1024 components. This process includes both mechanical and chemical methods to improve
1025 recovery efficiency. The first step is to physically free and separate the gallium-containing LED
1026 chips from the less valuable parts of the EoL LEDs. Once the chips are obtained, they are
1027 typically cut into small pieces and ground with a mill or mortar to produce a powder. The size
1028 of the particles can be adjusted by sieving the powder with different sieve apertures, with the
1029 recommended size usually being less than 1,000 μm due to the presence of chips in the range
1030 of 106-1,000 μm . After obtaining the powder, a thermal pre-treatment may be required to enrich
1031 the concentration of elements and modify the structure of the undissolved gallium, especially
1032 if the LED structure contains GaN (Maarefvand et al., 2020; Nagy et al., 2017; Swain et al.,
1033 2015a). This pre-treatment is critical to increase the solubility of gallium in leach solutions,
1034 which can ultimately lead to better recovery rates.

1035 To facilitate the recovery of LED chips from bulk material, polymers and adhesives (epoxy
 1036 resin and other additives) are removed in advance (Maarefvand et al., 2020; Zhan et al., 2020).
 1037 Polymers are typically removed by incineration due to their flammability and low melting point.
 1038 This process leaves a crispy residue that is easily removed. On the other hand, adhesives,
 1039 epoxies, and other additives can be removed using solvents such as acetone and anhydrous
 1040 ethanol. The use of these solvents helps to completely separate the chips from the waste LED
 1041 components. After the unwanted components have been removed, electrostatic separation is
 1042 used to separate the non-conductive fraction of the chips from the LED powder. This step
 1043 ensures that only the valuable components are recovered for further processing (Nagy et al.,
 1044 2017).

1045 For spent GaN LEDs, thermal treatment and pyrolysis play a critical role in the pre-treatment
 1046 process. These processes oxidize gallium nitride to gallium oxide in the air or convert gallium
 1047 nitride to gallium with nitrogen gas to improve solubility in leaching solutions (Maarefvand et
 1048 al., 2020; Zhou et al., 2019). Figure 7 shows the pre-treatment process for the LEDs.

1049



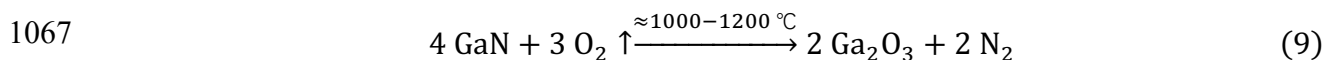
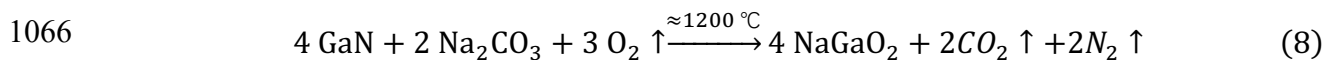
1050

1051 Figure 7 Flow chart of LEDs pre-treatment

1052

1053 Gallium nitride (GaN) is a highly durable crystal that has a high binding energy, making it
 1054 difficult to dissolve in lixivants. However, there are several methods that have been proposed
 1055 to improve the efficiency of gallium leaching from GaN. One such method is the chemical-
 1056 thermal treatment with mechanochemical activation, which involves the use of the alkaline salt
 1057 Na_2CO_3 . This treatment can convert GaN into soluble NaGaO_2 in the presence of Na_2CO_3 with
 1058 annealing, as reported by Swain et al. (2016b). Nagy et al. (2017) have also proposed a
 1059 chemical-thermal treatment with Na_2CO_3 that can improve the gallium leaching efficiency.
 1060 Another method involves thermal oxidation without oxidants, where insoluble GaN can be
 1061 converted to Ga_2O_3 in the air at a high temperature of 1000-1200 °C, as reported by Maarefvand
 1062 et al. (2020). The chemical reactions involved in the formation of NaGaO_2 and Ga_2O_3 are given

1063 by Equations (8) and (9), respectively. Other alkaline salts, such as LiBO₂ and NaOH, have
1064 also been used for alkali roasting in the recovery of gallium from spent LEDs (Chen et al.,
1065 2018a).



1068 Thermal treatment can also be used for direct gallium recovery. Zhan et al. (2018) performed
1069 vacuum metallurgical separation on GaAs-based LEDs to recover different metals based on
1070 their boiling and evaporation points at different pressure conditions. The system successfully
1071 separated gallium and arsenic, achieving a gallium recovery yield of 98.92% at high pressure
1072 of 20 Pa and 1273 °C in 60 min. However, the limited temperature gradient of the experimental
1073 equipment caused the overlapping of gallium and arsenic, making it difficult to obtain high
1074 purity of gallium and arsenic separately, requiring additional steps for purification.

1075 To determine the elemental composition of spent LEDs, acid digestion is commonly used. Chen
1076 et al. (2018a) reported that aqua regia with hydrofluoric acid (ratio 5/1) is efficient in
1077 completely dissolving solid samples. However, if the samples contain silver, nitric acid is
1078 recommended to avoid AgCl precipitation. The acidic leachate can then be analyzed using an
1079 inductively coupled plasma-optical emission spectrometer (ICP-OES) or atomic absorption
1080 spectroscopy (AAS) (Annoni et al., 2020; Chen et al., 2018a; Hu et al., 2014; Nagy et al., 2017;
1081 Pourhossein et al., 2021; Zhou et al., 2019).

1082 In addition to determining the total metal concentration of spent LEDs, various analytical
1083 techniques such as scanning electron microscopy (SEM), X-ray diffraction (XRD), energy
1084 dispersive spectroscopy (EDS), and X-ray fluorescence analysis (XRF) can be used for their
1085 characterization (Chen et al., 2018a; Hu et al., 2014; Maarefvand et al., 2020; Nagy et al., 2017;
1086 Swain et al., 2015a; Yang et al., 2023). These techniques can provide information on the crystal
1087 structure, elemental composition, and morphology of spent LEDs.

1088 **3.3.2 Gallium leaching from EoL LEDs via hydrometallurgical and** 1089 **biohydrometallurgical routes**

1090 Gallium recovery from LED industry waste and spent LEDs can be achieved by
1091 hydrometallurgical and biohydrometallurgical routes.

1092 Table 8 provides an overview of the different approaches that have been investigated in the
1093 literature. The GaN and GaAs wastes from the MOCVD process and the LED industry have

1094 been studied due to their similarity to the common chips from spent LEDs. Leaching of GaAs
 1095 waste is comparatively easier than that of GaN waste. However, the toxicity of arsenic during
 1096 the leaching process should be considered to prevent environmental contamination (Hu et al.,
 1097 2014; Mir et al., 2022).

1098 On the other hand, the insolubility of GaN, even in strong acids, makes it relatively difficult to
 1099 process. Therefore, numerous studies have been conducted to improve the gallium leaching
 1100 yield from GaN and GaAs by strong inorganic acids under different pressure and temperature
 1101 conditions, with or without catalysts.

1102 In addition, indirect bioleaching-based processes have also been tested to achieve optimal
 1103 gallium recovery. These processes use microorganisms to catalyze the leaching process, which
 1104 can increase the leaching yield while minimizing the environmental impact. However, further
 1105 research is needed to optimize bioleaching conditions for efficient gallium recovery. Overall,
 1106 hydrometallurgical and biohydrometallurgical routes offer promising avenues for the recovery
 1107 of gallium from LED industry waste and spent LEDs.

1108

1109 Table 8 Methods for gallium leaching from LED industry wastes and spent LEDs

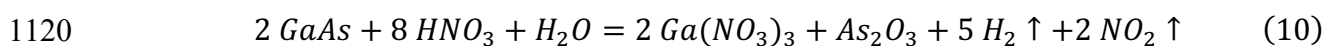
E-waste	In and Ga (mg/kg)	Leachant	Optimum conditions (S/L: g/mL)	Leaching yield	Other metals	Reference
Strong inorganic acid leaching process						
GaAs, scrap from LEDs	50.8% Ga	1.5 M HNO ₃	1/40 of S/L, 200 rpm agitation, 40 °C, 1.5 h	99.6% Ga	As	(Hu et al., 2014)
Waste GaN from MOCVD dust	62.1% Ga, 1.86% In	4 M HCl with 5 wt% NaNO ₃	1/20 of S/L, 400 rpm agitation, 100 °C, 1 h, NaNO ₃ as catalyst	89.1% Ga	Al, Fe	(Swain et al., 2015b)
waste GaN from LED industry dust	97.76% Ga, and 2.24% In	4 M HCl and 1/1 of Na ₂ CO ₃	1/50 of S/L, 400 rpm agitation, 100 °C leaching after annealing with Na ₂ CO ₃	73.7% Ga		(Swain et al., 2015a)
SMD LEDs (GaN)	712.9 Ga	4 M HCl and 1/1 of Na ₂ CO ₃	1/50 of S/L, 80 °C, 2 h leaching after annealing with Na ₂ CO ₃	99.5% Ga	Cu	(Nagy et al., 2017)
Waste LEDs (GaN) from used light		4 M HCl	93°C, 2 h for leaching after oxidation without an agent	91.4% Ga	Al	(Maarefvand et al., 2020)
GaN waste from LED industry	3.38% Ga	0.25 M HCl with pressure	1/30 of S/L, 200 °C (15 atm pressure), 3 h	98.5% Ga	As, Fe, Al, Si, and Cr	Chen et al., 2018a)
Waste LEDs	37 of Ga	Subcritical water, 3% H ₂ O ₂ ,	300 °C, 300 rpm agitation, 400 min	80.5% Ga	As, Ag	(Zhang et al., 2021)

Waste GaN from MOCVD dust	74% Ga, 6% In	2 M NaOH for Ga, 2 M H ₂ SO ₄ for In	1/10 of S/L, 500 rpm agitation, 80 °C, 3 h for Ga after annealing with Na ₂ CO ₃ , leaching residues in 1/20 of S/L, 600 rpm agitation, 80 °C, 4 h for In	90.0% Ga 94.3% In	Al, Mg, Si	(Fang et al., 2019)
MOCVD dust	71% Ga, 6.6% In	2 M NaOH for Ga	1/20 of S/L, 200 rpm agitation, 90 °C, 3 h for Ga, after calcinating at 1200 °C for 3 h	92.7% Ga with 99.3% purity	Al, Mg, Si	(Yang et al., 2023)
Organic acid leaching process						
Surface mounted device LEDs	116.43	0.7 M Oxalic acid	90 °C, 1/100 of S/L, 48-75 µm of particle size, 1 h	90.4% Ga	Fe and Cu	(Zhou et al., 2019)
Indirect bioleaching-based process						
GaN chemical		<i>Arthrobacter creatinolyticus</i>	pH 9, 15 days	18% Ga		(Maneesuwanarat, Teamkao et al., 2016)
Discarded pin-type LEDs	401 Ga and 124 In	Adapted <i>A. ferrooxidans</i> with biogenic ferric ion	1/50 of S/L, 29 °C, pH 2, 140 rpm agitation, 30 days for direct bioleaching	60% Ga	Sn, Cu, Ni, Ag, Al, Pb, Cr, As,	(Pourhosseini and Mousavi, 2018)
		4-5 g/L biogenic ferric ion from adapted <i>A. ferrooxidans</i> culture	1/50 of S/L, 29 °C, pH 2, 140 rpm agitation, 15 days for step-wise indirect bioleaching	84% Ga	Zn, Au, and Ba	(Pourhosseini & Mousavi, 2019)

1110

1111 3.3.2.1 Gallium leaching with strong mineral acids and alkaline

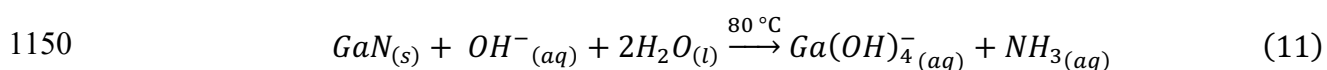
1112 Various strong inorganic acids such as HCl, HNO₃, and H₂SO₄ have been tested for leaching
1113 gallium from e-waste. HNO₃ was found to be the most effective leachant for gallium recovery
1114 from GaAs scrap when added at relatively high concentrations compared to HCl and H₂SO₄
1115 (Annoni et al., 2020). Hu et al. (2014) have confirmed that HNO₃ is the best technique for
1116 dissolving gallium and arsenic with high yields of 99.6% and 100%, respectively, under
1117 optimal conditions (1.5 M HNO₃ in 1.5 h at 40 °C). The reaction of GaAs with HNO₃ is an
1118 exothermic process and a self-catalytic reaction because the generated NO₂ gas enhances the
1119 reaction, according to the following chemical reaction:



1121 In contrast, when dealing with the type of GaN waste generated by the LED industry. Chen, et
1122 al. (2018a) found that the optimal acidic gallium leaching occurred with HCl when the optimal
1123 conditions were adjusted. However, the gallium leaching yield was very low (8.9%) even when
1124 the temperature was increased up to 90 °C to accelerate the reaction rate. Pre-treatment with
1125 alkaline salt (i.e. NaOH) significantly improved the gallium leaching yield to 73.3% with HCl.
1126 Also, the gallium leaching yield with HCl under optimal conditions was improved to more than
1127 90% after annealing with Na₂CO₃ (Swain et al., 2015b). Nagy et al. (2017) reported that 99.5%
1128 of gallium was leached from samples of new SMD LEDs. 91.4% of gallium could be achieved
1129 in the leaching process by using 4 M HCl at 93 °C for 2 h after thermal pre-treatment, even
1130 without oxidants (Maarefvand et al., 2020).

1131 Without high temperature pre-treatment, Chen et al. (2018a) reported a high gallium leaching
1132 yield of 98.5% using pressurized acid leaching with HCl at 200 °C and 15 atm vapor pressure,
1133 even with a low concentration of HCl (0.25 M). Zhang et al. (2021) found that high temperature
1134 and pressure in the presence of oxidants such as H₂O₂ for subcritical water treatment can lead
1135 to a high gallium leaching efficiency of more than 80%. However, high temperature and
1136 pressure require extra stringent measures to safely operate the experimental setup. Different
1137 catalysts (i.e. NaNO₃, HNO₃, H₂O₂, and Na₂CO₃) have been used in HCl leaching to improve
1138 gallium leaching efficiency. Swain et al. (2015b) found that NaNO₃ increased gallium leaching
1139 efficiency from 64.6% to 89.1%, and the following order of efficiency was Na₂CO₃ < H₂O₂ <
1140 HNO₃ < NaNO₃.

1141 Alkaline leaching with NaOH has also been investigated for gallium leaching from GaN-type
1142 wastes, due to the amphoteric property of gallium and the stability of Ga(OH)₄ chemical species
1143 in an alkaline solution. Fang et al. (2019) reported that gallium could be leached out with an
1144 efficient yield of 90% using 2 M NaOH at 80 °C, as the thermodynamic dissolution of GaN in
1145 the NaOH solution shows that the Gibbs free energy ($\Delta G_{80\text{ °C}} = -102.4 \text{ kg/mol}$) is negative, and
1146 the reaction (Eq. 11) is spontaneous at a temperature of 80 °C. Additionally, Yang et al. (2023)
1147 reported a gallium leaching yield of 92.7% with a purity of 99.3% using 2 M NaOH at 90 °C
1148 after calcination by converting nitrogen from GaN into diatomic nitrogen gas instead of
1149 ammonia or ammonium.

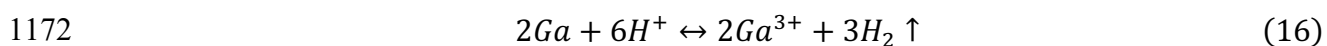
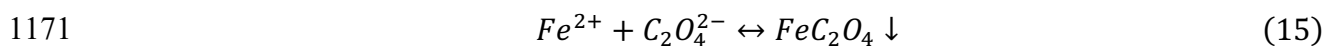
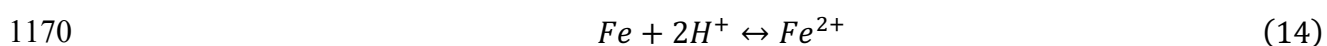
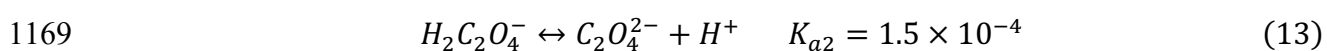
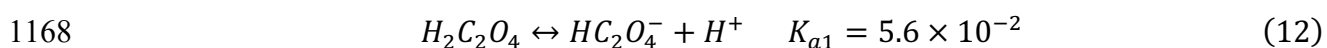


1151 **3.3.2.2 Gallium leaching with organic acids**

1152 Organic acids are being investigated as a potential alternative to mineral acids for gallium
1153 leaching from spent LEDs, due to their easier implementation and lower environmental impact.

1154 Zhou et al. (2019) conducted experiments to investigate the potential of three different organic
 1155 acids (oxalic acid, citric acid, and DL-malic acid) for gallium leaching from spent SMD LEDs.
 1156 The results showed that oxalic acid had the highest efficiency, with 83% of the gallium being
 1157 leached. This percentage was higher than citric acid (71%) and DL-malic acid (72%). After
 1158 optimizing the leaching conditions, a gallium leaching yield of more than 90% could be
 1159 achieved within 60 min.

1160 One reason for the high efficiency of gallium leaching with oxalic acid may be the formation
 1161 of iron oxalate precipitates (FeC_2O_4) resulting from the reaction of iron ions with oxalic acid.
 1162 This promotes the release of H^+ from oxalic acid, which is not observed with other organic
 1163 acids tested. Another reason is that oxalic acid can maintain a stable H^+ concentration during
 1164 the leaching process, which is critical for gallium dissolution. Similar reactions have been
 1165 reported for other metals, such as Ca^{2+} and Sr^{2+} (Cui et al., 2019). Therefore, oxalic acid
 1166 leaching shows potential as a promising recovery technique for gallium from EoL LEDs. The
 1167 possible related reactions of Fe and Ga leaching are:

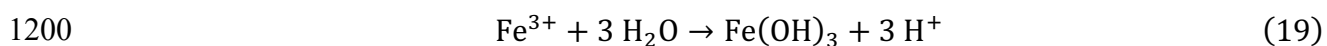
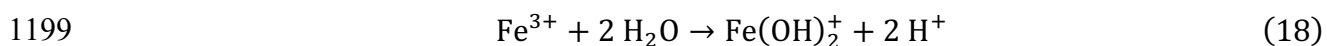
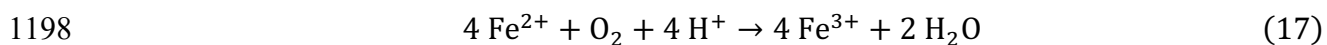


1173 **3.3.2.3 Gallium bioleaching**

1174 Bioleaching is an environmentally friendly and energy-saving method that has been
 1175 successfully applied to the recovery of gallium from waste LCDs. Although the number of
 1176 studies on the bioleaching of gallium from waste LEDs is limited, progress has been made in
 1177 recent years.

1178 The heterotrophic bacterium *Arthrobacter creatinolyticus* (*A. creatinolyticus*) has been studied
 1179 for gallium leaching from chemicals ($< 38 \mu\text{m}$ particle size). Although a low leaching yield
 1180 (18%) was achieved after 15 days of incubation, the results provide important insights into the
 1181 fundamental mechanisms of gallium bioleaching. In particular, the interaction of Ga with
 1182 amino acids, peptides, and proteins seems to be related to the binding mechanism with a
 1183 carboxyl group and an amine group by binding gallium ions from GaN and forming metal
 1184 complexes that promote the leaching of gallium from spent GaN (Maneesuwannarat, Vangnai,
 1185 et al., 2016).

1186 Iron-oxidizing bacteria, such as *A. ferrooxidans*, have been used to leach gallium from
1187 discarded pin-type LEDs (Pourhossein and Mousavi, 2018). The adaptation of these bacteria
1188 to tolerate toxic metals and flame retardants from spent LED media significantly increased the
1189 leaching efficiency of gallium. The results show that *A. ferrooxidans* was able to tolerate the
1190 maximum concentration of spent LED powder (20 g/L) and was able to reach approximately
1191 60% of gallium (Pourhossein and Mousavi, 2018). Iron, which is the largest metallic
1192 component in the total metal weight of LEDs, played an important role in maintaining the pH
1193 value stabilized at 2-2.5 in the direct bioleaching process by oxidation of ferrous ions and
1194 hydrolysis of ferric ions in the aqueous solution. Throughout the reaction process, the pH could
1195 be kept stable by the hydrolysis of ferric ions (Fe^{3+}), which releases H^+ into the solution, even
1196 though the above bacteria initially oxidize ferrous ions (Fe^{2+}) to ferric ions (Fe^{3+}) using protons.
1197 Related reactions of Fe are:



1201 Bioleaching can be a promising approach to improve gallium leaching from EoL products. One
1202 such method is the stepwise indirect bioleaching approach, which uses biogenic iron from
1203 adapted bacteria to enhance the recovery of gallium from spent LEDs. This method addresses
1204 the negative effects of bacterial adhesion in direct bioleaching of spent LEDs. The results
1205 showed that an 84% leaching yield of gallium was achieved at a pulp density of 20 g/L and pH
1206 2 within 15 days, which is an improvement over the 60% yield achieved by direct bioleaching
1207 (Pourhossein & Mousavi, 2019). This stepwise indirect bioleaching method is a low-cost,
1208 environmentally friendly, and easier controlled method that can recover gallium from low
1209 concentration sources. These results suggest that this approach could be a promising technique
1210 for the recovery of gallium from waste LEDs.

1211 **3.3.3 Gallium recovery from EoL LEDs via hydrometallurgical and** 1212 **biohydrometallurgical routes**

1213 Table 9 summarizes the methods implemented for the recovery of gallium from spent LEDs
1214 leachates as reported in peer-reviewed literature.

1215

1216 Table 9 Methods for gallium recovery from spent LEDs leachates

E-waste	In and Ga (mg/kg)	Extractant	Optimum conditions	Recovery yield	Other metals	Reference
Solvent extraction						
LEDs	8 of Ga in HCl leachate	Cyanex 272 for extraction and HCl for stripping	0.5 M Cyanex 272, 0.01 and 0.1 M HCl multi-stripping Ga	91% Ga extraction with 99% purity	Fe, Ni, Al, Cu, Ni, Mn	(Gupta et al., 2007)
Ionic liquids extraction						
GaAs and InAs from waste LEDs and semiconductors		[P ₄₄₄₁₀][Br ₃] as an ionic liquid, NaBr solution, pure water, and NaOH for stripping	Gallium was stripped by pure water before NaBr (remove As), and Indium was stripped by NaOH	96.5% Ga and 99% In precipitation	As	(Van den Bossche et al., 2019)
Membrane separation						
SMD red-emitting chip LEDs	1307 of Ga	Nanofiltration 90 membrane	10 atm pressure, 20-25 °C, 2.4 L/min of feed flow, pH 2-9	85% Ga	As, Zn, Fe, Cu, Si, Au	(Annoni et al., 2020)
Precipitation						
GaAs scraps of LEDs		0.1 M Na ₂ S	5 mL/min of flow rate, 0.7 of the molar ratios of S to (Ga+As) pH 3.5-7 for Ga	98.5% As precipitation, 98.5% Ga in solution	As	(Hu et al., 2014)
Waste LEDs		pH adjustment for Ga, NH ₄ OH for In	precipitation, pH 1-3 for In precipitation after residue dissolved in H ₂ SO ₄	99.8% Ga and 99.1% In		(Fang et al., 2019)
Supercritical liquid extraction						
Surface mounted device LEDs	41 of Ga and 21 of In	Anhydrous ethanol and ultrapure water	300 °C, 60% water in the water-ethanol mixture, 240 min	93.10% Ga and 85.72% In	As and Ag	(Zhan et al., 2020)
Indirect bioleaching-based process						
Wafer fabrication industry wastewater	4-35	DFOB and DFOE for complexation, EDTA for decomplexation	pH 2-9, molar ratio of Ga and DFOB/E of 1/1 for complexation, pH 3.5 with 6 times EDTA for	100% Ga complexation and > 95% Ga decomplexati	As, Al, Mg, Ca, Zn, P	(Jain et al., 2019)

1217

1218 3.3.3.1 Solvent extraction

1219 The recovery of gallium from spent LEDs leachates by solvent extraction has not been widely
1220 reported. Among the solvents tested, dialkylphosphine oxide (Cyanex 272) was found to be a
1221 superior extractant due to its low aqueous solubility, good recyclability, and resistance to
1222 hydrolysis compared to tributylphosphate (TBP) and di(2-ethylhexylphosphoric acid) (DEHPA)
1223 (Gupta et al., 2007). It is reported that gallium can be effectively recovered from spent LED
1224 leachates using Cyanex 272 solvent and ternary separations with various concentrations of HCl.
1225 It was found that 90-95% of the total gallium was extracted with 99% purity after adjusting the
1226 conditions. The good hydrolytic stability and regeneration of the Cyanex 272 extractant also
1227 make it a suitable candidate for large-scale recycling industries.

1228 However, the multi-step removal of non-target metals such as Ni, Mn, Cu, Al, and Fe increases
1229 the cost of gallium recovery. Therefore, there is a need to develop a simpler single-step method
1230 for selective recovery of gallium to reduce the overall process cost. Despite these limitations,
1231 the use of solvent extraction for gallium recovery from spent LED leachates has great potential
1232 and warrants further investigation.

1233 3.3.3.2 Ionic liquids extraction

1234 The use of ionic liquids (ILs) as an extraction method for target metal recovery has gained
1235 increasing attention due to their non-volatile and non-electrostatic charging properties. In
1236 recent years, a hydrophobic trihalide ionic liquid, tributyldecylphosphonium tribromide
1237 [P44410][Br₃], has been used as an oxidant for the extraction of gallium and indium from spent
1238 LEDs, including those containing GaAs and InAs. This approach has several advantages,
1239 including the avoidance of the highly toxic arsenic formation of AsH₃ during acid leaching and
1240 the ability to recycle ILs for multiple extraction cycles. Van den Bossche et al. (2019) reported
1241 the recovery of gallium and indium from semiconductors and LEDs containing GaAs and InAs
1242 using this method, achieving 96% recovery of gallium after stripping with ultrapure water and
1243 99% recovery of In(OH)₃ precipitated after stripping with NaOH solution. Finally, by adding
1244 Br₂ to the solution, ILs could be reused and recycled for another extraction cycle, contributing
1245 to a green and circular economy. The direct approach to recovering gallium and indium without
1246 the leaching step is a promising technique. However, this approach has not been implemented
1247 for spent GaN LED material.

1248 3.3.3.3 Membrane separation

1249 Membrane separation has been shown to be a promising approach for the purification of metals,
1250 including gallium (Annoni et al., 2020). Nanofiltration and ultrafiltration membranes have been
1251 tested for gallium recovery. The results show that even though gallium ions (radius size: 0.0621
1252 nm) easily pass through an ultrafiltration membrane (size > 100 nm), gallium precipitates are
1253 retained by the ultrafiltration membrane as pH increases (i.e. pH < 2.51, 22% of gallium
1254 precipitation). However, a nanofiltration membrane was a good way to reject gallium. The
1255 positive metal ions, such as gallium ions, are repelled due to the expected positive membrane
1256 charge in the nanofiltration membrane process when pH is low. The recovery yield of gallium
1257 from a synthetic solution can reach up to 98.4% when the pH is around 2. In actual acidic spent
1258 LED leachate, the recovery yield of gallium can achieve 85% using a nanofiltration membrane
1259 under optimal conditions of 10 atm pressure at room temperature and a feed flow rate of 2.4
1260 L/min. Additionally, the nanofiltration membrane does not degrade at pH 0.18, making it
1261 suitable for most acidic treated leachates. However, the cost of the recovery system is increased
1262 due to the need for acid control at low conditions, and the recovery yield and purity need to be
1263 improved. Despite these limitations, the use of nanofiltration membranes for gallium recovery
1264 offers a promising solution for the purification of this valuable metal.

1265 3.3.3.4 Precipitation

1266 Precipitation is a widely used method for recovering gallium from waste materials. This
1267 process involves adjusting the pH using an acid or a base. However, in the case of gallium and
1268 arsenic recovery from GaAs leachates, NaOH is not preferred due to the co-precipitation of
1269 these two metals. Hu et al. (2014) reported that the maximum precipitation percentage of
1270 gallium with $\text{Ga}(\text{OH})_3$ occurs in the pH range of 4-6, while arsenic precipitation reaches a
1271 maximum percentage at pH 6.

1272 Sodium sulfide (Na_2S) is an effective precipitant for gallium recovery from GaAs leachates.
1273 This approach achieves a highly selective separation of gallium and arsenic through Na_2S
1274 titration. The hydrolysis of S^{2-} and release of OH^- in solution can raise the pH to 1 in acidic
1275 leachates, resulting in 79% arsenic precipitation compared to 6% gallium precipitation. In this
1276 approach, Na_2S first reacts with As to form a precipitate of As_2O_3 rather than As_2S_3 , allowing
1277 the separation of gallium and arsenic (Hu et al., 2014).

1278 However, Chen et al. (2012) reported that the use of Na_2S solution not only recovered As but
1279 also co-precipitated Ga. The low separation efficiency of GaAs (49.1% Ga and 29.6% As
1280 precipitates) was attributed to the high addition flow rate of Na_2S solution, which could react

1281 with Ga and As simultaneously due to the excess of dissolved sulfide species. To improve the
1282 separation efficiency, Hu et al. (2014) optimized the Na₂S flow rate to 5 mL/min and found
1283 that 0.1 M Na₂S could precipitate 98.5% As and 1.5% Ga, resulting in the successful recovery
1284 of gallium from spent LEDs leachate.

1285 In addition, the precipitation of gallium and indium could also be achieved with high recovery
1286 yields (more than 99%) through pH adjustment using H₂SO₄ and NH₄OH solution, respectively.
1287 Fang et al. (2019) reported that adjusting the pH of the solution with H₂SO₄ solution to the
1288 range of 3.5-7 results in the maximum amount of Ga(OH)₃ precipitate. Similarly, adjusting the
1289 pH with NH₄OH solution in the range 1-3 resulted in the precipitation of In(OH)₃.

1290 Overall, chemical precipitation by adjusting pH with acid or base is a promising approach to
1291 recovering critical elements from waste materials. It is a simple and safe process, and the
1292 residue and leachate can be recycled for subsequent steps, resulting in a high recovery rate of
1293 critical elements.

1294 **3.3.3.5 Supercritical fluid separation**

1295 Supercritical fluid separation is an advanced technique that can effectively separate various
1296 metals from e-waste. One method that has been investigated is the use of a subcritical water-
1297 ethanol mixture, which has shown promising results in the recovery of gallium, indium, arsenic,
1298 and silver from e-waste LEDs. In a study conducted by Zhan et al. (2020), the optimum
1299 recovery conditions were found to be at a temperature of 300 °C and water content of 60% in
1300 the water-ethanol mixture, which allowed for the recovery of 93.1% gallium, 85.7% indium,
1301 93.8% arsenic, and 99.9% silver in only 4 h.

1302 This method has several advantages, including high efficiency, environmental friendliness, and
1303 the potential for large-scale application. The subcritical water-ethanol mixture is a non-toxic
1304 solvent that can be easily recycled and does not produce any harmful waste products. It also
1305 provides a sustainable solution for recovering valuable metals from e-waste, which can help
1306 reduce the environmental impact of this growing problem.

1307 **3.3.3.6 Indirect biorecovery-based approach**

1308 The use of an indirect biorecovery-based approach offers a promising and environmentally
1309 friendly approach for gallium recovery from low concentration wastewater. The first research
1310 to demonstrate the new technology for gallium recovery has been studied. Siderophores, such
1311 as desferrioxamine B (DFOB) and desferrioxamine E (DFOE) have been investigated for the
1312 selective and sensitive recovery of gallium from wafer fabrication wastewater (Hofmann et al.,

1313 2020; Jain et al., 2019). These natural chelator-siderophores, produced by the bacterium
1314 *Streptomyces*, were found to bind gallium with 100% yield and form more stable complexes
1315 than other metals, such as zinc. More importantly, this approach could selectively recover
1316 gallium without complexing non-target elements, such as arsenic, copper, magnesium, zinc,
1317 and calcium (Jain et al., 2019).

1318 The GaLIophore technology, which uses DFOB/DFOE to recover gallium from low
1319 concentration wastewater, has shown impressive results. In experiments, more than 90% of
1320 gallium decomplexation was achieved and DFOB/E regeneration was achieved with 100%
1321 efficiency by using ethylenediamine tetraacetic acid (EDTA) six times. This approach has been
1322 successfully applied to the recovery of gallium from wastewater by reversed-phase
1323 chromatography, and the recycling of DFOB/E has been demonstrated (Jain et al., 2019). The
1324 "GaLIophore technology" has been patented by a German company under the patent number
1325 DE102019108803B4 and its potential for widespread application in the field of gallium
1326 recovery is an exciting development for the future.

1327 **3.4 Indium and gallium recovery from EoL PVs via hydrometallurgical and** 1328 **biohydrometallurgical routes**

1329 The production of renewable energy through PVs, or solar panel systems, is a promising
1330 approach to mitigate the environmental impacts associated with non-renewable energy sources.
1331 However, the sustainability of PV technology is challenged by the scarcity and high demand
1332 for TCEs, such as indium and gallium, that are used in PV components. Therefore, it is
1333 imperative to establish efficient and cost-effective methods to recover indium and gallium from
1334 spent PVs, in order to reduce the dependence on primary resources and minimize the
1335 environmental impact (Schmidt et al., 2019).

1336 Unfortunately, the complex structure of PVs, which typically includes layers of different
1337 materials and coatings, and the low concentration of TCEs in spent PVs, pose significant
1338 challenges for the effective and selective recovery of these elements. As a result, conventional
1339 methods of metal extraction from primary resources are often unsuitable or inefficient for PV
1340 recycling, and alternative approaches must be explored. Two potential routes for the recovery
1341 of indium and gallium from spent PVs are hydrometallurgy and biohydrometallurgy. However,
1342 the complexity of the PVs structure and other factors have limited the application of critical
1343 metals recovery.

1344 **3.4.1 Pre-treatment of EoL PVs**

1345 Pre-treatment is a critical step in the recovery of valuable metals from spent PV modules and
1346 can be divided into two main stages. The first stage involves selective dismantling to remove
1347 hazardous or non-valuable components. This is followed by the second stage, which aims to
1348 upgrade or concentrate the target metals through mechanical and physical treatment
1349 (Maneesuwannarat, Teamkao, et al., 2016). The treatment process for EoL PVs typically
1350 involves dismantling the panels, cutting into smaller pieces, grinding into finer powders,
1351 screening through various hole sizes, and finally drying in an oven. While there is limited
1352 literature on the treatment of EoL PVs, Savvilotidou and Gidakos (2020) have reported on
1353 three methods for pre-concentrating EoL CIS panels after manual dismantling and cutting.
1354 These methods include thermal treatment and gravimetric process, mechanical shredding,
1355 screening, chemical treatment, and thermal treatment. Among the above methods tested, the
1356 first pre-concentration method proved successful in recovering 96.3% of indium from CIS
1357 panels. Pre-treatment, therefore, plays a crucial role in the efficient recovery of valuable metals
1358 from spent PV modules and can significantly improve the subsequent recovery process.

1359 **3.4.2 Indium and gallium leaching from EoL PVs via hydrometallurgical and** 1360 **biohydrometallurgical routes**

1361 Table 10 summarizes the literature leaching methods for indium and gallium from spent PVs
1362 (GaAs PV, CIGS, and CIS PV).

1363

E-waste	In and Ga (mg/kg)	Leachant	Optimum conditions (S/L: g/mL)	Leaching yield	Other metals	Reference
Inorganic and organic acid leaching process						
Spent CIS_CuInSe photovoltaic panels	0.02% In	1 M 30% H ₂ SO ₄	1/ 20 of S/L, 90 °C, 1h	87.3% In	Ag, Si	(Savvilotido u and Gidarakos, 2020)
Spent CIGS_CuIn _{0.5} Ga _{0.5} Se ₂	19% In 9% Ga	4 M H ₂ SO ₄	1/10 of S/L, 90 °C, 4 h after annealing with particle size <63 μm	98% In and Ga	Cu, Se	(Lv et al., 2019)
EoL CIGS panel_CuInGaSe ₂	600 In 90 Ga	1M citric acid and 0.4 M H ₂ O ₂	1/10 of S/L, 80 °C, 1 h	> 90% of In and Ga	Cu, Se	(Amato and Beolchini, 2019)
Alkali leaching process						
CIGS chamber waste		7 M NaOH	1/10 of S/L, 60 °C, 3 h	3.37% In 97.26% Ga	Cu	(Ma et al., 2020)
Indirect bioleaching-based process						
GaAs from solar cell waste		<i>Cellulosimicrobium funkei</i> (<i>C. funkei</i>)	Growth supernatant at death phase of <i>C. funkei</i> , 150 rpm agitation, pH 7, 30 °C, 15 days	70% Ga	As	(Maneesuwanarat, Vangnai et al., 2016)

1365

1366 3.4.2.1 Indium and gallium leaching with acids and alkali

1367 For CIS PVs, Savvilotidou and Gidarakos (2020) reported that efficient leaching of indium
 1368 (87.3% of leaching efficiency) from CIS PVs using sulfuric acid under optimal conditions of a
 1369 S/L ratio of 1/20 g/mL at 90 °C for 1 h after thermal pre-treatment and gravimetric separation.
 1370 The same leaching technique was also used for indium recovery from LCDs (Savvilotidou et
 1371 al., 2015).

1372 For CIGS PVs, the complexity of their structure, as well as the presence of numerous metals,
 1373 makes the leaching of indium and gallium more challenging. To address this challenge,
 1374 recovery methods combining pyrometallurgical and hydrometallurgical approaches have been
 1375 employed (Lv et al., 2019; Ma et al., 2020). In the hydrometallurgical leaching process, H₂SO₄
 1376 was used to leach indium and gallium after annealing, and approximately 98% of indium and

1377 gallium could be leached from spent CIGS panels under optimal conditions of 4 M H₂SO₄ (Lv
1378 et al., 2019).

1379 Other studies have tested different strong mineral acids (i.e. HCl, H₂SO₄, HNO₃) and organic
1380 acids (i.e. citric acid) as leachants in the presence of mobilizing agents, such as H₂O₂ and
1381 glucose (Amato and Beolchini, 2019). The results suggest that leaching indium and gallium
1382 from EoL CIGS PVs using citric acid and H₂O₂ as a catalyst could lead to high leaching yields
1383 of more than 90% at a temperature of 80 °C within 1 h. The use of glucose as a mobilizing
1384 agent in combination with citric acid further improved the leaching yield to over 70% in 3 h,
1385 while only citric acid leaching achieved a leaching yield of 40% (Amato and Beolchini, 2019).
1386 Furthermore, Ma et al. (2020) reported the use of NaOH to separate indium and gallium from
1387 indium gallium oxides based on their different dissolution characteristics. The results showed
1388 that using a concentration of 7 M NaOH obtained dissolution yields of indium and gallium of
1389 3.37% and 97.26%, respectively. This indicates that a high concentration of NaOH has a strong
1390 selectivity for separating indium and gallium, providing a promising method for their future
1391 recovery.

1392 **3.4.2.2 Indium and gallium bioleaching**

1393 Bioleaching has emerged as a promising and environmentally friendly method for recovering
1394 indium and gallium from EoL PVs. While research in this field is limited, Maneesuwanarat,
1395 Vangnai, et al. (2016) have made significant strides by investigating the use of microorganisms
1396 to leach gallium from GaAs scraps found in solar cells. Their study showed the potential of
1397 *Cellulosimicrobium funkei* (*C. funkei*) growth medium supernatant for gallium leaching. The
1398 presence of various amino acids produced and released by *C. funkei* in the growth medium
1399 supernatant was found to contribute to the leaching process based on the ability of *C. funkei* to
1400 solubilize gallium from GaAs by producing both organic acids and metabolites that can oxidize
1401 or reduce gallium ions. Encouragingly, the research successfully demonstrated the leaching of
1402 indium from thin-film GaAs solar cell waste using *C. funkei*, offering a promising and eco-
1403 friendly approach. Despite the lengthy incubation period of 15 days, the gallium leaching
1404 efficiency remained noteworthy, reaching approximately 70%. Nevertheless, further research
1405 is needed to fully uncover the potential of bioleaching in the recovery of indium and gallium
1406 from EoL PV panels.

1407 **3.4.3 Indium and gallium recovery from EoL PVs via hydrometallurgical and** 1408 **biohydrometallurgical routes**

1409 The recovery of valuable metals such as indium and gallium from EoL PVs (CIS and CIGS) is
1410 essential to meet the growing demand for these metals in various applications. Several methods
1411 have been proposed in the literature to achieve this goal, including hydrometallurgical and
1412 biohydrometallurgical routes. This section summarizes some of the main methods reported in
1413 the peer-reviewed literature.

1414 For CIS photovoltaic panel leachates, Savvilotidou and Gidaracos (2020) achieved indium
1415 recovery by adjusting the pH to 7.0-7.2 using NH_4OH solution for 24 h. They recovered 74.8%
1416 of pure indium hydroxide. Similarly, Van den Bossche et al. (2019) reported that more than
1417 99% of the indium could be precipitated by the addition of NaOH after the removal of gallium.

1418 In the case of CIGS material leachate, indium, and gallium were separated from copper by
1419 precipitation using NH_4OH solution due to the different precipitation pH values of the metals.
1420 Lv et al. (2019) achieved a precipitation efficiency of 99.6% for indium and 99.5% for gallium
1421 under optimal conditions of pH 3.5 within 400 rpm stirring at a temperature of 50 °C. The
1422 precipitates were then roasted at 800 °C to obtain indium and gallium oxide. The solubility
1423 constants of the different products (Cu, Ga, and In) are:

$$1424 \quad \text{Cu}(\text{OH})_2 \quad K_{sp} = 2.2 \times 10^{-20} \quad (20)$$

$$1425 \quad \text{Ga}(\text{OH})_3 \quad K_{sp} = 7.0 \times 10^{-36} \quad (21)$$

$$1426 \quad \text{In}(\text{OH})_3 \quad K_{sp} = 6.3 \times 10^{-34} \quad (22)$$

1427 However, it is difficult to achieve selective precipitation of indium and gallium due to the low
1428 solubility constants mentioned above. Therefore, solvent extraction was tested for the
1429 separation of indium and gallium after the removal of other metals, such as selenium and copper.
1430 Using di-(2-ethylhexyl) phosphoric acid (P204) as an extractant and kerosene as a diluent, Lv
1431 et al. (2019) were able to separate indium and gallium with high recovery efficiencies of 97.7%
1432 and 97.4%, respectively.

1433 To obtain pure gallium from spent PVs, electrolysis is always used after extraction by
1434 hydrometallurgical techniques. Chen et al. (2011) tested nickel-copper and platinum-stainless
1435 steel electrolysis to increase the gallium recovery efficiency from GaAs waste of silicon wafer
1436 fabs. The results show that the use of platinum-stainless steel could achieve more than 90% of
1437 gallium with a purity of 94%, while electrolysis with nickel-copper achieved a recovery yield
1438 of 56% of gallium with a purity of 92%. Therefore, platinum-stainless steel electrolysis would
1439 be a promising extraction method for gallium recovery that can contribute to significant
1440 economic gains in manufacturing.

1441 **3.5 Germanium recovery from EoL OFs via hydrometallurgical routes**

1442 In the global germanium market, nearly 30% of the total amount of germanium is supplied by
1443 obsolete products, particularly from the recycling of electronic devices. Recently, due to the
1444 rapid development of optical technologies has increased the demand for fiber optic cables
1445 containing germanium (Chen et al., 2017; Ruiz et al., 2018). Meanwhile, germanium is
1446 expected to increase in EoL products that can be recycled in the next two decades, as the
1447 lifetime of related electrical and electronic equipment is about 20 years. Therefore, the
1448 recycling of germanium from EoL OFs is seen as an encouraging way to obtain more
1449 germanium and reduce the tension caused by the scarcity of germanium sources. Considering
1450 the limited previous research on biohydrometallurgy, this section focuses only on exploring
1451 hydrometallurgical routes for germanium recovery from EoL optical fibers.

1452 **3.5.1 Pre-treatment of end-of-life OFs**

1453 There is a lack of comprehensive reports in the literature on the pre-treatment of spent optical
1454 fibers (OFs). However, a noteworthy study by Chen et al. (2017) provides a detailed method
1455 for a two-step pre-treatment approach. First, the samples were cut into 1-meter-long pieces
1456 using an electric saw. Next, a stripping machine was used to separate the pieces into different
1457 sections, including fibers, steel wires, plastic sheaths, and reinforcements. This process allowed
1458 the removal of the plastic sheaths, resulting in fiber bundle tubes consisting of glass fibers
1459 coated with acrylic resin. In the second pre-treatment step, fibers from the bundle tubes were
1460 ground to fine powder. This facilitated compositional analysis and served to streamline the
1461 subsequent leaching and extraction processes. In a more recent study, Chen et al. (2020)
1462 investigated the use of organic solvents such as acetone and ethanol to soften the plastics
1463 adhering to the fiber bundle tubes. The aim of this method was to obtain relatively pure glass
1464 fibers, as a plastic coating of more than 50% was found to be detrimental to germanium
1465 recovery efficiency. Overall, the research efforts of Chen et al. (2017, 2018b, 2020) shed light
1466 on the pre-treatment of spent OFs by providing a comprehensive methodology involving the
1467 removal of plastic sheaths and the extraction of glass fibers. The subsequent investigation of
1468 organic solvents for plastic softening further contributes to optimizing the recovery efficiency
1469 of valuable components from spent OFs.

1470 **3.5.2 Germanium leaching from OFs via hydrometallurgical routes**

1471 3.5.2.1 Germanium leaching with mineral acids

1472 After the pre-treatment of the sample, there are two different ways to leach germanium from
1473 spent OFs (Table 11) (Chen et al., 2017, 2018b, 2020). One is directly leaching by mineral
1474 acids, such as HCl, H₂SO₄, HNO₃, and HF. Considering the fact that decreased germanium
1475 leaching efficiency and the formation of germanium oxide precipitation in a strong acid
1476 solution, 0.1 M H₂SO₄ solution was studied as a leachant (Chen et al., 2017, 2018b, 2020).
1477 Since germanium is evenly distributed in materials and doped in silicon, it is necessary to
1478 remove or dissolve silicon before recovering germanium (Chen et al., 2018b). In the leaching
1479 process, hydrofluoric acid was added to dissolve silicon to extract germanium, as silicon only
1480 reacts with hydrofluoric acid. The optimal conditions for germanium and silicon leaching
1481 efficiency were achieved by adjusting the S/L ratio to 1/100 g/mL, at a temperature of 25 °C
1482 for 3 h and using mixed acids of 0.1M H₂SO₄ and 5% v/v HF, resulting in yields of 98.3% and
1483 99.5% for germanium and silicon, respectively (Chen et al., 2017).

1484 There is an alternative leaching method that involves alkali roasting followed by dilute sulfuric
1485 acid leaching. The alkali roasting process converts silica into a soluble form of silicate using
1486 chemicals such as NaOH and KOH at a temperature of 500 °C within 2 h. The results show
1487 that leaching efficiency was greater than 99.5% when the pH value was lower than 5. This is
1488 because several tests show that germanium and silicon would precipitate as the pH approaches
1489 neutral (Chen et al., 2018b).

1490 However, the use of hydrofluoric acid in direct leaching and roasting prior to acid leaching has
1491 potential drawbacks, such as environmental pollution and increased energy requirements.

1492

1493 Table 11 Methods for germanium leaching and recovery from spent OFs and associated
 1494 leachates

E-waste	Method	Leachant/Extractant	Optimum conditions (S/L: g/mL; O/A: organic/aqueous phase)	Ge leaching yield	Other metals	Reference
Waste fiber optic cables	Acid leaching	0.1 M H ₂ SO ₄ 5% v/v HF	1/100 of S/L, 25 °C, 3 h	98.3% (100 mg/L) Ge and 99.5% Si leaching		(Chen et al., 2017)
	Solvent extraction	0.1 M Trioctylamine (TOA) diluted into kerosene and mixed with 0.2 M tri-n-butyl phosphate (TBP), NaOH	Tartaric acid-germanium mole ratio of 1/4, 1/5 of O/A, pH 2, 5 min of extraction; 1.5 M NaOH, 1/1 of O/A, 5 min of stripping	91.3% extraction, 99.2% stripping	Si, Fe, Mg, and Ca	
Waste optical fibers	Roasting and acid leaching	NaOH, for roasting H ₂ SO ₄ for leaching	NaOH/SiO ₂ mole ratio of 6, 500 °C, 2 h for roasting; 1/40 of S/L, pH < 5 for leaching	> 99.5% Ge leaching		(Chen et al., 2018b)
	Solid-phase extraction	IRA900 resin and citric acid for extraction, 1 M HCl for stripping	Citric acid/Ge molar ratio of 4, pH 3 for extracting; 25 °C for stripping	92% extraction 99% stripping	Si, Fe, Mg, and Ca	

1495

1496 3.5.3 Germanium recovery from OFs via hydrometallurgical routes

1497 3.5.3.1 Solvent extraction

1498 Trioctylamine (TOA) has been found to be an effective and cost-effective extractant for
 1499 germanium recovery (Table 11) (Chen et al., 2017). Prior to extracting germanium from
 1500 leachate, the addition of tartaric acid, which reacts with germanium to form anion complexes,
 1501 could improve the efficiency of germanium extraction by increasing the ionic radius of the
 1502 complexes. Although silicon could react with tartaric acid, its extraction rate was slow and
 1503 negligible under the given reaction conditions of acid concentration and time. TOA as an
 1504 extractant was mixed with kerosene while adding tri-n-butyl phosphate (TBP), which could
 1505 avoid forming the third phase when separating germanium from silicon. The results showed
 1506 that under optimal conditions (pH 2, organic/aqueous phase ratio of 1/5, TOA and TBP
 1507 concentration of 0.1 M and 0.2 M, tartaric acid/germanium molar ratio of 5 in 5 min), the
 1508 germanium recovery efficiency could reach 91.3%, while the silicon extraction efficiency is

1509 less than 10%. After stripping with NaOH or chloride distillation, more than 99% of the
1510 germanium was recovered with GeO₂ or GeCl₄ (Chen et al., 2017).

1511 **3.5.3.2 Solid-phase extraction**

1512 Germanium could be efficiently adsorbed by anionic resins, such as amberlite IRA900 Cl⁻ and
1513 amberlite IRA958 Cl⁻ (Table 11) (Chen et al., 2018b). Therefore, anionic resins could be used
1514 to extract germanium with an agent of citric acid, which could react with germanium and form
1515 anion complexes. Chen et al. (2018b) reported the recovery of germanium from spent OFs
1516 using the anion resin IRA900 (Alfa-Aesar) in combination with citric acid agents. Germanium
1517 could be adsorbed in IRA900, while other metals, such as silicon and sodium, were hardly
1518 absorbed at the pH of 3. The sorption efficiency for germanium was found to be 92%, which
1519 was higher than that of other metals. By using HCl, 99% of the germanium could be removed
1520 from the resin. Finally, the concentration and calcination of the stripped germanium led to the
1521 production of GeO₂ with a purity of 99% at 500 °C.

1522 **4 Further research perspectives**

- 1523 1) Expanded research on EoL products as a secondary resource: There is limited research
1524 regarding the recovery of indium, gallium, and germanium from EoL products like PVs
1525 and OFs. While considerable research has been conducted on metal recovery from primary
1526 resources and related industrial wastes, more attention should be directed towards
1527 developing efficient and sustainable recovery methods for these TCEs from secondary
1528 waste streams like e-waste, not only limited to LCDs, LEDs, PVs, and OFs.
- 1529 2) Exploring specific pre-treatment methods: We emphasize the need for exploring specific
1530 pre-treatment methods for different electronic waste. The existing literature often lacks
1531 comprehensive pre-treatment approaches, mainly focusing on specific research targets. For
1532 example, pre-treatment methods for waste LCDs are well-established, but spent LEDs
1533 require more research due to their complex structures of different LED types and limited
1534 concentration methods for the target elements. Additionally, there is a research gap in pre-
1535 treatment methods for waste PVs and OFs. We encourage further research to develop
1536 efficient and customized pre-treatment methods for these specific targets.
- 1537 3) Improvement of biohydrometallurgical processes: Biohydrometallurgy shows great
1538 promise as an environmentally friendly approach for recovering indium, gallium, and
1539 germanium. However, the implementation of biohydrometallurgical processes for these
1540 TCEs from secondary products is still limited and poorly described in previous research.

1541 Further investigation and optimization of these eco-friendly methods are essential to
1542 facilitate the "closing the loop" in the recycling of EoL products and ensure a circular
1543 economy for TCEs.

1544 4) Technology integration: In order to achieve sustainable metal recovery from e-waste, it is
1545 crucial to integrate and combine various recovery technologies effectively with the
1546 development of a suitable flowsheet for circular hydrometallurgy (Binnemans & Jones,
1547 2022). In addition, developing integrated processes that combine hydrometallurgical and
1548 biohydrometallurgical methods can enhance metal recovery efficiency, minimize
1549 environmental impact, and maximize mass, energy, space, and time efficiency, like indirect
1550 bioleaching and biorecovery of gallium by using siderophores.

1551 **5 Conclusions**

1552 This review highlights the critical importance of indium, gallium, and germanium in high-tech
1553 applications. Sustainable recovery methods from EoL products like LCDs, LEDs, and OFs are
1554 being investigated, providing viable solutions to address supply shortages in the EU
1555 manufacturing industry and highlighting the potential of EoL products as secondary sources.
1556 Waste LCDs contain significant indium, waste LEDs offer promising gallium sources, waste
1557 PVs contain indium and gallium, and spent OFs can be a secondary source of germanium.
1558 These EoL products offer viable pathways to mitigate TCEs supply shortages.

1559 The recovery of indium, gallium, and germanium from EoL products primarily involves
1560 hydrometallurgical and biohydrometallurgical methods, which outcompete pyrometallurgical
1561 approaches in terms of performance. The hydrometallurgical approach includes leaching with
1562 mineral and organic acids, followed by selective recovery through various extraction methods,
1563 with pH, leaching agent, reaction time, temperature, and agitation rate being critical operating
1564 factors. Biohydrometallurgy, which employs microorganisms for selective metal recovery,
1565 holds promise as an eco-friendly EoL product recycling technique, but further research is
1566 necessary before full-scale implementation.

1567 Regarding the recovery of indium from EoL LCDs, pre-treatment involves manual dismantling
1568 and comminution to access the ITO film and concentrate indium. Various leaching methods,
1569 including strong mineral acids, organic acids (oxalic acid), and bioleaching (*A. ferrooxidans*
1570 and *A. thiooxidans*), are explored, achieving a high leaching yield (more than 95% in optimal
1571 conditions). Solvent extraction with DEHPA and D₂EHPA, precipitation with ammonium
1572 hydroxide, and cementation with zinc powder are effective extraction methods, but challenges
1573 remain in separating other elements from indium, like Al, Fe, Zn, and Sn. Solid-phase

1574 extraction, electrochemical separation, and supercritical fluid extraction show promise for high
1575 purification. Further research is needed to optimize these techniques for sustainable indium
1576 recycling.

1577 Recovering gallium from EoL LEDs presents challenges but is crucial due to its value as a
1578 metal source. Pre-treatment is vital for dissociating complex LED structures, with careful
1579 handling of toxic arsenic in GaAs LEDs and Na₂CO₃ annealing for GaN LEDs. Various
1580 leaching methods using strong mineral acids, alkaline leaching, and organic acids are being
1581 explored. HNO₃ and HCl were found to be effective for gallium recovery from GaAs and
1582 annealed GaN waste, respectively, achieving 99% leaching yield. Bioleaching with *A.*
1583 *ferrooxidans* shows promise. Solvent extraction and ionic liquid extraction offer high gallium
1584 purity but face non-target metal removal challenges. Nanofiltration, precipitation, and
1585 supercritical fluid separation provide sustainable options. Further optimization is needed for
1586 efficient and eco-friendly gallium recovery. The GaLIophore technology exhibits the potential
1587 for high gallium recovery from low concentration wastewater. Each method has distinct
1588 advantages and challenges, showing promise for sustainable gallium retrieval from discarded
1589 LEDs.

1590 Effective pre-treatment is essential for concentrating target metals from EoL PVs. For indium
1591 and gallium leaching, H₂SO₄ and citric acid with H₂O₂ demonstrated high leaching yields
1592 (around 90%) for CIGS PVs. NaOH alkali leaching showed a 97% yield for gallium. Indirect
1593 bioleaching with *C. funkei* showed potential, achieving approximately 70% gallium extraction
1594 yield. NH₄OH precipitation and solvent extraction with P204 achieved high efficiency in
1595 indium and gallium separated recovery (> 97%) from CIGS PVs. Platinum-stainless steel
1596 electrolysis exhibited promise for pure gallium extraction. Thus, developing efficient and eco-
1597 friendly methods is crucial to meet the demand for these valuable metals from EoL PVs.

1598 For the recovery of germanium from EoL OFs, pre-treatment involves removing plastic sheaths
1599 and extracting glass fibers to optimize the recovery process. Germanium leaching from waste
1600 OFs can be achieved using mineral acids or alkali roasting followed by acid leaching, with a
1601 high leaching yield of 98%. Hydrofluoric acid or alkali roasting effectively dissolves silicon,
1602 enabling efficient germanium extraction. In the extraction process, solvent extraction using
1603 TOA and tartaric acid shows promising results with a 91% germanium recovery rate and
1604 minimal silicon extraction (< 10%). Additionally, solid-phase extraction with anionic resins
1605 provides an effective method for selective germanium recovery from waste OFs. These
1606 hydrometallurgical routes offer environmentally friendly ways to obtain germanium from EoL
1607 OFs, contributing to sustainable resource utilization. Although biohydrometallurgical

1608 approaches have not been developed for EoL OFs at present, the development of this field is
1609 worth attention.

1610 Overall, the investigation of sustainable recovery technologies for indium, gallium, and
1611 germanium from EoL products is crucial for ensuring a stable and long-term supply of these
1612 TCEs for high-tech applications. Further advancements in the optimization and implementation
1613 of these recovery processes will contribute to efficient and environmentally friendly recycling
1614 of e-waste.

1615 **6 CRediT authorship contribution statement**

1616 **Kun Zheng:** Conceptualization, Data gathering, Writing – original draft, Writing – review &
1617 editing. **Marc F. Benedetti:** Conceptualization, Supervision, Writing – review & editing,
1618 Funding acquisition. **Eric D. van Hullebusch:** Conceptualization, Supervision, Writing –
1619 review & editing, Funding acquisition.

1620 **7 Declaration of Competing Interest**

1621 The authors declare that they have no known competing financial interests or personal
1622 relationships that could have appeared to influence the work reported in this paper.

1623 **8 Acknowledgments**

1624 The authors thank the Horizon 2020 ERA-MIN2 Project Siderophores assisted Biorecovery of
1625 Technology Critical Elements: Gallium (Ga), germanium (Ge), and indium (In) from end-of-
1626 life products - SIDEREC (Project ANR-19-MIN2-0001, 2019-2023) for financial support.

9 References

- Akcil, A., Agcasulu, I., & Swain, B. (2019). Valorization of waste LCD and recovery of critical raw material for circular economy: A review. *Resources, Conservation and Recycling*, *149*, 622–637. <https://doi.org/10.1016/j.resconrec.2019.06.031>
- Alfantazi, A. M., & Moskalyk, R. R. (2003). Processing of indium: A review. *Minerals Engineering*, *16*(8), 687–694. [https://doi.org/10.1016/S0892-6875\(03\)00168-7](https://doi.org/10.1016/S0892-6875(03)00168-7)
- Alguacil, F. J., & López, F. A. (2020). Dispersion-free extraction of In(III) from HCl solutions using a supported liquid membrane containing the HA324H+Cl⁻ ionic liquid as the carrier. *Scientific Reports*, *10*(1), 1–8. <https://doi.org/10.1038/s41598-020-70968-1>
- Amato, A., & Beolchini, F. (2019). End-of-life CIGS photovoltaic panel: A source of secondary indium and gallium. *Progress in Photovoltaics: Research and Applications*, *27*(3), 229–236. <https://doi.org/10.1002/pip.3082>
- Amthauer, G., Günzler, V., Hafner, S. S., & Reinen, D. (1982). The distribution of Fe³⁺ and Ga³⁺ between octahedral and tetrahedral sites in garnets, Y₃(Fe,Ga)₅O₁₂, at different temperatures. *Zeitschrift Fur Kristallographie - New Crystal Structures*, *161*(3–4), 167–186. <https://doi.org/10.1524/zkri.1982.161.3-4.167>
- Andrade, D. F., Machado, R. C., Bacchi, M. A., & Pereira-Filho, E. R. (2019). Proposition of electronic waste as a reference material-part 1: Sample preparation, characterization and chemometric evaluation. *Journal of Analytical Atomic Spectrometry*, *34*(12), 2394–2401. <https://doi.org/10.1039/c9ja00283a>
- Annoni, R., Lange, L. C., Santos Amaral, M. C., Silva, A. M., Assunção, M. C., Franco, M. B., & de Souza, W. (2020). Light emitting diode waste: Potential of metals concentration and acid reuse via the integration of leaching and membrane processes. *Journal of Cleaner Production*, *246*. <https://doi.org/10.1016/j.jclepro.2019.119057>
- Argenta, A. B., Reis, C. M., Mello, G. P., Dotto, G. L., Tanabe, E. H., & Bertuol, D. A. (2017). Supercritical CO₂ extraction of indium present in liquid crystal displays from discarded cell phones using organic acids. *Journal of Supercritical Fluids*, *120*, 95–101. <https://doi.org/10.1016/j.supflu.2016.10.014>
- Assefi, M., Maroufi, S., Nekouei, R. K., & Sahajwalla, V. (2018). Selective recovery of indium from scrap LCD panels using macroporous resins. *Journal of Cleaner Production*, *180*, 814–822. <https://doi.org/10.1016/j.jclepro.2018.01.165>
- Binnemans, K., & Jones, P. T. (2022). The Twelve Principles of Circular Hydrometallurgy.

- Bleiwas, D. I. (2010). Byproduct mineral commodities used for the production of photovoltaic cells. *US Geological Survey Circular*, 1365, 1–10. <https://doi.org/10.3133/cir1365>
- Bumba, J., Dytrych, P., Fajgar, R., Kastanek, F., & Solcova, O. (2018). Total Germanium Recycling from Electronic and Optical Waste [Research-article]. *Industrial and Engineering Chemistry Research*, 57(27), 8855–8862. <https://doi.org/10.1021/acs.iecr.8b01237>
- Cadore, J. S., Bertuol, D. A., & Tanabe, E. H. (2019). Recovery of indium from LCD screens using solid-phase extraction onto nanofibers modified with di-(2-ethylhexyl) phosphoric acid (DEHPA). *Process Safety and Environmental Protection*, 127, 141–150. <https://doi.org/10.1016/j.psep.2019.05.011>
- Castro, J. P., Pereira-Filho, E. R., & Bro, R. (2020). Laser-induced breakdown spectroscopy (LIBS) spectra interpretation and characterization using parallel factor analysis (PARAFAC): a new procedure for data and spectral interference processing fostering the waste electrical and electronic equipment (WEEE) . *Journal of Analytical Atomic Spectrometry*, 35(6), 1115–1124. <https://doi.org/10.1039/d0ja00026d>
- Chancerel, P., Rotter, V. S., Ueberschaar, M., Marwede, M., Nissen, N. F., & Lang, K. D. (2013). Data availability and the need for research to localize, quantify and recycle critical metals in information technology, telecommunication and consumer equipment. *Waste Management and Research*, 31, 3–16. <https://doi.org/10.1177/0734242X13499814>
- Charpentier Poncelet, A., Helbig, C., Loubet, P., Muller, S., Villeneuve, J., Laratte, B., Tuma, A., Sonnemann, G., Poncelet, A. C., Helbig, C., Loubet, P., Beylot, A., Poncelet, A. C., Helbig, C., Loubet, P., Beylot, A., Muller, S., Villeneuve, J., Laratte, B., ... Sonnemann, G. (2022). Losses and lifetimes of metals in the economy To cite this version : HAL Id : hal-03702553 Losses and lifetimes of metals in the economy. *Nature Sustainability*, 717–726.
- Chen, W., Chang, B. C., & Chiu, K. L. (2017). Recovery of germanium from waste Optical Fibers by hydrometallurgical method. *Journal of Environmental Chemical Engineering*, 5(5), 5215–5221. <https://doi.org/10.1016/j.jece.2017.09.048>
- Chen, W., Chang, B., & Chen, Y. (2018b). Using Ion-Exchange to Recovery of Germanium from Waste Optical Fibers by Adding Citric Acid. *IOP Conference Series: Earth and Environmental Science*, 159(1). <https://doi.org/10.1088/1755-1315/159/1/012008>

- Chen, W., Chang, B., & Shuai, C. (2020). Improve subsequent leaching efficiency and extraction rate of germanium in optical fibre cables with pre-treatment. *IOP Conference Series: Materials Science and Engineering*, 720(1). <https://doi.org/10.1088/1757-899X/720/1/012005>
- Chen, W., Hsu, L., & Wang, L. (2018a). Recycling the GaN waste from LED industry by pressurized leaching method. *Metals*, 8(10), 1–12. <https://doi.org/10.3390/met8100861>
- Chen, W. T., Chu, Y. C., Wei, J. M., Tsai, L. C., Tsai, F. C., Lin, C. P., & Shu, C. M. (2011). Gallium and arsenic recovery from waste gallium arsenide by wet refined methods. *Advanced Materials Research*, 194–196, 2115–2118. <https://doi.org/10.4028/www.scientific.net/AMR.194-196.2115>
- Chen, W. T., Tsai, L. C., Tsai, F. C., & Shu, C. M. (2012). Recovery of Gallium and Arsenic from Gallium Arsenide Waste in the Electronics Industry. *Clean - Soil, Air, Water*, 40(5), 531–537. <https://doi.org/10.1002/clen.201100216>
- Choi, D., Kim, Y. S., & Son, Y. (2014). Recovery of indium tin oxide (ITO) and glass plate from discarded TFT-LCD panels using an electrochemical method and acid treatment. *RSC Advances*, 4(92), 50975–50980. <https://doi.org/10.1039/c4ra11085d>
- Choi, J. H., Kim, S. O., Hilton, D. L., & Cho, N. J. (2014). Acid-catalyzed kinetics of indium tin oxide etching. *Thin Solid Films*, 565, 179–185. <https://doi.org/10.1016/j.tsf.2014.06.053>
- Ciacchi, L., Werner, T. T., Vassura, I., & Passarini, F. (2019). Backlighting the European Indium Recycling Potentials. *Journal of Industrial Ecology*, 23(2), 426–437. <https://doi.org/10.1111/jiec.12744>
- Cui, J., Zhu, N., Li, Y., Luo, D., Wu, P., & Dang, Z. (2020). Rapid and green process for valuable materials recovery from waste liquid crystal displays. *Resources, Conservation and Recycling*, 153, 104544. <https://doi.org/10.1016/j.resconrec.2019.104544>
- Cui, J., Zhu, N., Luo, D., Li, Y., Wu, P., Dang, Z., & Hu, X. (2019). The Role of Oxalic Acid in the Leaching System for Recovering Indium from Waste Liquid Crystal Display Panels [Research-article]. *ACS Sustainable Chemistry and Engineering*, 7(4), 3849–3857. <https://doi.org/10.1021/acssuschemeng.8b04756>
- Cui, J., Zhu, N., Mao, F., Wu, P., & Dang, Z. (2021). Biobleaching of indium from waste LCD panels by *Aspergillus niger*: Method optimization and mechanism analysis. *Science of the Total Environment*, 790, 148151. <https://doi.org/10.1016/j.scitotenv.2021.148151>

- de Oliveira, R. P., Benvenuti, J., & Espinosa, D. C. R. (2021). A review of the current progress in recycling technologies for gallium and rare earth elements from light-emitting diodes. *Renewable and Sustainable Energy Reviews*, *145*, 111090. <https://doi.org/10.1016/j.rser.2021.111090>
- Dhiman, S., & Gupta, B. (2020). Cyphos IL 104 assisted extraction of indium and recycling of indium, tin and zinc from discarded LCD screen. *Separation and Purification Technology*, *237*, 116407. <https://doi.org/10.1016/j.seppur.2019.116407>
- Dodson, J. R., Hunt, A. J., Parker, H. L., Yang, Y., & Clark, J. H. (2012). Elemental sustainability: Towards the total recovery of scarce metals. *Chemical Engineering and Processing: Process Intensification*, *51*, 69–78. <https://doi.org/10.1016/j.cep.2011.09.008>
- Elshkaki, A., & Graedel, T. E. (2013). Dynamic analysis of the global metals flows and stocks in electricity generation technologies. *Journal of Cleaner Production*, *59*, 260–273. <https://doi.org/10.1016/j.jclepro.2013.07.003>
- Erüst, C., Akcil, A., Gahan, C. S., Tuncuk, A., & Deveci, H. (2013). Biohydrometallurgy of secondary metal resources: A potential alternative approach for metal recovery. *Journal of Chemical Technology and Biotechnology*, *88*(12), 2115–2132. <https://doi.org/10.1002/jctb.4164>
- European Commission. (2011). *Role of critical metals in the future markets of clean energy technologies A Roadmap for moving to a competitive low carbon economy in 2050*. 95, 53–62. <https://doi.org/10.1016/j.renene.2016.03.102>
- European Commission. (2020). *Critical Raw Materials Factsheets (2020)*. <https://doi.org/10.2873/92480>
- Fang, S., Tao, T., Cao, H., Zheng, X., Hu, Y., Zhang, Y., & Sun, Z. (2019). Selective Recovery of Gallium (Indium) from Metal Organic Chemical Vapor Deposition Dust - A Sustainable Process. *ACS Sustainable Chemistry and Engineering*, *7*(10), 9646–9654. <https://doi.org/10.1021/acssuschemeng.9b01228>
- Ferella, F., Belardi, G., Marsilii, A., De Michelis, I., & Vegliò, F. (2016). Separation and recovery of glass, plastic and indium from spent LCD panels. *Waste Management*, *60*, 569–581. <https://doi.org/10.1016/j.wasman.2016.12.030>
- Filella, M., & May, P. M. (2023). The aqueous solution chemistry of germanium under conditions of environmental and biological interest: Inorganic ligands. *Applied Geochemistry*, *155*(January), 105631. <https://doi.org/10.1016/j.apgeochem.2023.105631>

- Fontana, D., Forte, F., Pietrantonio, M., & Pucciarmati, S. (2020). Recent developments on recycling end-of-life flat panel displays: A comprehensive review focused on indium. *Critical Reviews in Environmental Science and Technology*, 1–28. <https://doi.org/10.1080/10643389.2020.1729073>
- Fontana, Danilo, Forte, F., De Carolis, R., & Grosso, M. (2015). Materials recovery from waste liquid crystal displays: A focus on indium. *Waste Management*, 45, 325–333. <https://doi.org/10.1016/j.wasman.2015.07.043>
- Forti, V., Baldé, C. P., Kuehr, R., & Bel, G. (2020). *old_The Global E-waste Monitor 2020: Quantities, flows, and the circular economy potential*.
- Frenzel, M., Mikolajczak, C., Reuter, M. A., & Gutzmer, J. (2017). Quantifying the relative availability of high-tech by-product metals – The cases of gallium, germanium and indium. *Resources Policy*, 52, 327–335. <https://doi.org/10.1016/j.resourpol.2017.04.008>
- Gabriel, A. P., Baggio Giordani, B., Kasper, A., & Veit, H. M. (2018). Indium Extraction From Lcd Screens. *Detritus*, 1, 1. <https://doi.org/10.31025/2611-4135/2018.13704>
- Gabriel, A. P., Kasper, A. C., & Veit, H. M. (2020). Acid leaching of indium from the screens of obsolete LCD monitors. *Journal of Environmental Chemical Engineering*, 8(3), 103758. <https://doi.org/10.1016/j.jece.2020.103758>
- Gómez, M., Xu, G., Li, J., & Zeng, X. (2023). Securing Indium Utilization for High-Tech and Renewable Energy Industries. *Environmental Science and Technology*. <https://doi.org/10.1021/acs.est.2c07169>
- Grimes, S. M., Yasri, N. G., & Chaudhary, A. J. (2017). Recovery of critical metals from dilute leach solutions – Separation of indium from tin and lead. *Inorganica Chimica Acta*, 461, 161–166. <https://doi.org/10.1016/j.ica.2017.02.002>
- Gu, S., Fu, B., Dodbiba, G., Fujita, T., & Fang, B. (2018). Promising Approach for Recycling of Spent CIGS Targets by Combining Electrochemical Techniques with Dehydration and Distillation. *ACS Sustainable Chemistry and Engineering*, 6(5), 6950–6956. <https://doi.org/10.1021/acssuschemeng.8b00787>
- Gunn, G. (2014). Critical Metals Handbook. In G. Gunn (Ed.), *Critical Metals Handbook*. <https://doi.org/10.1002/9781118755341.ch14>
- Gupta, B., Mudhar, N., & Singh, I. (2007). Separations and recovery of indium and gallium using bis(2,4,4-trimethylpentyl)phosphinic acid (Cyanex 272). *Separation and Purification Technology*, 57(2), 294–303. <https://doi.org/10.1016/j.seppur.2007.04.011>

- Hamidnia, M., Luo, Y., & Wang, X. D. (2018). Application of micro/nano technology for thermal management of high power LED packaging – A review. *Applied Thermal Engineering*, *145*, 637–651. <https://doi.org/10.1016/j.applthermaleng.2018.09.078>
- Harper, E. M., Kavlak, G., Burmeister, L., Eckelman, M. J., Erbis, S., Sebastian Espinoza, V., Nuss, P., & Graedel, T. E. (2015). Criticality of the Geological Zinc, Tin, and Lead Family. *Journal of Industrial Ecology*, *19*(4), 628–644. <https://doi.org/10.1111/jiec.12213>
- Hoang Huy, V. P., Kim, I. T., & Hur, J. (2022). Gallium-Telluride-Based Composite as Promising Lithium Storage Material. *Nanomaterials*, *12*(19). <https://doi.org/10.3390/nano12193362>
- Hofmann, M., Retamal-Morales, G., & Tischler, D. (2020). Metal binding ability of microbial natural metal chelators and potential applications. *Natural Product Reports*. <https://doi.org/10.1039/C9NP00058E>
- Höll, R., Kling, M., & Schroll, E. (2007). Metallogenesis of germanium-A review. *Ore Geology Reviews*, *30*(3–4), 145–180. <https://doi.org/10.1016/j.oregeorev.2005.07.034>
- Houssaine Moutiy, E., Tran, L. H., Mueller, K. K., Coudert, L., & Blais, J. F. (2020). Optimized indium solubilization from LCD panels using H₂SO₄ leaching. *Waste Management*, *114*, 53–61. <https://doi.org/10.1016/j.wasman.2020.07.002>
- Hu, S., Xie, M., & Hsieh, Y. (2014). Resource Recycling of Gallium Arsenide Scrap Using Leaching-Selective Precipitation. *Environmental Progress & Sustainable Energy*, *33*(3), 676–680. <https://doi.org/10.1002/ep>
- Işıldar, A., van Hullebusch, E. D., Lenz, M., Du Laing, G., Marra, A., Cesaro, A., Panda, S., Akcil, A., Kucuker, M. A., & Kuchta, K. (2019). Biotechnological strategies for the recovery of valuable and critical raw materials from waste electrical and electronic equipment (WEEE) – A review. *Journal of Hazardous Materials*, *362*, 467–481. <https://doi.org/10.1016/j.jhazmat.2018.08.050>
- Jain, R., Fan, S., Kaden, P., Tsushima, S., Foerstendorf, H., Barthen, R., Lehmann, F., & Pollmann, K. (2019). Recovery of gallium from wafer fabrication industry wastewaters by Desferrioxamine B and E using reversed-phase chromatography approach. *Water Research*, *158*(2019), 203–212. <https://doi.org/10.1016/j.watres.2019.04.005>
- Jowkar, M. J., Bahaloo-Horeh, N., Mousavi, S. M., & Pourhossein, F. (2017). Old-Bioleaching of indium from discarded liquid crystal displays. *Journal of Cleaner Production*, *180*, 417–429. <https://doi.org/10.1016/j.jclepro.2018.01.136>

- Jowkar, M. J., Bahaloo-Horeh, N., Mousavi, S. M., & Pourhossein, F. (2018). Bioleaching of indium from discarded liquid crystal displays. *Journal of Cleaner Production*, *180*, 417–429. <https://doi.org/10.1016/J.JCLEPRO.2018.01.136>
- Kang, H. N., Lee, J. Y., & Kim, J. Y. (2011). Recovery of indium from etching waste by solvent extraction and electrolytic refining. *Hydrometallurgy*, *110*(1–4), 120–127. <https://doi.org/10.1016/j.hydromet.2011.09.009>
- Kim, C. W., Park, G. Y., Shin, J. C., & Kim, H. J. (2022). Efficiency Enhancement of GaAs Single-Junction Solar Cell by Nanotextured Window Layer. *Applied Sciences (Switzerland)*, *12*(2). <https://doi.org/10.3390/app12020601>
- Kot-Niewiadomska, A., Mineral, T., Guzik, K., & Mineral, T. (2022). *Safeguarding of mineral deposits as the basis of European Union raw materials security in the era of unstable geopolitical conditions*. <https://doi.org/10.5593/sgem2022/1.1/s03.046>
- Krishna Rama, C., Mulcahy, J., & O’donoghue, L. (2015). Investigation of Indium Recovery from End-of-life LCDs. *EPA Research Report-Krishna et Al. 2015*, 294. www.epa.ie
- Křištofová, P., Rudnik, E., & Miškufová, A. (2016). Hydrometallurgical Methods of Indium Recovery From Obsolete Lcd and Led Panels. *Metallurgy and Foundry Engineering*, *42*(3), 157. <https://doi.org/10.7494/mafe.2016.42.3.157>
- Lee, C. H., Jeong, M. K., Fatih Kilicaslan, M., Lee, J. H., Hong, H. S., & Hong, S. J. (2013). Recovery of indium from used LCD panel by a time efficient and environmentally sound method assisted HEBM. *Waste Management*, *33*(3), 730–734. <https://doi.org/10.1016/j.wasman.2012.10.002>
- Lee, H. S., & Nam, C. W. (1998). A study on the extraction of gallium from gallium arsenide scrap. *Hydrometallurgy*, *49*(1–2), 125–133. [https://doi.org/10.1016/s0304-386x\(98\)00016-4](https://doi.org/10.1016/s0304-386x(98)00016-4)
- Li, J., Gao, S., Duan, H., & Liu, L. (2009). Recovery of valuable materials from waste liquid crystal display panel. *Waste Management*, *29*(7), 2033–2039. <https://doi.org/10.1016/j.wasman.2008.12.013>
- Li, Y., Zhu, N., Wei, X., Cui, J., Wu, P., Li, P., Wu, J., & Lin, Y. (2020). Leaching of indium from waste LCD screens by oxalic acid in temperature-controlled aciduric stirred reactor. *Process Safety and Environmental Protection*, *133*, 137–148. <https://doi.org/10.1016/j.psep.2019.10.026>
- Licht, C., Peiró, L. T., & Villalba, G. (2015). Global substance flow analysis of gallium,

- germanium, and indium: Quantification of extraction, uses, and dissipative losses within their anthropogenic cycles. *Journal of Industrial Ecology*, 19(5), 890–903. <https://doi.org/10.1111/jiec.12287>
- Lokanc, M., Eggert, R., & Redlinger, M. (2015). The Availability of Indium: The Present, Medium Term, and Long Term. *National Renewable Energy Laboratory, No. NREL/S, 1–90*.
www.nrel.gov/publications.%0Awww.nrel.gov/publications.%0Awww.nrel.gov/publications.%0Ahttps://www.nrel.gov/docs/fy16osti/62409.pdf
- López-Yáñez, A., Alonso, A., Vengoechea-Pimienta, A., & Ramírez-Muñoz, J. (2019). Indium and tin recovery from waste LCD panels using citrate as a complexing agent. *Waste Management*, 96, 181–189. <https://doi.org/10.1016/j.wasman.2019.07.030>
- Lu, F., Xiao, T., Lin, J., Ning, Z., Long, Q., Xiao, L., Huang, F., Wang, W., Xiao, Q., Lan, X., & Chen, H. (2017). Resources and extraction of gallium: A review. *Hydrometallurgy*, 174, 105–115. <https://doi.org/10.1016/j.hydromet.2017.10.010>
- Luo, D., Zhu, N., Li, Y., Cui, J., Wu, P., & Wang, J. (2019). Simultaneous leaching and extraction of indium from waste LCDs with acidic ionic liquids. *Hydrometallurgy*, 189, 105146. <https://doi.org/10.1016/j.hydromet.2019.105146>
- Lu, Y., Xing, P., Ma, B., Liu, B., Wang, C., Zhang, Y., & Zhang, W. (2019). Separation and Recovery of Valuable Elements from Spent CIGS Materials [Research-article]. *ACS Sustainable Chemistry and Engineering*, 7, 19816–19823. <https://doi.org/10.1021/acssuschemeng.9b05121>
- Ma, B., Li, X., Liu, B., Xing, P., Zhang, W., Wang, C., & Chen, Y. (2020). Effective Separation and Recovery of Valuable Components from CIGS Chamber Waste via Controlled Phase Transformation and Selective Leaching [Research-article]. *ACS Sustainable Chemistry & Engineering*, 8, 3026–3037. <https://doi.org/10.1021/acssuschemeng.0c00138>
- Ma, E., & Xu, Z. (2013). Technological process and optimum design of organic materials vacuum pyrolysis and indium chlorinated separation from waste liquid crystal display panels. *Journal of Hazardous Materials*, 263, 610–617. <https://doi.org/10.1016/j.jhazmat.2013.10.020>
- Maarefvand, M., Sheibani, S., & Rashchi, F. (2020). Recovery of gallium from waste LEDs by oxidation and subsequent leaching. *Hydrometallurgy*, 191, 105230. <https://doi.org/10.1016/j.hydromet.2019.105230>
- Maneesuwannarat, S., Teamkao, P., Vangnai, A. S., Yamashita, M., & Thiravetyan, P. (2016).

- Possible mechanism of gallium bioleaching from gallium nitride (GAN) by *Arthrobacter creatinolyticus*: Role of amino acids/peptides/proteins bindings with gallium. *Process Safety and Environmental Protection*, 103, 36–45. <https://doi.org/10.1016/j.psep.2016.06.036>
- Maneesuwanarat, S., Vangnai, A. S., Yamashita, M., & Thiravetyan, P. (2016). Bioleaching of gallium from gallium arsenide by *Cellulosimicrobium funkei* and its application to semiconductor/electronic wastes. *Process Safety and Environmental Protection*, 99, 80–87. <https://doi.org/10.1016/j.psep.2015.10.008>
- Mejías, O., Parbhakar-Fox, A., Jackson, L., Valenta, R., & Townley, B. (2023). Indium in ore deposits and mine waste environments: Geochemistry, mineralogy, and opportunities for recovery. *Journal of Geochemical Exploration*, 107312. <https://doi.org/10.1016/j.gexplo.2023.107312>
- Mir, S., Vaishampayan, A., & Dhawan, N. (2022). A Review on Recycling of End-of-Life Light-Emitting Diodes for Metal Recovery. *Jom*, 74(2), 599–611. <https://doi.org/10.1007/s11837-021-05043-9>
- Nagao, M., Hayashi, A., & Tatsumisago, M. (2012). High-capacity Li 2S-nanocarbon composite electrode for all-solid-state rechargeable lithium batteries. *Journal of Materials Chemistry*, 22(19), 10015–10020. <https://doi.org/10.1039/c2jm16802b>
- Nagy, S., Bokányi, L., Gombkőto, I., & Magyar, T. (2017). Recycling of Gallium from End-of-Life Light Emitting Diodes. *Archives of Metallurgy and Materials*, 62(2), 1161–1166. <https://doi.org/10.1515/amm-2017-0170>
- Nancharaiah, Y. V., Mohan, S. V., & Lens, P. N. L. (2016). Biological and Bioelectrochemical Recovery of Critical and Scarce Metals. *Trends in Biotechnology*, 34(2), 137–155. <https://doi.org/10.1016/j.tibtech.2015.11.003>
- Nguyen, T. H., & Lee, M. S. (2019). A Review on Separation of Gallium and Indium from Leach Liquors by Solvent Extraction and Ion Exchange. *Mineral Processing and Extractive Metallurgy Review*, 40(4), 278–291. <https://doi.org/10.1080/08827508.2018.1538987>
- Nguyen, T. H., & Lee, M. S. (2021). A Review on Germanium Resources and its Extraction by Hydrometallurgical Method. *Mineral Processing and Extractive Metallurgy Review*, 42(6), 406–426. <https://doi.org/10.1080/08827508.2020.1756795>
- Nishida, Y., Nakane, K., & Satoh, T. (1997). Synthesis and properties of gallium-doped LiNiO₂ as the cathode material for lithium secondary batteries. *Journal of Power Sources*,

68(2), 561–564. [https://doi.org/10.1016/S0378-7753\(97\)02535-4](https://doi.org/10.1016/S0378-7753(97)02535-4)

- Ogi, T., Tamaoki, K., Saitoh, N., Higashi, A., & Konishi, Y. (2012). Recovery of indium from aqueous solutions by the Gram-negative bacterium *Shewanella algae*. *Biochemical Engineering Journal*, *63*, 129–133. <https://doi.org/10.1016/j.bej.2011.11.008>
- Pennesi, C., Amato, A., Occhialini, S., Critchley, A. T., Totti, C., Giorgini, E., Conti, C., & Beolchini, F. (2019). Adsorption of indium by waste biomass of brown alga *Ascophyllum nodosum*. *Scientific Reports*, *9*(1), 1–11. <https://doi.org/10.1038/s41598-019-53172-8>
- Pereira, E. B., Suliman, A. L., Tanabe, E. H., & Bertuol, D. A. (2018). Recovery of indium from liquid crystal displays of discarded mobile phones using solvent extraction. *Minerals Engineering*, *119*, 67–72. <https://doi.org/10.1016/j.mineng.2018.01.022>
- Pimputkar, S., Speck, J. S., Denbaars, S. P., & Nakamura, S. (2009). Prospects for LED lighting. *Nature Photonics*, *3*(4), 180–182. <https://doi.org/10.1038/nphoton.2009.32>
- Plotka-Wasyłka, J., Szczepańska, N., de la Guardia, M., & Namieśnik, J. (2016). Modern trends in solid phase extraction: New sorbent media. *TrAC - Trends in Analytical Chemistry*, *77*, 23–43. <https://doi.org/10.1016/j.trac.2015.10.010>
- Polman, A., Knight, M., Garnett, E. C., Ehrler, B., & Sinke, W. C. (2016). Photovoltaic materials: Present efficiencies and future challenges. *Science*, *352*(6283). <https://doi.org/10.1126/science.aad4424>
- Pourhossein, F., & Mousavi, S. M. (2018). Enhancement of copper, nickel, and gallium recovery from LED waste by adaptation of *Acidithiobacillus ferrooxidans*. *Waste Management*, *79*, 98–108. <https://doi.org/10.1016/j.wasman.2018.07.010>
- Pourhossein, F., & Mousavi, S. M. (2019). A novel step-wise indirect bioleaching using biogenic ferric agent for enhancement recovery of valuable metals from waste light emitting diode (WLED). *Journal of Hazardous Materials*, *378*, 120648. <https://doi.org/10.1016/j.jhazmat.2019.05.041>
- Pourhossein, F., Mousavi, S. M., Beolchini, F., & Lo Martire, M. (2021). Novel green hybrid acidic-cyanide bioleaching applied for high recovery of precious and critical metals from spent light emitting diode lamps. *Journal of Cleaner Production*, *298*, 126714. <https://doi.org/10.1016/j.jclepro.2021.126714>
- Pradhan, D., Panda, S., & Sukla, L. B. (2018). Recent advances in indium metallurgy: A review. *Mineral Processing and Extractive Metallurgy Review*, *39*(3), 167–180. <https://doi.org/10.1080/08827508.2017.1399887>

- Qin, J., Ning, S., Fujita, T., Wei, Y., Zhang, S., & Lu, S. (2021). Leaching of indium and tin from waste LCD by a time-efficient method assisted planetary high energy ball milling. *Waste Management*, *120*, 193–201. <https://doi.org/10.1016/j.wasman.2020.11.028>
- Rezaei, O., Mousavi, S. M., & Pourhossein, F. (2018). Recovery of Indium from Mobile Phone Touch Screen Using Adapted *Acidithiobacillus ferrooxidans*. *International Journal of Bioscience, Biochemistry and Bioinformatics*, *8*(2), 117–124. <https://doi.org/10.17706/ijbbb.2018.8.2.117-124>
- Rocchetti, L., Amato, A., & Beolchini, F. (2016). Recovery of indium from liquid crystal displays. *Journal of Cleaner Production*, *116*, 299–305. <https://doi.org/10.1016/j.jclepro.2015.12.080>
- Rocchetti, L., Amato, A., Fonti, V., Ubaldini, S., De Michelis, I., Kopacek, B., Vegliò, F., & Beolchini, F. (2015). Cross-current leaching of indium from end-of-life LCD panels. *Waste Management*, *42*, 180–187. <https://doi.org/10.1016/j.wasman.2015.04.035>
- Rosenberg, E. (2009). Germanium: Environmental occurrence, importance and speciation. *Reviews in Environmental Science and Biotechnology*, *8*(1), 29–57. <https://doi.org/10.1007/s11157-008-9143-x>
- Ruan, J., Guo, Y., & Qiao, Q. (2012). Recovery of Indium from Scrap TFT-LCDs by Solvent Extraction. *Procedia Environmental Sciences*, *16*, 545–551. <https://doi.org/10.1016/j.proenv.2012.10.075>
- Ruiz, A. G., Sola, P. C., & Palmerola, N. M. (2018). Germanium: Current and Novel Recovery Processes. *Advanced Material and Device Applications with Germanium*. <https://doi.org/10.5772/intechopen.77997>
- Sangine, E. (2020). Mineral Commodity Summaries 2020. In *United States Geological Survey* (Issue 703).
- Savvilitidou, V., & Gidarakos, E. (2020). Pre-concentration and recovery of silver and indium from crystalline silicon and copper indium selenide photovoltaic panels. *Journal of Cleaner Production*, *250*, 119440. <https://doi.org/10.1016/j.jclepro.2019.119440>
- Savvilitidou, V., Hahladakis, J. N., & Gidarakos, E. (2015). Leaching capacity of metals-metalloids and recovery of valuable materials from waste LCDs. *Waste Management*, *45*, 314–324. <https://doi.org/10.1016/j.wasman.2015.05.025>
- Schaeffer, N., Grimes, S. M., & Cheeseman, C. R. (2017). Use of extraction chromatography in the recycling of critical metals from thin film leach solutions. *Inorganica Chimica Acta*,

457, 53–58. <https://doi.org/10.1016/j.ica.2016.11.020>

Schmidt, F., Schäffer, A., & Lenz, M. (2019). Renewable energy from finite resources: Example of emerging photovoltaics. *Chimia*, 73(11), 874–879. <https://doi.org/10.2533/chimia.2019.874>

Sethurajan, M., van Hullebusch, E. D., Fontana, D., Akcil, A., Deveci, H., Batinic, B., Leal, J. P., Gasche, T. A., Ali Kucuker, M., Kuchta, K., Neto, I. F. F., Soares, H. M. V. M., & Chmielarz, A. (2019). Recent advances on hydrometallurgical recovery of critical and precious elements from end of life electronic wastes - a review. *Critical Reviews in Environmental Science and Technology*, 49(3), 212–275. <https://doi.org/10.1080/10643389.2018.1540760>

Sethurajan, M., van Hullebusch, E. D., & Nancharaiah, Y. V. (2018). Biotechnology in the management and resource recovery from metal bearing solid wastes: Recent advances. *Journal of Environmental Management*, 211, 138–153. <https://doi.org/10.1016/j.jenvman.2018.01.035>

Silveira, A. V. M., Fuchs, M. S., Pinheiro, D. K., Tanabe, E. H., & Bertuol, D. A. (2015). Recovery of indium from LCD screens of discarded cell phones. *Waste Management*, 45, 334–342. <https://doi.org/10.1016/j.wasman.2015.04.007>

Stephanie, W., Wade, A., & Garvin A, H. (2016). End-Of-Life Management: Solar Photovoltaic Panels. International Renewable Energy Agency and the International Energy Agency Photovoltaic Power Systems. In *National Renewable Energy Lab.(NREL), Golden, CO (United States)*,. <http://dx.doi.org/10.1016/j.solmat.2015.05.005><https://doi.org/10.1016/j.wasman.2018.01.036><http://dx.doi.org/10.1016/j.renene.2012.04.030><https://doi.org/10.1016/j.jclepro.2017.09.129><https://doi.org/10.1016/j.jclepro.2018.11.229><http://dx.doi.org/10.1016/j.jclepro.2017.09.129>

Swain, B., Mishra, C., Hong, H. S., & Cho, S. S. (2016a). Beneficiation and recovery of indium from liquid-crystal-display glass by hydrometallurgy. *Waste Management*, 57, 207–214. <https://doi.org/10.1016/j.wasman.2016.02.019>

Swain, B., Mishra, C., Kang, L., Park, K. S., Lee, C. G., & Hong, H. S. (2015a). Recycling process for recovery of gallium from GaN an e-waste of LED industry through ball milling, annealing and leaching. *Environmental Research*, 138, 401–408. <https://doi.org/10.1016/j.envres.2015.02.027>

Swain, B., Mishra, C., Kang, L., Park, K. S., Lee, C. G., Hong, H. S., & Park, J. J. (2015b).

- Recycling of metal-organic chemical vapor deposition waste of GaN based power device and LED industry by acidic leaching: Process optimization and kinetics study. *Journal of Power Sources*, 281, 265–271. <https://doi.org/10.1016/j.jpowsour.2015.01.189>
- Swain, B., Mishra, C., Lee, K. J., Hong, H. S., Park, K. S., & Lee, C. G. (2016b). Recycling of GaN, a Refractory eWaste Material: Understanding the Chemical Thermodynamics. *International Journal of Applied Ceramic Technology*, 13(2), 280–288. <https://doi.org/10.1111/ijac.12473>
- Takahashi, K., Sasaki, A., Dodbiba, G., Sadaki, J., Sato, N., & Fujita, T. (2009). Recovering indium from the liquid crystal display of discarded cellular phones by means of chloride-induced vaporization at relatively low temperature. *Metallurgical and Materials Transactions A: Physical Metallurgy and Materials Science*, 40(4), 891–900. <https://doi.org/10.1007/s11661-009-9786-4>
- Tan, L., Li, J., Wang, K., & Liu, S. (2009). Effects of defects on the thermal and optical performance of high-brightness light-emitting diodes. *IEEE Transactions on Electronics Packaging Manufacturing*, 32(4), 233–240. <https://doi.org/10.1109/TEPM.2009.2027893>
- Tang, Y. (2017). Copper Indium Gallium Selenide Thin Film Solar Cells. *Nanostructured Solar Cells*. <https://doi.org/10.5772/65291>
- Tao, J., Tao, Z., & Zhihong, L. (2021). Review on resources and recycling of germanium, with special focus on characteristics, mechanism and challenges of solvent extraction. *Journal of Cleaner Production*, 294(932), 126217. <https://doi.org/10.1016/j.jclepro.2021.126217>
- Ueberschaar, M., Otto, S. J., & Rotter, V. S. (2017). Challenges for critical raw material recovery from WEEE – The case study of gallium. *Waste Management*, 60, 534–545. <https://doi.org/10.1016/j.wasman.2016.12.035>
- Upadhyay, A., Alimohammadi, F., Van Aken, B., & Tehrani, R. (2021). Biogenic Synthesis of Self-Incorporated Indium Graphitic Composites from Electronic Waste Using *Eleocharis acicularis*. *ACS Sustainable Chemistry and Engineering*, 9(48), 16082–16091. <https://doi.org/10.1021/acssuschemeng.1c04326>
- USGS. (2013). *Historical statistics for mineral and material commodities in the United States (2013 version)*. 1–8. <http://minerals.usgs.gov/minerals/pubs/historical-statistics/>
- USGS. (2018). 2016 Minerals Yearbook-Gallium. *U.S. Geological Survey*, 23.1-23.4. <https://minerals.usgs.gov/minerals/pubs/commodity/lithium/myb1-2016-lithi.pdf>
- USGS. (2020). 2017 Minerals Yearbook. *U.S. Geological Survey*, 85.1-85.15.

- USGS. (2022). Mineral Commodity Summaries 2022. In *U.S. Geological Survey* (Issue 703).
- USGS. (2023). *Mineral commodity summaries 2023*.
- Van den Bossche, A., Vereycken, W., Vander Hoogerstraete, T., Dehaen, W., & Binnemans, K. (2019). Recovery of Gallium, Indium, and Arsenic from Semiconductors Using Tribromide Ionic Liquids [Research-article]. *ACS Sustainable Chemistry and Engineering*, 7(17), 14451–14459. <https://doi.org/10.1021/acssuschemeng.9b01724>
- Virolainen, S., Ibane, D., & Paatero, E. (2011). Recovery of indium from indium tin oxide by solvent extraction. *Hydrometallurgy*, 107(1–2), 56–61. <https://doi.org/10.1016/j.hydromet.2011.01.005>
- Wang, M. M., Zhang, C. C., & Zhang, F. S. (2016). An environmental benign process for cobalt and lithium recovery from spent lithium-ion batteries by mechanochemical approach. *Waste Management*, 51, 239–244. <https://doi.org/10.1016/j.wasman.2016.03.006>
- Wei, S., Liu, J., Zhang, S., Chen, X., Liu, Q., Zhu, L., Guo, L., & Liu, X. (2016). Stoichiometry, isotherms and kinetics of adsorption of In(III) on Cyanex 923 impregnated HZ830 resin from hydrochloric acid solutions. *Hydrometallurgy*, 164, 219–227. <https://doi.org/10.1016/j.hydromet.2016.05.006>
- Willner, J., Fornalczyk, A., Saternus, M., Sedlakova-Kadukova, J., & Gajda, B. (2022). LCD panels bioleaching with pure and mixed culture of *Acidithiobacillus*. *Physicochemical Problems of Mineral Processing*, 58(1), 15–23. <https://doi.org/10.37190/ppmp/143580>
- Wood, S. A., & Samson, I. M. (2006). The aqueous geochemistry of gallium, germanium, indium and scandium. *Ore Geology Reviews*, 28(1), 57–102. <https://doi.org/10.1016/j.oregeorev.2003.06.002>
- Xie, Y., Wang, S., Tian, X., Che, L., Wu, X., & Zhao, F. (2019). Leaching of indium from end-of-life LCD panels via catalysis by synergistic microbial communities. *Science of the Total Environment*, 655, 781–786. <https://doi.org/10.1016/j.scitotenv.2018.11.141>
- Xu, L., Xiong, Y., Wang, L., Tian, Y., Tong, B., You, J., & Zhao, Z. (2021). A novel method for selective recovery of indium from end-of-life liquid crystal displays by 15-crown-5 ether and its derivatives. *Hydrometallurgy*, 202, 105601. <https://doi.org/10.1016/j.hydromet.2021.105601>
- Yam, F. K., & Hassan, Z. (2005). Innovative advances in LED technology. *Microelectronics Journal*, 36(2), 129–137. <https://doi.org/10.1016/j.mejo.2004.11.008>
- Yang, J., Retegan, T., & Ekberg, C. (2013). Indium recovery from discarded LCD panel glass

- by solvent extraction. *Hydrometallurgy*, 137, 68–77.
<https://doi.org/10.1016/j.hydromet.2013.05.008>
- Yang, Y., Zheng, X., Tao, T., Rao, F., Gao, W., Huang, Z., Leng, G., Min, X., Chen, B., & Sun, Z. (2023). A sustainable process for selective recovery of metals from gallium-bearing waste generated from LED industry. *Waste Management*, 167, 55–63.
<https://doi.org/10.1016/j.wasman.2023.05.018>
- Yen, F. C., Chang, T. C., Laohaprapanon, S., Chen, Y. L., & You, S. J. (2016). Recovery of indium from LCD waste by solvent extraction and the supported liquid membrane with strip dispersion using D2EHPA as the extractant. *Solvent Extraction Research and Development*, 23(1), 63–73. <https://doi.org/10.15261/serdj.23.63>
- Ylä-Mella, J., & Pongrácz, E. (2016). Drivers and constraints of critical materials recycling: The case of indium. *Resources*, 5(4). <https://doi.org/10.3390/resources5040034>
- Yu, Z., Han, H., Feng, P., Zhao, S., Zhou, T., Kakade, A., Kulshrestha, S., Majeed, S., & Li, X. (2020). Recent advances in the recovery of metals from waste through biological processes. In *Bioresource Technology* (Vol. 297, p. 122416). Elsevier.
<https://doi.org/10.1016/j.biortech.2019.122416>
- Zeng, X., Wang, F., Sun, X., & Li, J. (2015). Recycling Indium from Scraped Glass of Liquid Crystal Display: Process Optimizing and Mechanism Exploring. *ACS Sustainable Chemistry and Engineering*, 3(7), 1306–1312.
<https://doi.org/10.1021/acssuschemeng.5b00020>
- Zhan, L., Wang, Z., Zhang, Y., & Xu, Z. (2020). Recycling of metals (Ga, In, As and Ag) from waste light-emitting diodes in sub/supercritical ethanol. *Resources, Conservation and Recycling*, 155, 104695. <https://doi.org/10.1016/j.resconrec.2020.104695>
- Zhan, L., Xia, F., Xia, Y., & Xie, B. (2018). Recycle Gallium and Arsenic from GaAs-Based E-Wastes via Pyrolysis-Vacuum Metallurgy Separation: Theory and Feasibility. *ACS Sustainable Chemistry and Engineering*, 6(1), 1336–1342.
<https://doi.org/10.1021/acssuschemeng.7b03689>
- Zhan, L., Xia, F., Ye, Q., Xiang, X., & Xie, B. (2015). Novel recycle technology for recovering rare metals (Ga, In) from waste light-emitting diodes. *Journal of Hazardous Materials*, 299, 388–394. <https://doi.org/10.1016/j.jhazmat.2015.06.029>
- Zhang, K., Li, B., Wu, Y., Wang, W., Li, R., Zhang, Y. N., & Zuo, T. (2017). Recycling of indium from waste LCD: A promising non-crushing leaching with the aid of ultrasonic wave. *Waste Management*, 64(100), 236–243.

<https://doi.org/10.1016/j.wasman.2017.03.031>

Zhang, K., Wu, Y., Wang, W., Li, B., Zhang, Y., & Zuo, T. (2015). Recycling indium from waste LCDs: A review. *Resources, Conservation and Recycling*, *104*(100), 276–290.

<https://doi.org/10.1016/j.resconrec.2015.07.015>

Zhang, L., Song, Q., & Xu, Z. (2019). Thermodynamics, Kinetics Model, and Reaction Mechanism of Low-Vacuum Phosphate Reduction Process for Germanium Recovery from Optical Fiber Scraps. *ACS Sustainable Chemistry and Engineering*, *7*(2), 2176–2186.

<https://doi.org/10.1021/acssuschemeng.8b04882>

Zhang, L., & Xu, Z. (2016). A review of current progress of recycling technologies for metals from waste electrical and electronic equipment. *Journal of Cleaner Production*, *127*, 19–

36. <https://doi.org/10.1016/j.jclepro.2016.04.004>

Zhang, Y., Zhan, L., & Xu, Z. (2021). Recycling Ag, As, Ga of waste light-emitting diodes via subcritical water treatment. *Journal of Hazardous Materials*, *408*, 124409.

<https://doi.org/10.1016/j.jhazmat.2020.124409>

Zhao, L., Chen, B., & Wang, D. (2013). Effects of electrochemically active carbon and indium (III) oxide in negative plates on cycle performance of valve-regulated lead-acid batteries during high-rate partial-state-of-charge operation. *Journal of Power Sources*, *231*, 34–38.

<https://doi.org/10.1016/j.jpowsour.2012.12.083>

Zhou, J., Zhu, N., Liu, H., Wu, P., Zhang, X., & Zhong, Z. (2019). Recovery of gallium from waste light emitting diodes by oxalic acidic leaching. *Resources, Conservation and Recycling*, *146*, 366–372.

<https://doi.org/10.1016/j.resconrec.2019.04.002>

Supplementary Materials for

Recovery technologies for indium, gallium, and germanium from end-of-life products (electronic waste) – A review

Kun Zheng¹, Marc F. Benedetti¹, Eric D. van Hullebusch^{1*}

¹ Université Paris Cité, Institut de Physique du Globe de Paris, CNRS, F-75005 Paris, France

* Corresponding author: vanhullebusch@ipgp.fr (Eric D. van Hullebusch)

Number of Pages: 5

Number of Texts: 1

Number of Figures: 3

Number of Tables: 1

Supporting Text of Contents

Text S1 Methodology for literature selection2

Figure of Contents

Figure S1 Common LED chip structure. Modified from Tan et al. (2009).....3

Figure S2 Schematic structure of CIGS PV and GaAs PV. Modified from Polman et al. (2016)

.....3

Figure S3 Typical structure of OFs. Modified from Zhang et al. (2019)3

Table of Contents

Table S1 Summary of indium, gallium, and germanium stability constants with different ligands in the optimal conditions from the literature.4

Text S1 Methodology for literature selection

In this section, we explain the methodology and criteria that were utilized for the selection of relevant literature, with emphasis on traceability and transparency. Our goal is to ensure that the selected articles were highly relevant and recently published (within the last 8 years) regarding the research topic, thereby supporting the foundation of this review.

Data collection was carried out in scientific databases such as ScienceDirect, SpringerLink, and Google Scholar. The search terms include indium (or gallium or germanium) leaching (or bioleaching or extraction or recovery), critical metal recovery, secondary source, electronic waste (or waste electrical and electronic equipment (WEEE) or end-of-life (EoL) products) pre-treatment or hydrometallurgy (or biohydrometallurgy), waste (or spent or end-of-life or discarded) light crystal displays (LCDs) (or LCD monitors/panels/screens/glass), waste (or spent or end-of-life or discarded) light emitting diodes (LEDs) (or GaN/GaAs or MOCVD dust or LED industry), waste (or spent or end-of-life or discarded) photovoltaics (PVs) (or CIS/CIGS panels or solar cell), and waste (or spent or end-of-life or discarded) optical fibers (or fiber optics).

The literature selection process focused exclusively on original research articles while excluding review articles, books, reports, and non-scholarly sources that lacked peer-reviewed research findings. Additionally, we only considered research samples sourced from electronic waste to coordinate with our research theme, categorizing them into distinct sections based on different types of electronic waste. Our methodology also entailed considering pre-treatment methods for concentrating indium, gallium, and germanium from a batch of electronic waste, followed by the evaluation of hydrometallurgical and biohydrometallurgical routes for leaching and extraction, excluding pyrometallurgical processes.

To efficiently manage the selected literature, we employed the Mendeley reference management tool. Finally, we accurately extracted key information related to the research topic, encompassing methods, findings, and limitations, from the chosen literature. This extracted data was thoughtfully integrated into the review article to provide readers with a comprehensive understanding of the research topic.

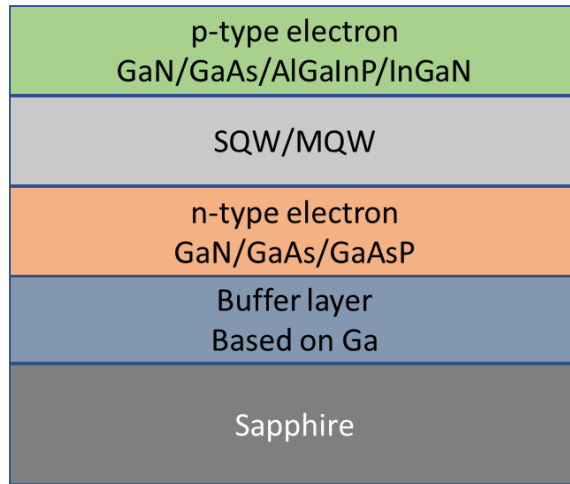


Figure S1 Common LED chip structure. Modified from Tan et al. (2009)

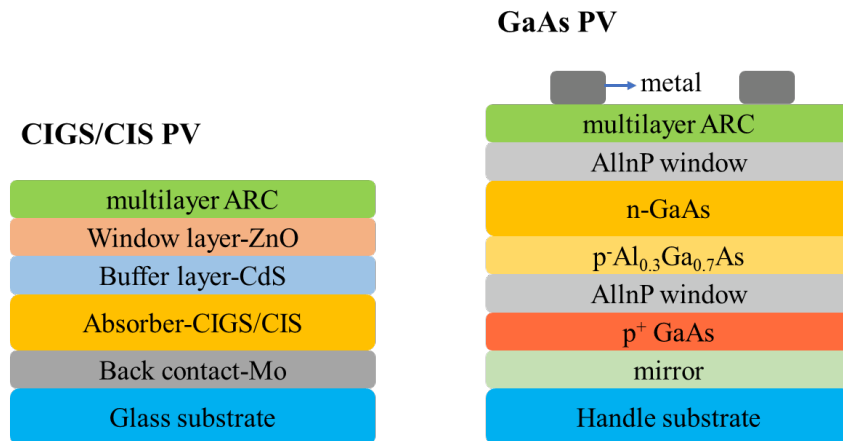


Figure S2 Schematic structure of CIGS PV and GaAs PV. Modified from Polman et al. (2016)

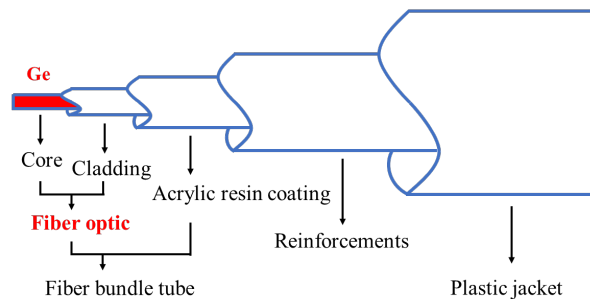


Figure S3 Typical structure of OFs. Modified from Zhang et al. (2019)

Table S1 Summary of indium, gallium, and germanium stability constants with different ligands in the optimal conditions from the literature.

Ligand	Species	log K	Ionic strength and temperature	Reference
Hydroxide	InOH ²⁺	-4.31	0.1 M KNO ₃ , 25 °C	(Wood & Samson, 2006)
	GaOH ²⁺	-2.6	0 M, 25 °C	(Wood & Samson, 2006)
	H ₄ GeO ₄ ⁰	-9.27	0.1 M KNO ₃ , 20 °C	(Wood & Samson, 2006)
	Ge(OH) ₄	55.6	0.1 M KNO ₃ , 25 °C, pH 1-2	(Filella & May, 2023)
Fluoride	InF ²⁺	12.5	1 M NaClO ₄ , 25 °C	(Wood & Samson, 2006)
	GaF ²⁺	5.58	25 °C	(Wood & Samson, 2006)
	GeF ₄	5.17	20 °C	(Filella & May, 2023)
Sulphate	InSO ₄ ⁺	3.04	0 M, 25 °C	(Wood & Samson, 2006)
	GaSO ₄ ⁺	2.77	0 M, 25 °C	(Wood & Samson, 2006)
Phosphate	In(HPO ₄) ⁺	7.4	0.2 M	(Wood & Samson, 2006)
	Ga(HPO ₄) ⁺	7.26	1 M NaClO ₄ , 25 °C	(Wood & Samson, 2006)
Chloride	InCl ²⁺	4.3	2 M NaClO ₄ , 25 °C	(Wood & Samson, 2006)
	GaCl ²⁺	0.01	0.69M HClO ₄ , 20 °C	(Wood & Samson, 2006)
Bisulfide	In(HS) ²⁺	10.5	1 M NaClO ₄ , 25 °C	(Wood & Samson, 2006)
Nitrate	InNO ₃ ²⁺	0.41	> 1 M NO ₃ ⁻	(Ashworth & Frisch, 2017)

References

- Wood, S. A., & Samson, I. M. (2006). The aqueous geochemistry of gallium, germanium, indium and scandium. *Ore Geology Reviews*, 28(1), 57–102. <https://doi.org/10.1016/j.oregeorev.2003.06.002>
- Filella, M., & May, P. M. (2023). The aqueous solution chemistry of germanium under conditions of environmental and biological interest: Inorganic ligands. *Applied Geochemistry*, 155(January), 105631. <https://doi.org/10.1016/j.apgeochem.2023.105631>
- Ashworth, C., & Frisch, G. (2017). Complexation Equilibria of Indium in Aqueous Chloride, Sulfate and Nitrate Solutions: An Electrochemical Investigation. *Journal of Solution Chemistry*, 46(9–10), 1928–1940. <https://doi.org/10.1007/s10953-017-0675-y>
- Tan, L., Li, J., Wang, K., & Liu, S. (2009). Effects of defects on the thermal and optical performance of high-brightness light-emitting diodes. *IEEE Transactions on Electronics Packaging Manufacturing*, 32(4), 233–240. <https://doi.org/10.1109/TEPM.2009.2027893>
- Polman, A., Knight, M., Garnett, E. C., Ehrler, B., & Sinke, W. C. (2016). Photovoltaic materials: Present efficiencies and future challenges. *Science*, 352(6283). <https://doi.org/10.1126/science.aad4424>
- Zhang, L., Song, Q., & Xu, Z. (2019). Thermodynamics, Kinetics Model, and Reaction Mechanism of Low-Vacuum Phosphate Reduction Process for Germanium Recovery from Optical Fiber Scraps. *ACS Sustainable Chemistry and Engineering*, 7(2), 2176–2186. <https://doi.org/10.1021/acssuschemeng.8b04882>